ANTI-METHOTREXATE FAB FRAGMENTS FOR OPTIMIZATION OF INTRAPERITONEAL METHOTREXATE CHEMOTHERAPY

by

Evelyn Lobo

August, 2002

A dissertation submitted to the
Faculty of the Graduate School of State
University of New York at Buffalo
in partial fulfillment of the requirements
for the degree of

Doctor of Philosophy

Department of Pharmaceutical Sciences

Table of Contents

ABSTRACT

This research group has proposed that anti-drug antibodies may be utilized to improve the safety and efficacy of intraperitoneal chemotherapy by imparting regio-specific alterations in drug disposition, increasing the ratio of peritoneal drug exposure relative to systemic drug exposure. The primary objectives of this dissertation work were to test the hypotheses that anti-chemotherapeutic antibodies would reduce drug-induced toxicity, increase the maximum tolerated dose of drug, and improve drug efficacy in the treatment of peritoneal tumors. A stepwise approach was employed, using methotrexate (MTX) as a model drug. Firstly, a high-performance liquid chromatographic assay was developed to quantify MTX concentrations in biologic samples, including those containing anti-MTX antibodies. The anti-cancer effect of MTX was evaluated in cell culture using sarcoma-180 cells and Ehrlich ascites cells. MTX pharmacokinetics and toxicokinetics were assessed in mice, following MTX administration over a wide range of doses (2.5 – 1000 mg/kg), given by a variety of dosing protocols (i.p. bolus injection, and i.p. infusion 24 – 168 h). These data were characterized with a robust mathematical model that related the time-course of MTX exposure to MTX-induced toxicity. The mathematical model was used to predict, via computer simulation, the influence of anti-MTX antibodies on MTX disposition and MTX-induced toxicity. Hybridoma cells were developed to secrete monoclonal anti-MTX IgG antibodies. Methods were developed to produce and purify anti-MTX IgG, and to produce and purify anti-MTX Fab fragments (AMF). In vivo experiments were conducted in mice to test predictions of the mathematical

model, and to test the hypothesis that anti-MTX antibodies allow increases in the maximally tolerated i.p. dose of MTX. Additional studies, using Swiss-Webster mice bearing sarcoma-180 cells, were conducted to test the hypothesis that AMF allows increases in the efficacy of i.p. MTX therapy of peritoneal tumors.

MTX-induced body weight loss was found to be highly dependent on the time-course of MTX exposure. The maximally tolerated dose of MTX reduced more than 200-fold when the administration protocol was changed from bolus injection (760 mg/kg) to 72 h infusion (3.8 mg/kg). These data were well characterized with a pharmacokinetic-pharmacodynamic model, which was then utilized to predict the influence of anti-MTX antibodies on MTX disposition and MTX-induced toxicity. Interestingly, the model predicted that antibody administration could lead to increases in toxicity, as well as the expected decreases in toxicity, depending on the dosing protocol employed, the affinity of the antibody, and the kinetics of antibody disposition. Predictions of increased toxicity (i.e., agonistic effects of the anti-drug antibodies) and decreased toxicity (i.e., antagonistic effects) were tested in vivo, and results were found to be very similar to those predicted by the model. Additionally, as hypothesized, intravenous AMF was shown to significantly reduce MTX-induced body weight loss and MTX related mortality, following i.p. MTX therapy. With AMF administration, the maximally tolerated dose of MTX was found to increase to more than 5-fold that observed in control animals. Additionally, combination therapy with i.p. MTX and s.c. AMF extended the survival of mice bearing peritoneal tumors (i.e., relative to the

survival of control animals and animals treated with the maximally tolerated dose of MTX). Consequently, this dissertation work suggests that anti-drug antibodies may allow improvements in the safety and efficacy of the intraperitoneal chemotherapy of peritoneal cancers.

PREFACE

This dissertation evaluated an approach that utilized anti-drug antibodies to improve therapeutic selectivity (i.e. the ratio of drug efficacy to drug toxicity) of intraperitoneal chemotherapy. The approach calls for the systemic administration of anti-drug antibodies to reduce systemic drug exposure and systemic drug toxicities of intraperitoneal drug therapy. The approach was investigated with methotrexate (MTX) as a model chemotherapeutic drug and anti-methotrexate antibodies in an animal model of peritoneal tumor.

Each chapter is intended for submission to a particular scientific journal for publication. The chapters are written in the format required by that journal. Each chapter presents the research investigations with its own introduction and conclusions. Chapter 1 is a short review of literature reports regarding the utility of anti-drug antibodies to reduce systemic drug toxicities for small molecules. The review discusses the influence of anti-drug antibodies on drug pharmacokinetics and its implications on drug pharmacodynamics.

Chapter 2 describes a sensitive high performance liquid chromatographic assay for determining MTX concentration in the presence of anti-MTX antibodies. The assay was validated for accuracy and precision in determining total (bound and unbound) and free (unbound) MTX concentration in mouse and rat plasma in the presence and in the absence of anti-MTX Fab fragments.

Chapter 3 presents systematic investigations of the pharmacokinetics and toxicodynamics of MTX following intraperitoneal administration of MTX in mice. MTX was administered either as bolus injection or as constant-rate infusion. MTX-induced toxicity was characterized with a pharmacokinetic-pharmacodynamic model that related the time course of MTX plasma exposure to the magnitude of MTX-induced nadir body weight loss.

Chapter 4 discusses the application of the pharmacokinetic-pharmacodynamic model for MTX toxicity to make predictions regarding MTX disposition and MTX toxicity in the presence of anti-MTX antibodies. Computer simulations were conducted to evaluate the ability of anti-MTX antibodies to reduce MTX-induced systemic toxicities. The predictions of the model were tested in mice with anti-MTX IgG and anti-MTX Fab fragments.

Chapter 5 examined the utility of systemic anti-MTX Fab to permit dose escalation following i.p. MTX therapy and allow for enhancement of MTX efficacy in mice bearing peritoneal tumors. The pharmacokinetics of anti-MTX Fab were investigated following i.v. and s.c. route of administration. Dose escalation studies were conducted following s.c. administration of anti-MTX Fab and i.p. administration of MTX. The survival curves were evaluated following i.p. MTX treatment either with or without s.c. AMF.

For many chemotherapeutic drugs, chemotherapeutic selectivity (i.e., the ratio of drug efficacy to drug toxicity) is dependent on the administration protocol. In chapter 7, an approach was investigated to allow prediction of in vivo chemotherapeutic selectivity with in vivo toxicity data and in vitro cytotoxicity data. The approach was examined with MTX in two murine cancer cell lines, sarcoma 180 and Ehrlich ascites cells in vitro and in mice bearing peritoneal tumors.

Recently, a simple approach was introduced to model pharmacokinetic-pharmacodynamic time delays through the use of transit compartments. In chapter 6, the transit compartment model was evaluated to describe the time course of cell growth observed from MTX treatment in two cancer cell lines grown in culture. The transit compartment model was developed to incorporate a series of transfer steps to characterize the time delay in MTX exposure and MTX effects.

Lastly, chapter 8 summarizes the conclusions of the research results presented in this dissertation.

CHAPTER ONE

Utility of anti-drug antibodies to optimize cancer chemotherapy

Summary

Anti-drug antibodies have been successfully applied in the treatment of drug poisoning and drug overdose to prevent or reverse life-threatening adverse effects. During the past decade, there has been increasing interest in utilizing anti-drug antibodies to prevent or reverse toxicities associated with cancer chemotherapy. The interaction of drug and anti-drug antibodies often leads to dramatic alterations in the time course of drug disposition and in the magnitude and time course of drug effects. In most cases, administration of anti-drug antibodies leads to the development of inactive drug-antibody complexes, minimization of unbound drug concentrations, and reversal of drug effects. However, in many cases, administration of anti-drug antibodies has led to an increase in the magnitude of drug effect, perhaps due to alterations in the tissue distribution of drug, or perhaps due to alterations in the time course of drug exposure. This report reviews the influence of anti-drug antibodies on drug pharmacokinetics and drug pharmacodynamics, and discusses strategies where anti-drug antibodies may be used to mitigate the toxicities associated with cancer chemotherapy.

Introduction

Antibodies directed against drugs, venoms, toxins, and endogenous substances (hereafter collectively referred to as anti-drug antibodies), have been applied to prevent, reverse, or attenuate the pharmacologic effects of their ligand. For example, antibodies remain to be the primary treatment for snake and insect venom poisoning [1]. Anti-drug antibodies have been shown to provide protection against life threatening toxicities associated with endotoxins and cytokines [2, 3], and several antibodies are effective in the treatment of intentional or accidental overdose of small molecule drugs, including morphine, digitalis, colchicine, and antidepressants [4-7]. Perhaps due to these successes, there has been a growing interest in investigating the use of anti-drug antibodies to prevent adverse effects related to cancer chemotherapy [8, 9].

In general, antineoplastic agents are not selective, killing not only cancer cells but also rapidly proliferating normal cells (e.g. gastrointestinal tract epithelial cells, bone marrow stem cells, etc.) [10]. Consequently, cancer chemotherapy is associated with a host of adverse effects (e.g., stomatitis, mucositis, neutropenia, thrombocytopenia, anemia, etc.) [10-12]. These adverse effects are of great clinical importance, affecting patient's quality of life and often leading to dose reduction, delays in subsequent drug treatment, and, in some cases, discontinuation of drug therapy.

Several strategies have been employed to prevent or palliate the systemic toxicities of chemotherapeutic drugs. Anti-emetic agents are used to manage nausea and vomiting associated with initiation of chemotherapy [13]. Epithelial growth factor, pilocarpine, glutamine and oral cryotherapy have been tested to reduce inflammation of the oral mucosa [14]. Colony stimulating factors and erythopoietin have been applied to manage bone marrow suppression by increasing neutrophil, platelet and red cell production [15, 16]. In current clinical practice, multiple supportive therapies are often employed to mitigate the adverse effects of chemotherapy.

The unique ability of anti-drug antibodies to rapidly and efficiently neutralize toxins in venom poisoning, septic shock, and drug overdose has fueled interest in utilizing anti-drug antibodies to prevent, minimize, or reverse systemic toxicities of chemotherapeutic drugs. The review primarily focuses on the influence of anti-drug antibodies on drug pharmacokinetics and its implications for drug pharmacodynamics. An understanding of the effects of anti-drug antibodies on drug pharmacokinetics and pharmacodynamics may expedite the development of successful strategies for minimization of chemotherapeutic toxicity with anti-drug antibodies.

Antibody Ligand Interaction

Immunglobulins (IgG, IgA, IgD, IgE, and IgM) are a unique family of specialized proteins that bind ligands with high specificity and affinity. The interaction

between the ligand and the antibody binding site is bimolecular and reversible, and governed by the law of mass action described as follows,

$$[L] + [A] \underset{k_{off}}{\overset{k_{on}}{\rightleftharpoons}} [LA] \qquad \text{Eq. 1}$$

$$K_{eq} = \frac{k_{on}}{k_{off}} = \frac{[LA]}{[L][A]} \qquad \text{Eq. 2}$$

where [L] is the concentration of the unbound ligand, [A] is the concentration of unoccupied binding sites, [LA] is the concentration of antibody-ligand complex, k_{on} is the second order association rate constant, k_{off} is the first order dissociation rate constant, and K_{eq} is the equilibrium affinity constant of the antibody-ligand complex. In most cases, the pharmacologic effects of ligands are highly correlated with concentrations of unbound ligand. In the presence of anti-ligand antibodies, unbound ligand concentrations will be dependent on the equilibrium affinity of the antibody and the concentration of the antibody binding sites.

As a result of the bimolecular nature of antibody – ligand interaction, antibody – ligand binding is dependent not only on the molar ratio of ligand and binding sites, but also on their absolute quantities. For example, eq 2 may be rearranged to solve for equilibrium concentrations of L, LA, and A, given initial concentrations and K_{eq}. Assuming that K_{eq} is equivalent to 10^8 M^{-1}, an initial concentration of 0 for LA, and equimolar initial concentrations of L and A = 10^{-8} M, then the equilibrium concentrations may be estimated to be: 6.2×10^{-9} M (for L and A) and 3.8×10^{-9} M (for LA), where the fraction of drug bound is 0.38 (i.e., fraction bound

= LA/(L+LA)). Again if it is assumed that K_{eq} is equivalent to 10^8 M^{-1}, initial concentration of 0 for LA, and L and A, but where equimolar initial concentrations of L and A = 1 M, then the equilibrium concentrations may be estimated to be: 9.99×10^{-5} M (for L and A) and 0.9999 M (for LA), where the fraction of drug bound is 0.9999. So, although equimolar amounts of L and A were considered in each example, the extent of drug binding is predicted to be dramatically different. As such, the effects of anti-drug antibody on drug disposition and drug effects will be dependent not only on the molar ratio of antibody and drug, but also on the absolute quantities present in vivo.

Antibody Pharmacokinetics

Intact antibody, most commonly of the IgG isotype, and its fragments such as $F(ab)_2$, Fab/c, Fab and Fv have been employed as antidotes to reduce toxic effects arising from drug overdose [17-20]. Intact IgG and its fragments differ in their number of binding sites (two molar binding sites per mole of IgG and $F(ab)_2$; one molar binding site per mole of Fab/c, Fab and Fv), molecular weight (IgG, ~150 kDa; $F(ab)_2$ and Fab/c, ~100 kDa; Fab, ~50 kDa; Fv, ~25 kDa) and disposition characteristics [21].

The disposition of antibodies and their fragments is governed, in part, by their molecular weight. For example, rates of antibody distribution and elimination are likely to be largely determined by rate processes that are sensitive to molecular size (e.g., rates of extravascation, diffusion, and glomerular filtration). Consistent

with this expectation, antibody volume of distribution, clearance, and half-life, are often correlated with the molecular weight of the antibody or fragment (e.g., Table I) [22]. However, it is important to note that IgG elimination is influenced, in part, by its interaction with FcRn, which protects IgG from intracellular catabolism [23]. As such, IgG is eliminated more slowly than higher molecular weight immunoglobulins (e.g., IgM), and much more slowly than predicted based on molecular weight [24]. In most studies, the volume of distribution of intact immunoglobulins (IgG, IgA, IgD, IgE, and IgM) approximates blood volume, whereas Fab fragments are often found to distribute to a volume approximating the extracellular fluid volume [25, 26]. Fab and Fv fragments are sufficiently small to allow substantial renal filtration, and these fragments demonstrate rapid elimination relative to intact immunoglobulins, $F(ab)_2$, and Fab (Table I).

Antibodies also differ in their metabolic sites and routes of elimination. Intact immunoglobulins demonstrate little elimination via renal filtration, and are primarily cleared via catabolism in the liver, gut, and spleen [27, 28]. Investigations of the metabolism of murine monoclonal IgG1 in mice indicate that 73% of the IgG1 was catabolized in the gut, 20% in the liver, and 4% in the spleen [29]. On the other hand, the kidney was found to be the main organ of clearance for $F(ab)_2$ and Fab. In mice, nearly 50% and 73% of total catabolism for $F(ab)_2$ and Fab was accounted for by the kidneys [29].

Although not thoroughly studied for all antibody isotypes and fragments, the kinetics of antibody elimination are often found to be dependent on the species of antibody origin. For example, Bazin-Redureau et al. investigated the disposition of mouse IgG1, rat IgG1, and human IgG1 in rats (Table II) [22]. The clearance and terminal half-life of mouse IgG1 were found to significantly different from rat and human IgG1. However, the distribution volumes of IgG were not dependent on the species origin. Table III, IV and V presents the pharmacokinetic parameters of IgG, $F(ab)_2$ and Fab in different species [25, 30, 31]. Interestingly, Scherrmann and coworkers found that while Fab clearance scaled well across species [31], a similar relationship could not be developed for IgG (personal communications). This finding may be related to interspecies differences in IgG affinity for FcRn [32].

Influence of anti-drug antibodies on drug pharmacokinetics

Administration of anti-drug antibodies in the systemic circulation can drastically alter the time course of drug exposure. The changes in the disposition of the drug are governed by the disposition of the antibody, affinity of the antibody, the molar dose ratio of the antibody : drug and the dosing protocol employed. Typically, an equimolar dose of systemic anti-drug antibody would increase the total plasma drug concentrations due to the high affinity of the drug for the antibody leading to the redistribution of drug from tissues into the systemic circulation [33]. The redistribution of drug from the tissues would reduce total drug concentrations in the tissues [34-37]. Additionally, the binding of the drug to the antibody would

likely decrease the free (or unbound) drug concentrations and the free fraction of drug in plasma. Figure 1 illustrates the alterations in the time course of total and free colchicine following anti-colchicine Fab administration or 0.9% sterile NaCL [38].

In addition to reducing free plasma drug concentrations, antibody fragments may also reduce the cumulative free drug exposure [39]. Renal filtration of drug-antibody complexes would provide an additional pathway for drug elimination. Several studies with anti-drug Fab fragments have demonstrated increased urinary elimination of drug. In rats, the percent of colchicine dose eliminated in urine increased from 9 ± 0.7% to 38 ± 6.9% with anti-colchicine Fab treatment [38]. Anti-desipramine Fab was found to increase the total urinary excretion of desipramine by 7-fold as compared to a non-specific Fab in rats [40]. The percent of methotrexate eliminated in the urine increased from 8.2 ± 1.4% to 25.7 ± 3.8% in rats treated with anti-methotrexate Fab [39]. Perhaps due to direct elimination of methotrexate-Fab complexes, the cumulative systemic exposure of free methotrexate (AUCf) was reduced by approximately 55% in this study. Unlike antibody fragments, intact IgG has limited renal elimination and may not reduce the cumulative exposure to free drug. Instead degradation of the drug : anti-drug IgG complex may lead to localization of the drug in the metabolizing organ or recycling of the drug into the systemic circulation.

Several chemotherapeutic drugs demonstrate short elimination half-lives (i.e. less than 12 h) [41, 42]. The binding of such drugs to the antibody with long half-lives would potentially increase the half-life of the drug and increase the duration of free drug exposure. For example, Schermann et al. found that the terminal half-life of free colchicine increased from 10.7 h in non-immunized animals to 32.4 h in colchicine-immunized animals [43]. For schedule dependent chemotherapeutic drugs, where effects are dependent on dose and the duration of exposure, an increase in the duration of free drug exposure may potentially lead to increases in drug toxicities.

By enhancing the elimination of anti-drug antibodies, it might be possible to decrease the half-life of the drug and allow further reductions in cumulative free drug exposure. Several strategies have been proposed to achieve this goal. For example, pre-clinical and clinical investigations have investigated the use of cationic amino acids to enhance the renal elimination Fab fragments [44-46]. Proksch et al. have found that systemic alkalinization with sodium bicarbonate increased urine flow, Fab excretion rate, and Fab elimination in the urine [47]. More recently, cationized IgG and Fab were found to demonstrate increased clearance and reduced terminal half-lives as compared to their native antibodies [48].

Influence of anti-drug antibodies on drug pharmacodynamics

Systemic toxicities of chemotherapeutic drugs are often highly correlated with peak plasma drug concentration [49-51], steady state plasma concentration, cumulative systemic exposure [52, 53], or time above a threshold concentration [54]. If chemotherapeutic toxicity is related to peak drug concentration, systemic administration of anti-drug antibodies and its fragments would typically decrease peak free drug concentration, and produce favorable reduction in systemic toxicities. In cases where toxicities are dependent on cumulative exposure to free drug, antibody fragments such as $F(ab)_2$, Fab and sFv may decrease systemic toxicities as there may be significant elimination of drug-antibody complexes.

For many chemotherapeutics, toxicity v. dose relationships are dependent on the time course of drug exposure (and, thus, dependent on the time course of drug administration). In most cases, apparent potency of the drug increases with increases in the duration of drug exposure (i.e., where toxicity v. dose relationships shift to the left with increasing duration of drug exposure). For example, in clinical studies with topotecan, the maximally tolerated dose reduced from 22.5 mg/kg (following 30 min infusion) to 3.4 mg/kg (following 120 h infusion) [55]. Similarly, in preclinical studies conducted in this laboratory, the maximally tolerated dose of methotrexate reduced from 760 mg/kg, following bolus administration, to 3.8 mg/kg, following 72 h infusion [56]. This phenomenon is likely due, in part, to the fact that many chemotherapeutics exhibit cell cycle phase-specific toxicity, where drug potency is greatest during a specific stage of

the cell cycle. By extending the duration of drug exposure, a greater fraction of cells may ‘cycle’ into the stage associated with high drug potency. Because anti-drug antibodies will typically exhibit longer half-lives than those of the target drug, it is possible that beneficial reductions in cumulative exposure to free drug may be offset by increases in the duration of drug exposure. That is, in cases where effect v. dose relationships shift leftward with increases in the duration of drug exposure, administration of anti-drug antibodies may increase drug toxicity (rather than producing the desired reduction in drug toxicity).

There have been several reports in the literature demonstrating increased drug toxicities following anti-drug antibody administration. Investigations with anti-interluekin antibodies have shown that the administration of anti-interleukin-6 antibodies led to a 30% increase in interleukin-6 induced fibrinogen levels in mice [57]. Anti-interleukin-3 monoclonal antibodies increased mucosal mast cell number by 16-fold compared to results observed in mice treated with interleukin-3 alone [58]. Similarly, IgE production in mice treated with IL-4 binding protein increased five-fold compared to IgE production following administration of IL-4 alone [59].

Similarly, reoccurrence of drug toxicities observed in drug overdose and in venom poisoning has been related to changes in the time course of drug exposure [60, 61]. Anti-digoxin Fab treatment in digoxin poisoning has occasionally shown a rebound increase in free digoxin concentrations after initial

decrease in free digoxin concentrations and may possibly be related to the recurrence of digoxin toxicities [62, 63]. Apart from toxicities due to alteration in the time course of drug exposure, anti-drug antibodies administration may lead to additional toxicities arising from redistribution of drug and localization of drug in certain tissues. For example, systemic monoclonal anti-amantin Fab resulted in enhanced kidney damage to due localization of amanitin (a mushroom toxin)-Fab complex in the kidneys [64]. As such, it is often difficult to predict the effects of anti-drug antibodies.

Pharmacokinetic models may be applied to predict the effects of anti-drug antibodies on the drug disposition [37, 39]. A pharmacokinetic-toxicodynamic model for drug toxicity that relates the time course of drug exposure to drug toxicity may be valuable in predicting the effects of anti-drug antibody on drug toxicity. The pharmacokinetic model might allow the prediction of changes in drug disposition with anti-drug antibodies, and the toxicodynamic model might then permit prediction of drug toxicities resulting from the changes in drug disposition. Computer simulations would also allow evaluation of the effect of molar dose ratio (drug : antibody), antibody affinity, and mode of administration on drug toxicities.

The coadministration of anti-drug antibodies for chemotherapeutic drugs has largely been observed to reduce drug toxicities. Savaraj et al. demonstrated that coadministration of polyclonal anti-doxorubicin antibody preparations increased

the survival of mice treated with a toxic dose of doxorubicin [65]. Later, murine monoclonal anti-doxorubicin IgG were developed and shown to significantly reduce body weight loss and mortality following i.v. doxorubicin in mice [8]. Animal treated with anti-doxorubicin IgG and doxorubicin had a survival rate of 90% compared to the survival rate of 10% in animals treated with doxorubicin alone. Coadministration of murine monoclonal anti-vinca IgG and vinca (toxic dose) produced no deaths whereas vinca administration alone caused 70% mortality in mice [66].

Optimization of chemotherapy

The ability of anti-drug antibodies to reduce systemic toxicity may be utilized to enhance therapeutic selectivity (i.e., the ratio of drug efficacy to drug toxicity) of cancer chemotherapy. By reducing systemic toxicities, anti-drug antibodies may allow for dose escalation of drug therapy and enhance the therapeutic efficacy of drug therapy. Two research groups have been investigating the administration of anti-drug antibodies to reduce systemic drug toxicities and achieve improvements in therapeutic efficacy of drug therapy: Balsari and coworkers have been investigating the utility of local administration of anti-drug antibodies to treat systemic toxicities following drug therapy [9, 67-69], and Balthasar and coworkers have been investigating the use of systemic administration of anti-drug antibodies to enhance the selectivity of regional chemotherapy [37, 39, 70, 71].

Local administration of anti-drug antibodies may result in high antibody concentration in the locally applied tissue relative to the blood. Following drug administration, drug that reaches the site of toxicity would likely bind to the anti-drug antibody to form drug-antibody complex and thereby reduce free drug exposure in tissues (such as gastrointestinal lining, bone marrow and hair follicle) associated with systemic toxicities. The approach was examined with doxorubicin and monoclonal anti-doxorubicin IgG2a (MAD11) in animal models. Local administration of anti-doxorubicin IgG to the skin, oral mucosa, gastrointestinal tract and bone marrow was examined for protection against doxorubicin induced alopecia, mucositis, body weight loss and bone marrow suppression [9, 67-69].

Local application of anti-doxorubicin IgG (0.1 mg/rat/day) to head, neck and abdomen of 8-day old rats treated with i.p. doxorubicin (2 mg/kg/day) for a week was observed to retain full coat of fur whereas 90% of the rats treated with i.p. doxorubicin alone showed severe alopecia ($p<0.003$) [67]. After 10 days of doxorubicin administration, skin biopsy sections of rats cotreated with anti-doxorubicin IgG were found to have normal morphology whereas skin section from rats treated with doxorubicin showed considerable loss of hair follicles. Antibody concentrations in the skin were found to be nearly 400-fold greater than in the blood after 4 to 16 h of topical antibody application. However, anti-doxorubicin antibody did not provide protection from doxorubicin induced mortality.

Oral administration of anti-doxorubicin IgG was examined to protect against gastrointestinal mucositis associated with doxorubicin [68]. Photomicrograph sections of the small intestine showed that oral anti-doxorubicin IgG (50 mg/kg, 1ml) inhibited doxorubicin induced apoptosis in mice treated with i.p. doxorubicin (12 mg/kg). Following oral antibody administration, less than 0.5% protein related radioactivity (molecular weight less than 14,000) was detected in the blood. Anti-doxorubicin IgG also significantly ($p<0.05$) reduced the body weight loss of i.p. doxorubicin treated mice. As the animals were monitored for only 2 weeks, it is not clear if anti-doxorubicin IgG improved the overall survival of the animals.

Local application of anti-doxorubicin IgG to the oral mucosa was evaluated for protection against doxorubicin-induced damage to the oral mucosa [9]. On oral application of anti-doxorubicin IgG, tongue near the tunica submucosa showed high concentrations of IgG whereas no absorption was observed in the cheek mucosa. Doxorubicin-induced apoptosis in tongue was examined following application of 20 mg/kg of MAD11 on the tongue and 2 h or 24 h later i.v. administration of 30 mg/kg doxorubicin. Examination of photomicrographs of parasagittal sections of the tongue revealed reduction in apoptotic cells at 4 h, 8 h and 24 h after treatment in animals (2 h dosing interval). No reduction in apoptotic cells was observed when anti-doxorubicin IgG was applied 24 h after i.v doxorubicin treatment. Although, oral anti-doxorubicin IgG may prevent apoptosis in the tongue, it may not provide protection against doxorubicin-induced body weight loss and bone marrow suppression.

Administration of anti-doxorubicin IgG in the tibial bone marrow was investigated for protection of doxorubicin-induced myelotoxicity [69]. Anti-doxorubicin IgG (2.5 mg/kg) in the right tibia of i.p doxorubicin (16 mg/kg) treated mice significantly decreased the percent of apoptotic cell in the right tibia but not in the contralateral tibia. This may partly be explained by a nearly 90-fold lower concentrations in the contralateral tibia than in the right tibia. Intratibial MAD11 (15 mg/kg) increased the survival rate from 60% to 100% in animals treated with i.p. doxorubicin (14 mg/kg). Efficacy studies in mice bearing P388 leukemia cells in the peritoneum showed that intratibial MAD11 (50 mg/kg) did not alter the survival of i.p. doxorubicin (16 mg/kg).

Local delivery of anti-drug antibodies was proposed as a supportive therapy to treat severe systemic toxicities arising from chemotherapy in clinical setting. Although locally applied anti-drug antibodies may likely produce reductions in free drug exposure and reductions in local drug toxicities, it may not provide protection against drug toxicities in other tissues. Dose escalation of drug therapy with local delivery of anti-drug antibodies remains to be demonstrated. Concerns related to the stability of the antibody at the site of application, extent of absorption, dose of the antibody required and delivery of the antibody also need to be addressed [72].

Balthasar and coworkers have proposed that systemic anti-drug antibodies could be utilized to produce site-specific alterations in drug disposition, increasing the

ratio of local drug exposure relative to systemic drug exposure [37, 39, 70, 71]. For example, in the treatment of peritoneal tumors, intraperitoneal chemotherapy may be combined with systemic administration of anti-drug antibodies (Figure 2). The presence of anti-drug antibodies in the systemic circulation would lead to rapid binding of drug upon absorption from the peritoneum, thereby reducing systemic exposure to unbound drug, and limiting the distribution of the drug to sites associated with systemic drug toxicities.

Pharmacokinetic studies conducted in rats with i.p. methotrexate and i.v anti-methotrexate Fab fragments (produced from polyclonal rabbit IgG) demonstrated that anti-methotrexate Fab reduced peak free methotrexate plasma concentration and cumulative systemic exposure (AUC) to free methotrexate without significantly altering peritoneal free methotrexate exposure [39]. Toxicity studies were conducted in mice with i.p. methotrexate and i.v. murine monoclonal anti-methotrexate Fab. Methotrexate-induced body weight loss and methotrexate-related mortality were significantly reduced following i.v. anti-methotrexate Fab fragments (550 mg/kg over 72 h infusion) + i.p methotrexate (5 mg/kg over 72 h infusion) compared to administration of i.v. saline (over 72 h infusion) + i.p. methotrexate (5 mg/kg over 72 h infusion) [70]. Further, anti-methotrexate Fab allowed for a 5-fold increase in the maximally tolerated dose of i.p. methotrexate (1.9 mg/kg i.p. methotrexate alone v 10 mg/kg i.p. methotrexate + s.c anti-methotrexate Fab). Preliminary methotrexate efficacy studies in mice bearing peritoneal tumors showed that the percent increase in life span was increased

from 33% following methotrexate (i.p. 1.9 mg/kg, n=9) alone to 100% following anti-methotrexate Fab (s.c.) + methotrexate (i.p. 7.5 mg/kg, n=3) treatment [71].

Limitations and concerns

The use of anti-drug antibodies for optimization of chemotherapy may be limited by (1) the high cost of production and purification of anti-drug antibodies, (2) the safety regarding administration of high doses of antibodies, (3) the immunogenicity of antibodies, (4) the toxicity risks associated with drug-antibody interaction, and (5) the fate of the complex. Poorly potent chemotherapeutic drugs (10 to 100 mg/kg) may require very high doses of antibody to reduce systemic toxicities and to achieve dose escalation. Genetic engineering and protein expression technology may allow for economical and high yield production of antibody and antibody fragments. High doses of Fab fragments (7.5 g/kg in rats and 5.3 g/kg in dogs) were well tolerated in animals [73, 74]. In dogs, administration of 5.3 g/kg of human Fab resulted in transient increase in serum creatinine concentration and urine output [74]. In humans, doses up to 1.6 g of ovine Fab in patients with digoxin poisoning have been tolerated without any adverse effects [5].

Administration of murine monoclonal antibodies has been observed to result in human anti-mouse antibody response. The immunological response may result in severe hypersensitivity reactions and rapid clearance of the antibody from the body. Protein engineering technologies may be applied to develop humanized

antibodies in an effort to minimize human immune response without altering drug binding affinity [75]. Lastly, risks associated with the development of toxicities resultant from drug-antibody complex remains unpredictable and the fate of the drug-antibody complex unknown.

Conclusions

Anti-drug antibodies may alter drug disposition and produce reductions in systemic drug exposure by reducing peak free plasma drug concentrations and cumulative free plasma drug exposure, thereby reducing systemic drug toxicities. However, redistribution of drug due to drug-antibody interaction may alter the time course of drug exposure, and may possibly increase toxicities of chemotherapeutic drugs. The ability of systemic anti-drug antibodies to reduce systemic drug exposure may be applied to selectively enhance drug exposure of intracavitary drug therapy. The effect of anti-drug antibodies on the drug disposition and drug effects may be highly important in the development and evaluation of targeting strategies to improve the safety and efficacy of cancer chemotherapy.

References

1. Sullivan JB, Jr. 1987. Past, present, and future immunotherapy of snake venom poisoning. Ann Emerg Med 16: 938-44.

2. Teng NN, Kaplan HS, Hebert JM, Moore C, Douglas H, Wunderlich A, Braude AI. 1985. Protection against gram-negative bacteremia and endotoxemia with human monoclonal IgM antibodies. Proc Natl Acad Sci U S A 82: 1790-4.

3. Bendtzen K, Hansen MB, Ross C, Svenson M. 1998. High-avidity autoantibodies to cytokines. Immunol Today 19: 209-11.

4. Berkowitz B, Spector S. 1972. Evidence for active immunity to morphine in mice. Science 178: 1290-2.

5. Antman EM, Wenger TL, Butler VP, Jr., Haber E, Smith TW. 1990. Treatment of 150 cases of life-threatening digitalis intoxication with digoxin-specific Fab antibody fragments. Final report of a multicenter study. Circulation 81: 1744-52.

6. Putterman C, Ben-Chetrit E, Caraco Y, Levy M. 1991. Colchicine intoxication: clinical pharmacology, risk factors, features, and management. Semin Arthritis Rheum 21: 143-55.

7. Pentel PR, Keyler DE. 1995. Drug-specific antibodies as antidotes for tricyclic antidepressant overdose. Toxicol Lett 82-83: 801-6.

8. Balsari A, Menard S, Colnaghi MI, Ghione M. 1991. Anti-drug monoclonal antibodies antagonize toxic effect more than anti- tumor activity of doxorubicin. Int J Cancer 47: 889-92.

9. Balsari A, Rumio C, Morelli D, Sfondrini L, Nardini E, Barajon I, Menard S. 2001. Topical administration of a doxorubicin-specific monoclonal antibody prevents drug-induced mouth apoptosis in mice. Br J Cancer 85: 1964-7.

10. Jansman FG, Sleijfer DT, de Graaf JC, Coenen JL, Brouwers JR. 2001. Management of chemotherapy-induced adverse effects in the treatment of colorectal cancer. Drug Saf 24: 353-67.

11. Wojtaszek C. 2000. Management of chemotherapy-induced stomatitis. Clin J Oncol Nurs 4: 263-70.

12. Kintzel PE. 2001. Anticancer drug-induced kidney disorders. Drug Saf 24: 19-38.

13. Gralla RJ. 2002. New agents, new treatment, and antiemetic therapy. Semin Oncol 29: 119-24.

14. Knox JJ, Puodziunas AL, Feld R. 2000. Chemotherapy-induced oral mucositis. Prevention and management. Drugs Aging 17: 257-67.

15. Cebon JS, Morstyn G. 1990. The potential role of granulocyte-macrophage colony stimulating factor (GM-CSF) in cancer chemotherapy. Cancer Surv 9: 131-55.

16. Itri LM. 2002. Managing cancer-related anaemia with epoetin alfa. Nephrol Dial Transplant 17: 73-7.

17. Pentel PR, Brunn GJ, Pond SM, Keyler DE. 1991. Pretreatment with drug-specific antibody reduces desipramine cardiotoxicity in rats. Life Sci 48: 675-83.

18. Brunn GJ, Keyler DE, Ross CA, Pond SM, Pentel PR. 1991. Drug-specific F(ab')2 fragment reduces desipramine cardiotoxicity in rats. Int J Immunopharmacol 13: 841-51.

19. Smith TW, Haber E, Yeatman L, Butler VP, Jr. 1976. Reversal of advanced digoxin intoxication with Fab fragments of digoxin- specific antibodies. N Engl J Med 294: 797-800.

20. Shelver WL, Keyler DE, Lin G, Murtaugh MP, Flickinger MC, Ross CA, Pentel PR. 1996. Effects of recombinant drug-specific single chain antibody Fv fragment on [3H]-desipramine distribution in rats. Biochem Pharmacol 51: 531-7.

21. Pavlinkova G, Beresford GW, Booth BJ, Batra SK, Colcher D. 1999. Pharmacokinetics and biodistribution of engineered single-chain antibody constructs of MAb CC49 in colon carcinoma xenografts. J Nucl Med 40: 1536-46.

22. Bazin-Redureau MI, Renard CB, Scherrmann JM. 1997. Pharmacokinetics of heterologous and homologous immunoglobulin G, F(ab')2 and Fab after intravenous administration in the rat. J Pharm Pharmacol 49: 277-81.

23. Ghetie V, Ward ES. 2002. Transcytosis and catabolism of antibody. Immunol Res 25: 97-113.

24. Haisma HJ, Kessel MA, Silva C, van Muijen M, Roos JC, Bril H, Martens HJ, McCabe R, Boven E. 1990. Human IgM monoclonal antibody 16.88: pharmacokinetics and distribution in mouse and man. Br J Cancer Suppl 10: 40-3.

25. Lin YS, Nguyen C, Mendoza JL, Escandon E, Fei D, Meng YG, Modi NB. 1999. Preclinical pharmacokinetics, interspecies scaling, and tissue distribution of a humanized monoclonal antibody against vascular endothelial growth factor. J Pharmacol Exp Ther 288: 371-8.

26. Sabouraud AE, Urtizberea M, Benmoussa K, Cano NJ, Scherrmann JM. 1992. Fab-bound colchicine appears to adopt Fab fragment disposition in rats. J Pharm Pharmacol 44: 1015-9.

27. Wochner RD, Strober W, Waldmann TA. 1967. The role of the kidney in the catabolism of Bence Jones proteins and immunoglobulin fragments. J Exp Med 126: 207-21.

28. Mitrenga D, Arnold W, Muller O, Mayersbach HV. 1975. The fate of injected human IgG in the mouse liver: Uptake, immunological inactivation, and lysosomal reactions. Cell Tissue Res 156: 359-76.

29. Covell DG, Barbet J, Holton OD, Black CD, Parker RJ, Weinstein JN. 1986. Pharmacokinetics of monoclonal immunoglobulin G1, F(ab')2, and Fab' in mice. Cancer Res 46: 3969-78.

30. Bazin-Redureau M, Pepin S, Hong G, Debray M, Scherrmann JM. 1998. Interspecies scaling of clearance and volume of distribution for horse antivenom F(ab')2. Toxicol Appl Pharmacol 150: 295-300.

31. Grene-Lerouge NA, Bazin-Redureau MI, Debray M, Scherrmann JM. 1996. Interspecies scaling of clearance and volume of distribution for digoxin-specific Fab. Toxicol Appl Pharmacol 138: 84-9.

32. Ober RJ, Radu CG, Ghetie V, Ward ES. 2001. Differences in promiscuity for antibody-FcRn interactions across species: implications for therapeutic antibodies. Int Immunol 13: 1551-9.

33. Rosenblum MG, Murray JL, Stuckey S, Newman RA, Chaney S, Khokhar AR. 1990. Modification of methyliminodiacetato-trans-R,R-1,2-diamminocyclohexane platinum(II) pharmacology using a platinum-specific monoclonal antibody. Cancer Chemother Pharmacol 25: 405-10.

34. Terrien N, Urtizberea M, Scherrmann JM. 1989. Influence of goat colchicine specific antibodies on murine colchicine disposition. Toxicology 59: 11-22.

35. Pentel PR, Keyler DE, Brunn GJ, Milavetz JM, Gilbertson DG, Matta SG, Pond SM. 1991. Redistribution of tricyclic antidepressants in rats using a

drug- specific monoclonal antibody: dose-response relationship. Drug Metab Dispos 19: 24-8.

36. Valentine JL, Owens SM. 1996. Antiphencyclidine monoclonal antibody therapy significantly changes phencyclidine concentrations in brain and other tissues in rats. J Pharmacol Exp Ther 278: 717-24.

37. Balthasar JP, Fung HL. 1994. Utilization of antidrug antibody fragments for the optimization of intraperitoneal drug therapy: studies using digoxin as a model drug. J Pharmacol Exp Ther 268: 734-9.

38. Sabouraud AE, Urtizberea M, Cano NJ, Grandgeorge M, Rouzioux JM, Scherrmann JM. 1992. Colchicine-specific Fab fragments alter colchicine disposition in rabbits. J Pharmacol Exp Ther 260: 1214-9.

39. Balthasar JP, Fung HL. 1996. Inverse targeting of peritoneal tumors: selective alteration of the disposition of methotrexate through the use of anti- methotrexate antibodies and antibody fragments. J Pharm Sci 85: 1035-43.

40. Keyler DE, Le Couteur DG, Pond SM, St Peter JV, Pentel PR. 1995. Effects of specific antibody Fab fragments on desipramine

pharmacokinetics in the rat in vivo and in the isolated, perfused liver. J Pharmacol Exp Ther 272: 1117-23.

41. Aisner J, Van Echo DA, Whitacre M, Wiernik PH. 1982. A phase I trial of continuous infusion VP16-213 (etoposide). Cancer Chemother Pharmacol 7: 157-60.

42. Lokich J, Anderson N. 1997. Dose intensity for bolus versus infusion chemotherapy administration: review of the literature for 27 anti-neoplastic agents. Ann Oncol 8: 15-25.

43. Scherrmann JM, Urtizberea M, Pierson P, Terrien N. 1989. The effect of colchicine-specific active immunization on colchicine toxicity and disposition in the rabbit. Toxicology 56: 213-22.

44. DePalatis LR, Frazier KA, Cheng RC, Kotite NJ. 1995. Lysine reduces renal accumulation of radioactivity associated with injection of the [177Lu]alpha-[2-(4-aminophenyl) ethyl]-1,4,7,10- tetraaza-cyclodecane-1,4,7,10-tetraacetic acid-CC49 Fab radioimmunoconjugate. Cancer Res 55: 5288-95.

45. Pimm MV. 1995. Preventing renal uptake of 111In from labelled monoclonal antibody fragments. Nucl Med Commun 16: 710-1.

46. Behr TM, Becker WS, Sharkey RM, Juweid ME, Dunn RM, Bair HJ, Wolf FG, Goldenberg DM. 1996. Reduction of renal uptake of monoclonal antibody fragments by amino acid infusion. J Nucl Med 37: 829-33.

47. Proksch JW, Gentry WB, Owens SM. 1998. Pharmacokinetic mechanisms for obtaining high renal coelimination of phencyclidine and a monoclonal antiphencyclidine antigen-binding fragment of immunoglobulin G in the rat. J Pharmacol Exp Ther 287: 616-24.

48. Hong G, Bazin-Redureau MI, Scherrmann JM. 1999. Pharmacokinetics and organ distribution of cationized colchicine- specific IgG and Fab fragments in rat. J Pharm Sci 88: 147-53.

49. Fogli S, Danesi R, De Braud F, De Pas T, Curigliano G, Giovannetti G, Del Tacca M. 2001. Drug distribution and pharmacokinetic/pharmacodynamic relationship of paclitaxel and gemcitabine in patients with non-small-cell lung cancer. Ann Oncol 12: 1553-9.

50. Nagai N, Ogata H, Wada Y, Tsujino D, Someya K, Ohno T, Masuhara K, Tanaka Y, Takahashi H, Nagai H, Kato K, Koshiba Y, Igarashi T, Yokoyama A, Kinameri K, Kato T, Kurita Y. 1998. Population pharmacokinetics and pharmacodynamics of cisplatin in patients with

cancer: analysis with the NONMEM program. J Clin Pharmacol 38: 1025-34.

51. Lyass O, Uziely B, Ben-Yosef R, Tzemach D, Heshing NI, Lotem M, Brufman G, Gabizon A. 2000. Correlation of toxicity with pharmacokinetics of pegylated liposomal doxorubicin (Doxil) in metastatic breast carcinoma. Cancer 89: 1037-47.

52. Jodrell DI, Egorin MJ, Canetta RM, Langenberg P, Goldbloom EP, Burroughs JN, Goodlow JL, Tan S, Wiltshaw E. 1992. Relationships between carboplatin exposure and tumor response and toxicity in patients with ovarian cancer. J Clin Oncol 10: 520-8.

53. Zhou H, Choi L, Lau H, Bruntsch U, Vries EE, Eckhardt G, Oosterom AT, Verweij J, Schran H, Barbet N, Linnartz R, Capdeville R. 2000. Population pharmacokinetics/toxicodynamics (PK/TD) relationship of SAM486A in phase I studies in patients with advanced cancers. J Clin Pharmacol 40: 275-83.

54. Ohtsu T, Sasaki Y, Tamura T, Miyata Y, Nakanomyo H, Nishiwaki Y, Saijo N. 1995. Clinical pharmacokinetics and pharmacodynamics of paclitaxel: a 3-hour infusion versus a 24-hour infusion. Clin Cancer Res 1: 599-606.

55. Rowinsky EK, Verweij J. 1997. Review of phase I clinical studies with topotecan. Semin Oncol 24: S20-3-S20-10.

56. Lobo ED, Balthasar JP. 2002. Pharmacokinetic-pharmacodynamic modeling of methotrexate toxicity in mice. J Pharm Pharmcol, for submission Thesis Chapter 3, 71.

57. May LT, Neta R, Moldawer LL, Kenney JS, Patel K, Sehgal PB. 1993. Antibodies chaperone circulating IL-6. Paradoxical effects of anti-IL-6 "neutralizing" antibodies in vivo. J Immunol 151: 3225-36.

58. Finkelman FD, Madden KB, Morris SC, Holmes JM, Boiani N, Katona IM, Maliszewski CR. 1993. Anti-cytokine antibodies as carrier proteins. Prolongation of in vivo effects of exogenous cytokines by injection of cytokine-anti-cytokine antibody complexes. J Immunol 151: 1235-44.

59. Sato TA, Widmer MB, Finkelman FD, Madani H, Jacobs CA, Grabstein KH, Maliszewski CR. 1993. Recombinant soluble murine IL-4 receptor can inhibit or enhance IgE responses in vivo. J Immunol 150: 2717-23.

60. Seifert SA, Boyer LV. 2001. Recurrence phenomena after immunoglobulin therapy for snake envenomations: Part 1. Pharmacokinetics and

pharmacodynamics of immunoglobulin antivenoms and related antibodies. Ann Emerg Med 37: 189-95.

61. Boyer LV, Seifert SA, Cain JS. 2001. Recurrence phenomena after immunoglobulin therapy for snake envenomations: Part 2. Guidelines for clinical management with crotaline Fab antivenom. Ann Emerg Med 37: 196-201.

62. Ujhelyi MR, Robert S, Cummings DM, Colucci RD, Green PJ, Sailstad J, Vlasses PH, Zarowitz BJ. 1993. Influence of digoxin immune Fab therapy and renal dysfunction on the disposition of total and free digoxin. Ann Intern Med 119: 273-7.

63. Ujhelyi MR, Robert S. 1995. Pharmacokinetic aspects of digoxin-specific Fab therapy in the management of digitalis toxicity. Clin Pharmacokinet 28: 483-93.

64. Faulstich H, Kirchner K, Derenzini M. 1988. Strongly enhanced toxicity of the mushroom toxin alpha-amanitin by an amatoxin-specific Fab or monoclonal antibody. Toxicon 26: 491-9.

65. Savaraj N, Allen LM, Sutton C, Troner M. 1980. Immunological modification of adriamycin cardiotoxicity. Res Commun Chem Pathol Pharmacol 29: 549-59.

66. Gutowski MC, Fix DV, Corvalan JR, Johnson DA. 1995. Reduction of toxicity of a vinca alkaloid by an anti-vinca alkaloid antibody. Cancer Invest 13: 370-4.

67. Balsari AL, Morelli D, Menard S, Veronesi U, Colnaghi MI. 1994. Protection against doxorubicin-induced alopecia in rats by liposome-entrapped monoclonal antibodies. Faseb J 8: 226-30.

68. Morelli D, Menard S, Colnaghi MI, Balsari A. 1996. Oral administration of anti-doxorubicin monoclonal antibody prevents chemotherapy-induced gastrointestinal toxicity in mice. Cancer Res 56: 2082-5.

69. Morelli D, Menard S, Cazzaniga S, Colnaghi MI, Balsari A. 1997. Intratibial injection of an anti-doxorubicin monoclonal antibody prevents drug-induced myelotoxicity in mice. Br J Cancer 75: 656-9.

70. Lobo ED, Soda DM, Balthasar JP. 2002. Application of pharmacokinetic-pharmacodynamic modeling to predict the kinetic and dynamic effects of

anti-methotrexate antibodies in mice. J Pharm Exp Ther, for submission Thesis Chapter 4, 108.

71. Lobo ED, Tayab ZR, Balthasar JP. 2002. Utility of anti-methotrexate Fab fragments for the optimization of intraperitoneal methotrexate therapy: Dose escalation and methotrexate efficacy enhancement in a peritoneal model of tumor. J Pharm Exp Ther, for submission Thesis Chapter 5, 149.

72. Reilly RM, Sandhu J, Alvarez-Diez TM, Gallinger S, Kirsh J, Stern H. 1995. Problems of delivery of monoclonal antibodies. Pharmaceutical and pharmacokinetic solutions. Clin Pharmacokinet 28: 126-42.

73. Pentel PR, Keyler DE, Gilbertson DG, Ruth G, Pond SM. 1988. Pharmacokinetics and toxicity of high doses of antibody Fab fragments in rats. Drug Metab Dispos 16: 141-5.

74. Keyler DE, Shelver WL, Landon J, Sidki A, Pentel PR. 1994. Toxicity of high doses of polyclonal drug-specific antibody Fab fragments. Int J Immunopharmacol 16: 1027-34.

75. Winter G, Harris WJ. 1993. Humanized antibodies. Immunol Today 14: 243-6.

76. Gordon MS, Talpaz M, Margolin K, Holmgren E, Sledge GW, Benjamin R, Stalter S, Shak S, Adelman D. 1998. Phase I trial of recombinant humanized monoclonal anti-vascular endothelial growth factor (anti-VEGF Mab) in patients with metastatic cancer. Proc Am Soc Clin Oncol 17: 210a.

77. Schaumann W, Kaufmann B, Neubert P, Smolarz A. 1986. Kinetics of the Fab fragments of digoxin antibodies and of bound digoxin in patients with severe digoxin intoxication. Eur J Clin Pharmacol 30: 527-33.

Captions for Figures

Figure 1. Alteration of the time course of drug plasma exposure by anti-drug Fab. Rabbits were administered 0.1 mg/kg i.v. colchicine over 15 min. After 1.5 h, either anti-colchicine Fab (0.5 molar dose of colchicine) or 0.9% NaCL was infused over 15 min. A. The concentration-time profile of total colchicine. Total colchicine concentrations were increased several fold following anti-colchicine Fab administration. B. The concentration-time profile of free colchicine. Free colchicine concentrations decreased rapidly following anti-colchicine Fab administration. However, after 6 h free colchicine concentrations were higher than those observed with colchicine administration alone [38].

Figure 2. Schematic representation of systemic administration of anti-drug antibodies for optimization of intraperitoneal drug therapy.

Figure 1

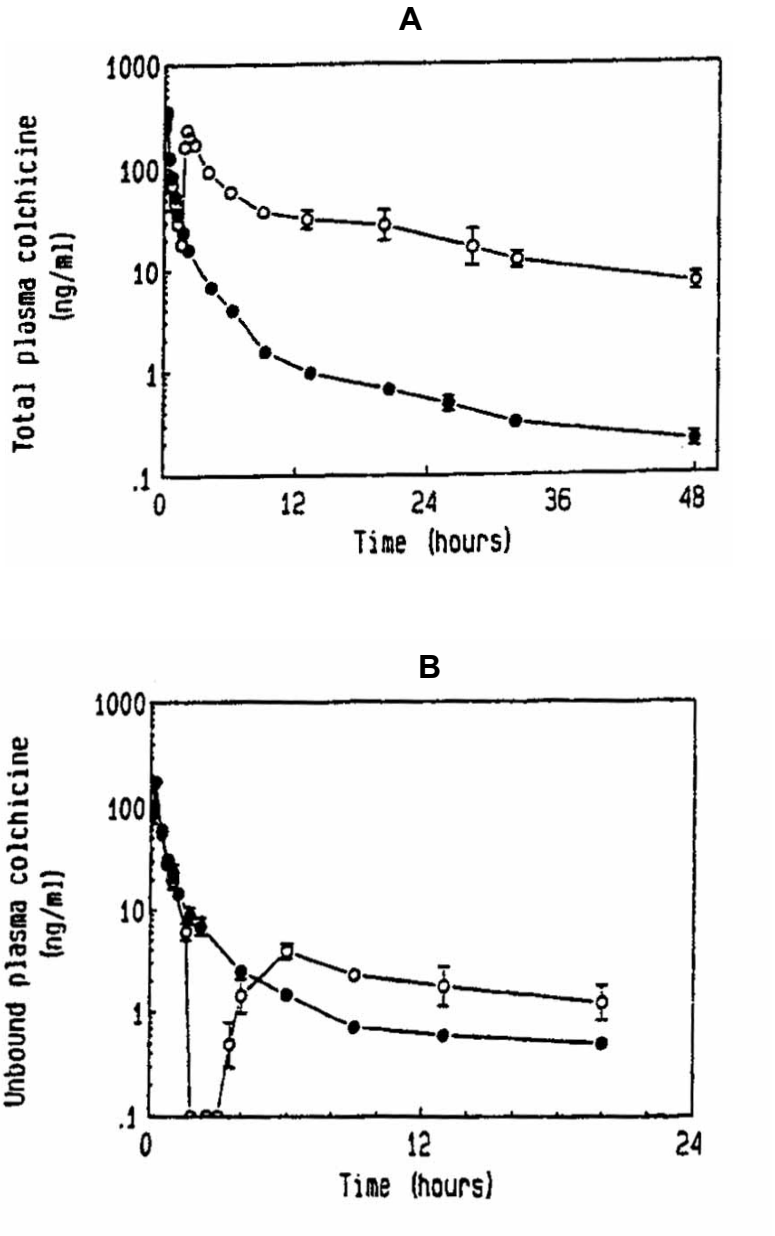
A
Total plasma colchicine (ng/ml)
1000
100
10
1
.1
0
12
24
36
48
Time (hours)
B
Unbound plasma colchicine (ng/ml)
1000
100
10
1
.1
0
12
24
Time (hours)

Figure 2

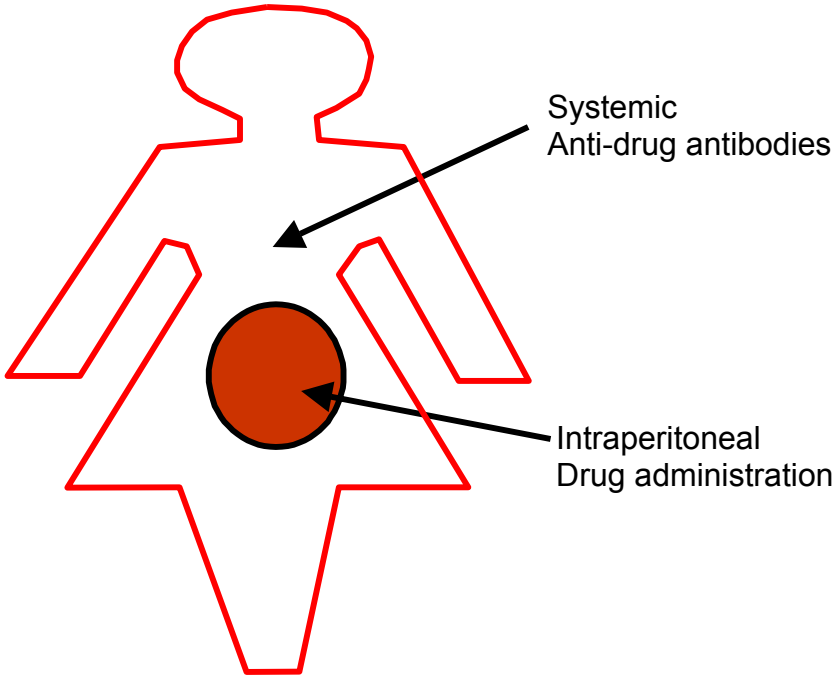
Systemic
Anti-drug antibodies
Intraperitoneal
Drug administration

Table I

Pharmacokinetic parameters for monoclonal mouse antibody in rat[a]

	IgG1	$F(ab)_2$	Fab
$t_{1/2\alpha}$ (h)	8.4 ± 1.2	3.3 ± 0.8	0.89 ± 0.05
$t_{1/2\beta}$ (days)	8.1 ± 0.8	0.7 ± 0.04	0.41 ± 0.03
V_d (ml/kg)	133.9 ± 4.5	124.3 ± 5.2	382 ± 29.6
V_{ss} (ml/kg)	125.0 ± 4.0	90.7 ± 8.5	186.7 ± 23.3
CL (ml/kg/day)	11.6 ± 1.1	123.5 ± 6.8	640 ± 9.6

[a] Rats were administered 0.7 mg/kg i.v dose of mouse monoclonal digoxin specific antibody (n=6) [22]. $t_{1/2\alpha}$, distribution half-life; $t_{1/2\beta}$, elimination half-life; V_d, volume of distribution; V_{ss}, volume of distribution at steady state; CL, total body clearance.

Table II

Pharmacokinetic parameters of species specific IgG1 in rats[a]

	Murine IgG1	Rat IgG1	Human IgG1
$t_{1/2\alpha}$ (h)	8.4 ± 1.2	6.1 ± 0.96	6.8 ± 1.9
$t_{1/2\beta}$ (h)	8.1 ± 0.8	6.1 ± 0.14	5.3 ± 0.6
V_d (ml/kg)	133.9 ± 4.5	141.0 ± 8.8	145.3 ± 14.8
V_{ss} (ml/kg)	125.0 ± 3.9	131.6 ± 7.7	133.6 ± 12.8
CL (ml/kg/day)	11.6 ± 1.1	16.1 ± 1.1	19.1 ± 3.7

[a]An i.v. dose of 0.7 mg/kg of polyclonal human IgG1, monoclonal rat IgG1 and monoclonal mouse IgG1 was administered to the rats (n=6) [22]. $t_{1/2\alpha}$, distribution half-life; $t_{1/2\beta}$, elimination half-life; V_d, volume of distribution; V_{ss}, volume of distribution at steady state; CL, total body clearance.

Table III

Pharmacokinetic parameters of humanized IgG in different species.[a]

	Mouse	Rat	Monkeys	Human
$t_{1/2\alpha}$ (h)	1.2	6.6 ± 1.9	10.6 ± 1.6	-
$t_{1/2\beta}$ (days)	6.8	12.3 ± 3.2	8.6 ± 0.4	17
V_d (ml/kg)	53.0	30.8 ± 2.7	36.0 ± 2.2	-
V_{ss} (ml/kg)	152	79.5 ± 12.0	65.9 ± 6.9	-
CL (ml/kg/day)	15.7	4.8 ± 1.1	5.6 ± 0.5	4.3

[a]Intravenous administration of monoclonal recombinant humanized VEGF IgG at 9.3 mg/kg in mice (n=24) and 10 mg/kg in rats (n=3), monkeys (n=4) [25] and human [76]. Parameters were obtained on non-compartmental analysis of the plasma concentration time data. $t_{1/2\alpha}$, distribution half-life; $t_{1/2\beta}$, elimination half-life; V_d, volume of distribution; V_{ss}, volume of distribution at steady state; CL, total body clearance.

Table IV

Pharmacokinetic parameters of $F(ab)_2$ in different species.[a]

	Mouse	Rat	Rabbit
$t_{1/2\alpha}$ (h)	1.42	2.7 ± 0.3	4.3 ± 1.2
$t_{1/2\beta}$ (h)	13.7	21.7 ± 0.6	61.4 ± 7.0
V_d (ml/kg)	86.4	56.5 ± 5.6	46.6 ± 5.2
V_{ss} (ml/kg)	165.3	116.7 ± 10.6	94.4 ± 7.1
CL (ml/kg/h)	9.5	4.6 ± 0.5	1.2 ± 0.08

[a]Intravenous administration of horse anti-venom $F(ab)_2$ at 10 mg/kg in mice (n=5, pooled samples), rats (n=6), rabbits (n=5) [30]. Parameters were obtained on non-compartmental analysis of the plasma concentration time data. $t_{1/2\alpha}$, distribution half-life; $t_{1/2\beta}$, elimination half-life; V_d, volume of distribution; V_{ss}, volume of distribution at steady state; CL, total body clearance.

Table V

Pharmacokinetic parameters of Fab in different species.[a]

	Mouse	Rat	Rabbit	Human
$t_{1/2\alpha}$ (h)	0.19	0.27 ± 0.02	0.7 ± 0.07	-
$t_{1/2\beta}$ (h)	1.5	3.17 ± 0.22	7.02 ± 0.43	14.0 ± 5.5
V_d (ml/kg)	76.9	68.9 ± 18.6	56.9 ± 2.9	430 ± 120
V_{ss} (ml/kg)	192.3	228.0 ± 75.2	158.4 ± 14.4	-
CL (ml/kg/h)	191.5	103.6 ± 20.0	39.2 ± 4.1	19.4 ± 6.0

[a]Intravenous administration of anti-digoxin Fab (Digidot) of 10 mg/kg in mice (n=5, pooled samples), rats (n=6), rabbits (n=5) [31] and human patients (n=7) [77]. Parameters were obtained on non-compartmental analysis of the plasma concentration time data. $t_{1/2\alpha}$, distribution half-life; $t_{1/2\beta}$, elimination half-life; V_d, volume of distribution; V_{ss}, volume of distribution at steady state; CL, total body clearance.

CHAPTER TWO

Highly sensitive high performance liquid chromatographic assay for methotrexate in the presence and absence of anti-methotrexate antibody fragments in rat and mouse plasma

This chapter has been published in J Chromatogr B Biomed Sci Appl 736 (1999) 191-99.

Abstract

Recently, Balthasar and Fung have proposed that anti-methotrexate antibody fragments may be employed to enhance the selectivity of intraperitoneal methotrexate (MTX) therapy. This current work presents a sensitive high performance liquid chromatographic method for measuring plasma concentrations of total (i.e., bound and unbound) MTX and free (unbound) MTX in rat and mouse plasma, in the presence or absence of therapeutic anti-MTX antibody fragments. The assay involves pre-column derivatization of MTX by sodium hydrosulfite to 2,4-diamino-6-methylpteridine. The limit of quantitation for MTX by this assay was 1.25 ng in rat plasma, mouse plasma, and mouse plasma ultrafiltrate, which corresponds to a concentration of 25 ng/ml for a 50 µl sample. The limit of quantitation was found to be 2.5 ng in rat plasma ultrafiltrate (i.e., 50 ng/ml in 50 µl rat plasma ultrafiltrate). The method was shown to be quite accurate, as the mean assayed concentration of quality control samples was within 10% of theoretical values. We have applied the method to the investigation of MTX pharmacokinetics in mice and rats, following the administration of MTX alone or following simultaneous administration of MTX and anti-MTX Fab fragments (AMF). The method has been shown to be suitable for the assay of total and free MTX in the plasma of these species and will enable the testing of pharmacokinetic hypotheses regarding the influence of AMF on the disposition of MTX.

Keywords : Methotrexate, pharmacokinetics, anti-MTX Fab fragment, antibody

1. Introduction

Traditional drug targeting approaches attempt to enhance the selectivity of drug action by increasing the efficiency of drug delivery to desired sites of drug activity. Conversely, inverse targeting strategies attempt to increase selectivity by reducing the efficiency of drug delivery to sites associated with drug toxicities. Recently, Balthasar and Fung have demonstrated the utility of anti-MTX antibodies and antibody fragments in an inverse targeting strategy designed to enhance the pharmacokinetic selectivity of intraperitoneal MTX therapy for peritoneal tumors [1]. Their inverse targeting approach calls for simultaneous intravenous administration of anti-MTX antibodies and intraperitoneal administration of MTX. The presence of anti-MTX antibodies in systemic circulation leads to a rapid complexation of MTX diffusing out of the peritoneum and entering the blood. However, the large molecular weight of the anti-MTX antibodies limits their rate of entry into the peritoneal cavity; consequently, this strategy produces regiospecific alterations in MTX binding. This selective alteration of drug binding has been shown to produce dramatic, regiospecific alterations in the pharmacokinetics of the target drug. Specifically, it has been shown that systemic administration of anti-MTX antibodies may decrease maximal free MTX plasma concentrations and also decrease the cumulative systemic exposure to free MTX, while not altering peritoneal exposure to free MTX. Consequently, this combined therapy has been shown to increase the pharmacokinetic selectivity of intraperitoneal chemotherapy by decreasing the

fraction of drug available for distribution to sites associated with systemic toxicities.

These preliminary studies have suggested that therapeutic benefits may result from the proposed inverse targeting strategy; however, many questions remain regarding proposed pharmacokinetic and therapeutic hypotheses. Testing proposed pharmacokinetic hypotheses requires the availability of a sensitive assay capable of accurately quantifying both total and unbound concentrations of MTX in plasma. Preliminary studies had been conducted with the use of radio-labeled MTX [1]; however, administration of radio-labeled drug to animals is inconvenient, expensive, and raises safety concerns. Consequently, we had hoped to identify a suitable MTX assay for use in our pharmacokinetic investigations.

Numerous methods for MTX analysis have been reported in the literature. These include HPLC analysis with ultraviolet detection [2-6] and fluorescence detection [7-10], radioimmunoassay [11-14], dihydrofolate reductase inhibition assay [15], enzyme-multiplied immunoassay [16], fluorescence polarization immunoassay [17], enzyme immunoassay [18], and capillary zone electrophoresis with laser induced fluorescence detection [19]. For our purposes, HPLC approaches provide the greatest compromise between sensitivity, selectivity, assay time and assay expense.

The most sensitive HPLC assays have employed either pre-column [7, 8] or post-column derivatization [20-23] of MTX coupled with fluorescence detection. However, no HPLC assay has been validated for application to the quantitation of ng/ml concentrations of MTX in rat and mouse plasma. Moreover, no HPLC assay has been shown to be capable of accurately measuring total and unbound MTX concentrations in the presence of therapeutic anti-MTX antibodies. Consequently, we have attempted to modify existing assays for these applications.

In our search to find a sensitive HPLC assay that could detect MTX both in plasma and plasma ultrafiltrate, we found that the assay reported by Deen et al. appeared most useful [8]. This HPLC assay involved pre-column derivatization of MTX, followed by fluorescence detection. The method reported a limit of detection of 2.3 ng/ml for MTX starting with 1.0 ml of human plasma. Although this method was not as sensitive as some of the post-column derivatization assays reported [21], it was simple and could be implemented with standard HPLC equipment. Unfortunately, when we applied the method to the analysis of MTX in rat plasma we observed lower sensitivity compared to results reported by Deen et al. [8], inconsistent recoveries and high variability. We have, however, successfully adapted the method of Deen et al. for our purposes.

In this paper, we describe a simple and convenient HPLC procedure that allows the determination of MTX in the presence and absence of anti-MTX antibody.

The method utilizes pre-column derivatization of MTX by sodium hydrosulfite to a fluorescent derivative 2,4-diamino-6-methylpteridine as reported previously [8]. The assay was validated for its reproducibility and accuracy over a concentration range of 25 - 500 ng/ml. The limit of quantitation for MTX by this assay was 1.25 ng in rat plasma, mouse plasma, and mouse plasma ultrafiltrate, and 2.5 ng in rat plasma ultrafiltrate.

2. Experimental

2.1 Chemicals & Reagents

Methotrexate (>98% pure, HPLC), folic acid (approximately 98% pure), and sodium hydrosulfite were purchased from Sigma (St Louis, MO, USA). Methanol was HPLC grade and all other chemicals were analytical grade. Anti-MTX Fab fragments were produced in our laboratory and characterized as previously described [24].

2.2 Chromatographic instrumentation and system

The HPLC system consisted of Waters (Milford, MA) components, including a Novopak® C18 column (150 x 3.9 mm), a model 515 pump, a model 474 scanning fluorescence detector and a model 717 autosampler. Waters Millenium32 software was used for instrument control, data acquisition and processing.

The mobile phase comprised of 0.1 M Tris (trishydroxymethylaminomethane) buffer (pH 7.0) and methanol (9:1), and was filtered (0.45 µm pore size) and

degassed prior to use. A constant mobile phase flow rate of 1 ml/min was used for separation. The fluorescence detector was set at excitation and emission wavelengths of 367 nm and 463 nm, respectively.

2.3 Sample preparation

2.3.1 Standards and Quality Control Samples.

Stock solutions of MTX (50 µg/ml) and folic acid (50 µg/ml) were prepared in distilled water and stored at 4ºC. Working standards were prepared in the concentration range of 15.6-500 ng/ml with phosphate buffered saline (PBS, pH 7.4). Folic acid at 1.0 or 5.0 µg/ml was used as an internal standard. Quality control samples (QCs) for MTX were prepared by spiking rat / mouse plasma with appropriate amounts of MTX. QCs for AMF containing MTX were prepared by spiking plasma containing 20% AMF with MTX. Filtered rat / mouse plasma was obtained by ultrafiltration in Centrifree tubes (30,000 MW cutoff, YM membrane; Amicon, Beverly, MA) at 25ºC at 1000 *g* for 30 min.

2.3.2 Derivatization

a. For total MTX in rat plasma

Reduction of MTX was carried out in glass vials. A reaction solution was prepared containing 100 µl plasma (blank rat plasma in case of standards), 25 µl of folic acid (1.0 µg/ml), 100 µl of PBS (containing MTX in case of standards), 100 µl of 2 M sodium acetate / 5 M acetic acid buffer (pH 6.0), 50 µl of freshly prepared sodium hydrosulfite (10 mg/ml) solution. The solution was heated at

92ºC for 20 min. The solution was then cooled to room temperature, centrifuged at 200 *g* for 2 min. 175 µl of the supernatant was injected on the column.

b. For total MTX in mouse plasma

Reduction of MTX was carried out as above with slight modification. A solution was prepared to contain 50 µl plasma (blank mouse plasma in case of standards), 25 µl of folic acid (5.0 µg/ml), 100 µl of PBS (containing MTX in case of standards), 75 µl of 2 M sodium acetate / 5 M acetic acid buffer (pH 6.0) and 50 µl of freshly prepared sodium hydrosulfite solution (10 mg/ml). The solution was heated at 92ºC for 30 min. The solution was cooled, centrifuged, and 200 µl of the supernatant was injected on the column.

c. For free MTX in rat / mouse plasma

Starting with 50 µl of ultrafiltrate rat / mouse plasma, the procedure for sample preparation was the same as described in for total MTX in mouse plasma.

2.4 Assay Validation

Assay validation was performed by assessing the intra- and inter-day accuracy and precision in quantifying MTX in QCs. Intra-day variability was assessed through the analysis of QCs in triplicate, and inter-day variability was determined through the analyses of QCs on 3 different days. Accuracy was determined by calculating the concentration present using standard curve and comparing it to known (spiked) concentrations. The limit of quantitation was defined as the MTX concentration in the lowest QC yielding an intra-assay coefficient of variation less

than 10% and producing a mean assayed concentration within 10% of the theoretical concentration.

2.5 MTX Pharmacokinetics in mice

An i.p. bolus of 10 mg/kg MTX in sterile saline solution was administered to a group of 3 male Swiss-Webster mice. Blood samples (20-60 µl) were obtained from the saphenous vein at 15, 30, 60, 120, 180, 240 min. Plasma was separated from blood samples via centrifugation at approximately 10,000 *g* for 2 min. Samples were diluted, if appropriate, and analyzed for MTX concentration.

2.6 MTX pharmacokinetics in absence and presence of anti-MTX Fab in the rat

An abdominal aortal cannula was inserted into two female Sprague-Dawley rats (225-250 g) under ketamine (50 mg/kg, Fort Dodge Laboratories, Fort Dodge, IA) and xylazine (10 mg/kg, Miles, Shawne Mission, KA) anesthesia. MTX, 2.0 µmol/kg (909 µg/kg) in sterile saline, was administered as an intraarterial (i.a.) bolus, followed with continuous i.a. infusion of sterile saline over 6 h. Blood samples (0.1 - 0.3 ml) were drawn from the aortal cannula at 15, 30, 60, 90, 120 min and placed in heparinized microcentrifuge tubes. After centrifugation, aliquots of plasma were analyzed for total MTX concentration. Analysis of MTX in the presence of AMF was demonstrated by administering continuous i.a. infusion of 0.4 µmol/kg AMF for 6 h with an i.a. bolus of MTX (2.0 µmol/kg) at 4 h of the infusion. Free MTX concentration was determined following ultrafiltration of 100 µl of plasma at 1000 *g* $\times$ 30 min in Centrifree tubes at 25°C.

3. Results and discussion

3.1 Development of the assay

Deen et al. introduced a sensitive HPLC method for the analysis of MTX in human plasma which included a pre-column reduction of MTX to a fluorescent product [8]. However, when we applied this procedure to small volumes of rat and mouse plasma, we observed high variability and lower sensitivity than that reported by Deen et al. The authors used 70% perchloric acid to deproteinate the plasma samples, and then added NaOAc / NaOH buffer to neutralize samples to pH 5.6-6.0 prior to derivatization. Also, Deen et al. reported that the derivatization reaction was highly pH dependent, with a reaction maximum near pH 6.0 [8]. Preliminary studies in PBS confirmed this observation (data not shown). However, we found that we could reduce assay variability by eliminating the acidification and neutralization steps. In rat plasma, maximum MTX response was achieved near pH 5.0 as shown in Fig. 1. In addition, we found that we could reduce assay variability by lowering the reaction temperature from 100ºC to 92ºC and increasing the reaction time from 15 to 30 min (Fig. 2). The original method used mobile phase of 0.005 M tetrabutylammonium phoshate in water with 25% methanol at 1.4 ml/min; however, we found that we could reduce the assay run-time while maintaining resolution by using a methanol / Tris buffer (pH: 7.0) mobile phase at a flow rate of 1 ml/min. This modification reduced the run-time from approximately 15 min (as reported by Deen et al.) to approximately 8 min.

It was interesting to find that the authors reported higher fluorescence response (4 times) in PBS as compared to plasma; in our hands, we observed a greater slope in the linear relationship between detector response and MTX concentration in plasma samples relative to PBS samples (plasma slope = 0.0085, r^2 = 0.992; PBS slope = 0.0052, r^2 = 0.948). We then proceeded to investigate the effect of protein and plasma on the fluorescence response from MTX samples. The slope of the standard curves increased in the order of bovine serum albumin 3.1% > bovine serum albumin 6.7% > rat plasma. Assay response was shown to be dependent on the inclusion of plasma and on the concentration of bovine serum albumin added to the reaction mixture. Therefore, we decided to use standards containing rat plasma to analyze MTX in rat plasma and standards containing mouse plasma to analyze MTX in mouse plasma. Standards containing plasma ultrafiltrate produced poor correlations between concentration and response. However, we found that we could stabilize the reaction and improve assay response through the addition of rat or mouse plasma to the reaction mixture. Fig. 3 shows typical chromatograms obtained from HPLC analysis of mouse and rat plasma containing MTX. Retention times were approximately 3 and 7 min for folic acid (the internal standard) and MTX, respectively. There was no interference from either reaction products or endogenous substances.

Although the majority of MTX is eliminated unchanged in man and in rodents, pharmacokinetic investigations conducted in these species have demonstrated

that a fraction of MTX is metabolized to 7-hydroxymethotrexate and 2,4-diamino-N^{10}-methyl-pteroic acid. For example, following high-dose MTX therapy in man, approximately 70-94% of the dose is recovered as the parent compound, 0.4-11% as 7-hydroxymethotrexate, and 0.01% as 2,4-diamino-N^{10}-methylpteroic acid [25]. Following MTX doses of 4-10 mg/kg in rats, about 80-90% of the dose was eliminated as the parent compound and approximately 10% was metabolized to 7-hydroxymethotrexate [26,27]. Unfortunately, 7-hydroxy methotrexate is not commercially available and, consequently, we were unable to assess assay selectivity in samples containing both MTX and 7-hydroxymethotrexate. However, Bremnes et al. have found that the concentrations of the major MTX metabolite, 7-hydroxymethotrexate, are only 1-10% of the concentrations of parent drug following a 10 mg/kg iv bolus dose in rats [26]. Consequently, in spite of our inability to assure assay selectivity, we do not expect significant interference from MTX metabolites in our proposed preclinical investigations.

3.2 Validation of the assay

Calibration curves were linear over the concentration range of 15.6 to 500 ng/ml in mouse and rat plasma (typically, r^2 values were greater than 0.995). The intra-day and inter-day coefficient of variation for total MTX in rat plasma was less than 8%, and less than 9% for mouse plasma (Tables I, II). For free MTX in rat and mouse plasma ultrafiltrate, coefficients of variation were less than 11% (Table III). The recoveries of free and total MTX from spiked rat and mouse

plasma were within 10% of theoretical values. The limit of quantitation for MTX by this assay was 1.25 ng in rat plasma, mouse plasma, and mouse plasma ultrafiltrate, which corresponds to a concentration of 25 ng/ml for a 50 µl sample. The limit of quantitation was found to be 2.5 ng in rat plasma ultrafiltrate (i.e., 50 ng/ml in 50 µl rat plasma ultrafiltrate).

3.3 Pharmacokinetics in mice

The MTX concentration time profile following an i.p. bolus of 10 mg/kg MTX in Swiss Webster mice is shown in Fig. 4. The data was fitted to a two compartment model using the Scientist program (Micromath, Salt Lake City, UT). The fitted parameters were clearance (2.22 ± 0.22 l/kg/h) and volume of distribution (0.80 ± 0.53 l/kg). The half life of MTX in these mice was found to be 36.8 ± 7.6 min. These values are very similar to those reported by Osman et al. for i.p. bolus of 50 mg/kg in female Swiss albino mice with clearance at 1.85 ± 0.07 l/kg/h, volume of distribution of 1.28 ± 0.14 l/kg and half life of 28.4 ± 2.4 min [28].

3.4 Pharmacokinetics in rats

The concentration time profile of MTX after i.a. administration of 2.0 µmol/kg (909 µg/kg) is shown in Fig. 5. Fitting the data to a two compartment model resulted in clearance value of 1.0 l/kg/h, volume of distribution in the central compartment of 0.41 l/kg and half life of 28 min. These values compare well with those reported by Slordal et al. in male Wistar rats at a dose of 1.0 mg/kg with clearance of 1.16 ± 0.14 l/kg/h, central volume of distribution of 0.26 ± 0.04 l/kg and half life of 25.6

± 3.0 min [29]. The disposition of MTX following continuous i.a. infusion of AMF and bolus MTX is shown in Fig. 5. Non-compartmental fitting of the data gave a clearance value of 0.32 l/kg/h. The low clearance of MTX in the presence of AMF is due to the slow elimination of MTX bound to the antibody. With MTX administration alone, the free MTX fraction at 2 h was 88% while in presence of the antibody free MTX fraction was less than 1%. This is in agreement with our hypothesis that circulating anti-MTX antibody will reduce the free fraction of MTX in the systemic circulation.

4. Conclusion

In this paper, we have presented a sensitive and validated HPLC method to analyze total and free MTX in rat and mouse plasma in the presence and absence of anti-MTX antibody fragments. This is the only HPLC assay, to our knowledge, that is capable of measuring both free and total MTX in rat and mouse plasma. The assay will enable the testing our pharmacokinetic hypotheses regarding the influence of AMF on the disposition of MTX in these species.

Acknowledgements

This work was supported through a Faculty Development Grant from the Parental Drug Association and through a New Investigator Grant from the American Association of Colleges of Pharmacy, both awarded to JPB.

References

1. J.P. Balthasar, H.L. Fung, J. Pharm. Sci. 85 (1996) 1035.
2. C.P. Collier, S.M. MacLeod, S.J. Soldin, Ther. Drug. Monit. 4 (1982) 371.
3. D.A. Cairnes, W.E. Evans, J. Chromatogr. 231 (1982) 103.
4. N. So, D.P. Chandra, I.S. Alexander, V.J. Webster, D.W. O'Gorman Hughes, J. Chromatogr. 337 (1985) 81.
5. H.N. Alkaysi, A.M. Gharaibeh, M.A. Salem, Ther. Drug. Monit. 12 (1990) 191.
6. S. Belz, C. Frickel, C. Wolfrom, H. Nau, G. Henze, J. Chromatogr. B Biomed. Appl. 661 (1994) 109.
7. J.A. Nelson, B.A. Harris, W.J. Decker, D. Farquhar, Cancer Res. 37 (1977) 3970.
8. W.M. Deen, P.F. Levy, J. Wei, R.D. Partridge, Anal. Biochem. 114 (1981) 355.
9. J. Salamoun, J. Frantisek, J. Chromatogr. 378 (1986) 173.
10. J. Salamoun, M. Smrz, F. Kiss, A. Salamounova, J. Chromatogr. 419 (1987) 213.
11. C. Bohuon, F. Duprey, C. Boudene, Clin. Chim. Acta. 57 (1974) 263.
12. V. Raso, R. Schreiber, Cancer Res. 35 (1975) 1407.
13. J.W. Paxton, F.J. Rowell, Clin. Chim. Acta. 80 (1977) 563.
14. T. Anzai, N. Jaffe, Y.M. Wang, J. Chromatogr. 415 (1987) 445.
15. L.C. Falk, D.R. Clark, S.M. Kalman, T.F. Long, Clin. Chem. 22 (1976) 785.

16. P.R. Finley, R.J. Williams, F. Griffith, D.A. Lichti, Clin. Chem. 26 (1980) 341.

17. L. Slordal, P.S. Prytz, I. Pettersen, J. Aarbakke, Ther. Drug. Monit. 8 (1986) 368.

18. R.G. Buice, W.E. Evans, J. Karas, C.A. Nicholas, P. Sidhu, A.B. Straughn, M.C. Meyer, W.R. Crom, Clin. Chem. 26 (1980) 1902.

19. M.C. Roach, P. Gozel, R.N. Zare, J. Chromatogr. 426 (1988) 129.

20. O. Beck, P. Seideman, M. Wennberg, C. Peterson, Ther. Drug. Monit. 13 (1991) 528.

21. G. Lu, H.W. Jun, J. Liquid Chromatogr. 18 (1995) 155.

22. F. Albertioni, B. Pettersson, O. Beck, C. Rask, P. Seideman, C. Peterson, J. Chromatogr. B Biomed. Appl. 665 (1995) 163.

23. E.A. McCrudden, S.E. Tett, J. Chromatogr. B. 721 (1999) 87.

24. J.P. Balthasar, H.L. Fung, J. Pharm. Sci. 84 (1995) 2.

25. H. Breithaupt, K. E., Cancer Treat. Rep. 66 (1982) 1733.

26. R.M. Bremnes, L. Slordal, E. Wist, J. Aarbakke, Cancer Res. 49 (1989) 2460.

27. L. Fahrig, H. Brasch, H. Iven, Cancer Chemother. Pharmacol. 23 (1989) 156.

28. A.M. Osman, S.F. Saad, S.Y. Saad, A.B. El-Aaser, M.M. El-Merzabani, Chemotherapy. 40 (1994) 227.

29. L. Slordal, R. Jaeger, J. Kjaeve, J. Aarbakke, Pharmacol. Toxicol. 63 (1988) 81.

TABLE I : Accuracy and precision for MTX in rat plasma

A. Total MTX in presence of AMF

Intra-day Variability

QC (ng/ml)	Mean Assay Response	SD	% CV	% Recovery
500	508.5	8.7	1.7	101.7
250	267.2	6.4	2.4	106.9
100	102.9	5.4	5.2	102.9
25	26.7	2.1	7.9	106.9

Inter-day Variability

QC (ng/ml)	Mean Assay Response	SD	% CV	% Recovery
500	515.5	9.4	1.8	103.1
250	267.7	19.4	7.2	107.1
100	98.3	2.7	2.7	98.3
25	25.3	1.4	5.7	101.1

B. Total MTX in the absence of AMF

Intra-day Variability

QC (ng/ml)	Mean Assay Response	SD	% CV	% Recovery
500	508.5	8.7	1.7	101.7
100	102.9	5.4	5.2	102.9
25	26.7	2.1	7.9	106.9

Inter-day Variability

QC (ng/ml)	Mean Assay Response	SD	% CV	% Recovery
500	515.5	9.4	1.8	103.1
100	98.3	2.7	2.7	98.3
25	25.3	1.4	5.7	101.1

TABLE II : Accuracy and precision for MTX in mouse plasma.

A. Total MTX in presence of AMF

Intra-day Variability

QC (ng/ml)	Mean Assay Response	SD	% CV	% Recovery
250	251.2	18.5	7.4	100.5
50	50.9	4.5	8.9	101.9
25	24.5	1.3	5.4	98.0

Inter-day Variability

QC (ng/ml)	Mean Assay Response	SD	% CV	% Recovery
250	270.9	13.9	5.2	108.4
50	54.9	0.5	0.9	109.9
25	26.3	1.6	6.0	105.2

B. Total MTX in absence of AMF

Intra-day Variability

QC (ng/ml)	Mean Assay Response	SD	% CV	% Recovery
250	262.3	13.9	5.3	104.9
100	100.4	2.5	2.5	100.4
25	26.0	1.9	7.5	104.0

Inter-day Variability

QC (ng/ml)	Mean Assay Response	SD	% CV	% Recovery
250	259.0	10.5	4.1	103.6
100	97.9	2.7	2.8	97.9
25	26.4	1.2	4.7	105.8

TABLE III : Accuracy and precision for free MTX

A. In rat plasma

Intra-day Variability

QC (ng/ml)	Mean Assay Response	SD	% CV	% Recovery
500	549.4	5.2	0.9	109.9
100	107.8	2.5	2.3	107.8
50	54.9	1.1	2.0	109.7

Inter-day Variability

QC (ng/ml)	Mean Assay Response	SD	% CV	% Recovery
500	548.5	28.6	5.2	109.7
100	109.8	1.3	1.2	109.8
50	52.9	2.3	4.3	105.9

B. In mouse plasma

Intra-day Variability

QC (ng/ml)	Mean Assay Response	SD	% CV	% Recovery
250	272.6	12.7	4.7	109.0
100	101.1	4.7	4.6	101.1
25	26.4	0.9	3.3	105.5

Inter-day Variability

QC (ng/ml)	Mean Assay Response	SD	% CV	% Recovery
250	260.9	26.5	10.2	104.3
100	97.9	7.4	7.6	97.9
25	26.2	0.8	2.9	104.6

CAPTIONS FOR FIGURES

Fig. 1. The effect of pH on the derivatization reaction was investigated by assessing detector response from rat plasma samples containing MTX (100 ng/ml). Reaction solutions were buffered to pH 4, 5, 6, 7, or 7.6 (n=3).

Fig. 2. The effect of reaction time on the completeness and variability of the derivatization reaction was investigated by assessing detector response from rat plasma samples containing MTX (100 ng/ml). The derivatization reaction was allowed to proceed for 10, 20, 30, or 45 min (n=3). The 30 minute reaction time provided the most desirable combination of response magnitude and variability for our purposes.

Fig. 3. Typical chromatograms obtained from the analysis of (a) 'blank' mouse plasma; (b) mouse plasma (obtained during a pharmacokinetic experiment) containing methotrexate at an assayed concentration of 33.2 ng/ml; (c) 'blank' rat plasma; and (d) rat plasma (obtained during a pharmacokinetic experiment) containing methotrexate at an assayed concentration of 20.6 ng/ml.

Fig. 4. MTX concentration time profile in mice following an i.p. bolus of 10 mg/kg; n=3. Data was fitted to two compartment mammillary model using Scientist program.

Fig. 5. MTX concentration time profile in rat with continuous i.a. infusion of anti-MTX Fab fragment over 6 h and i.a. bolus of 2.0 μmol/kg MTX. The fit concentration time profile is shown as the smooth line, while observed concentrations are represented as closed circles (total MTX concentration, following MTX administered alone), open circles (free MTX concentration, following MTX administered alone), and closed triangles (total MTX concentration, following AMF and MTX administration).

Fig. 1

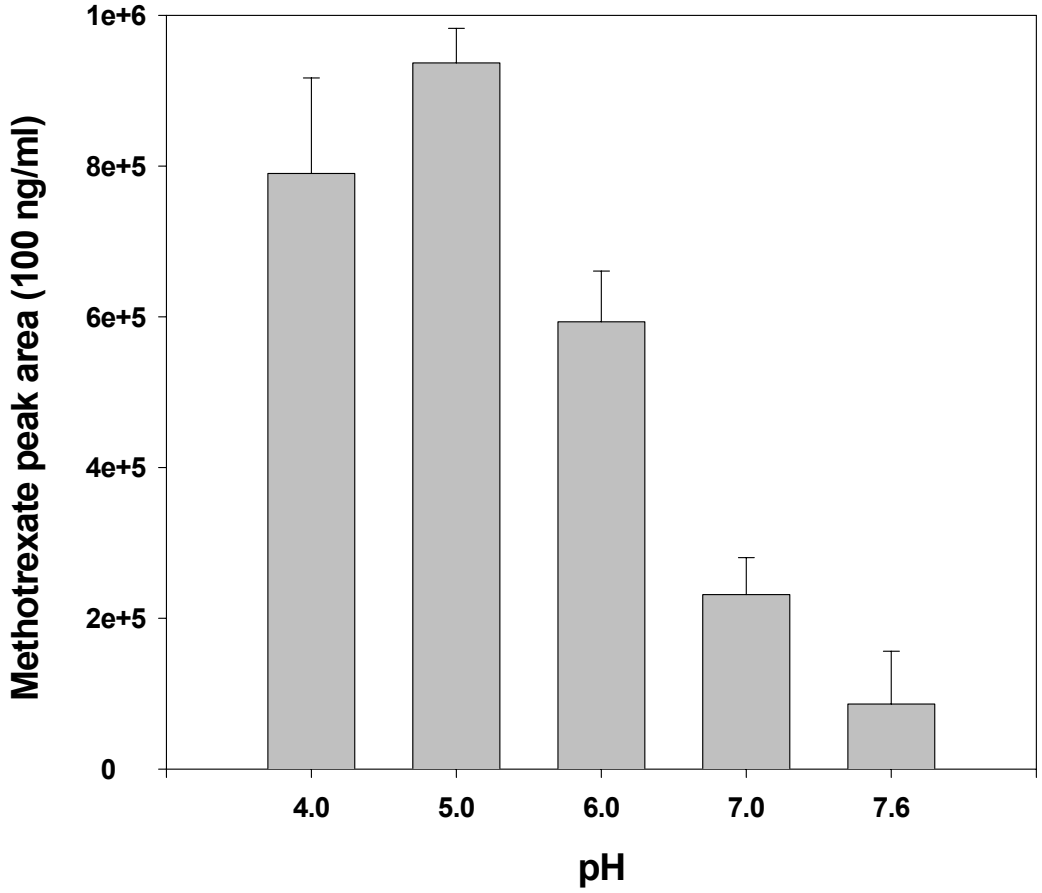
Methotrexate peak area (100 ng/ml)
1e+6
8e+5
6e+5
4e+5
2e+5
0
4.0
5.0
6.0
7.0
7.6
pH

Fig. 2

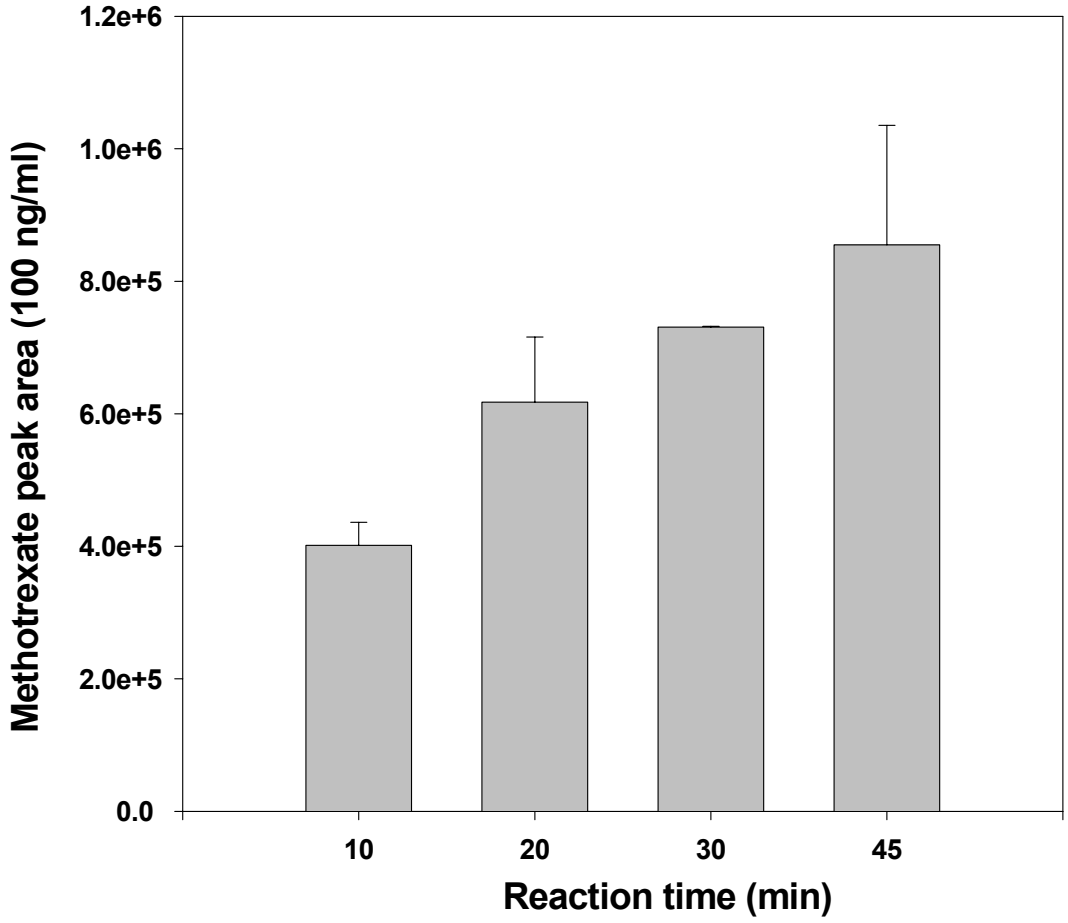
1.2e+6
1.0e+6
8.0e+5
6.0e+5
4.0e+5
2.0e+5
0.0
Methotrexate peak area (100 ng/ml)
10
20
30
45
Reaction time (min)

Fig. 3

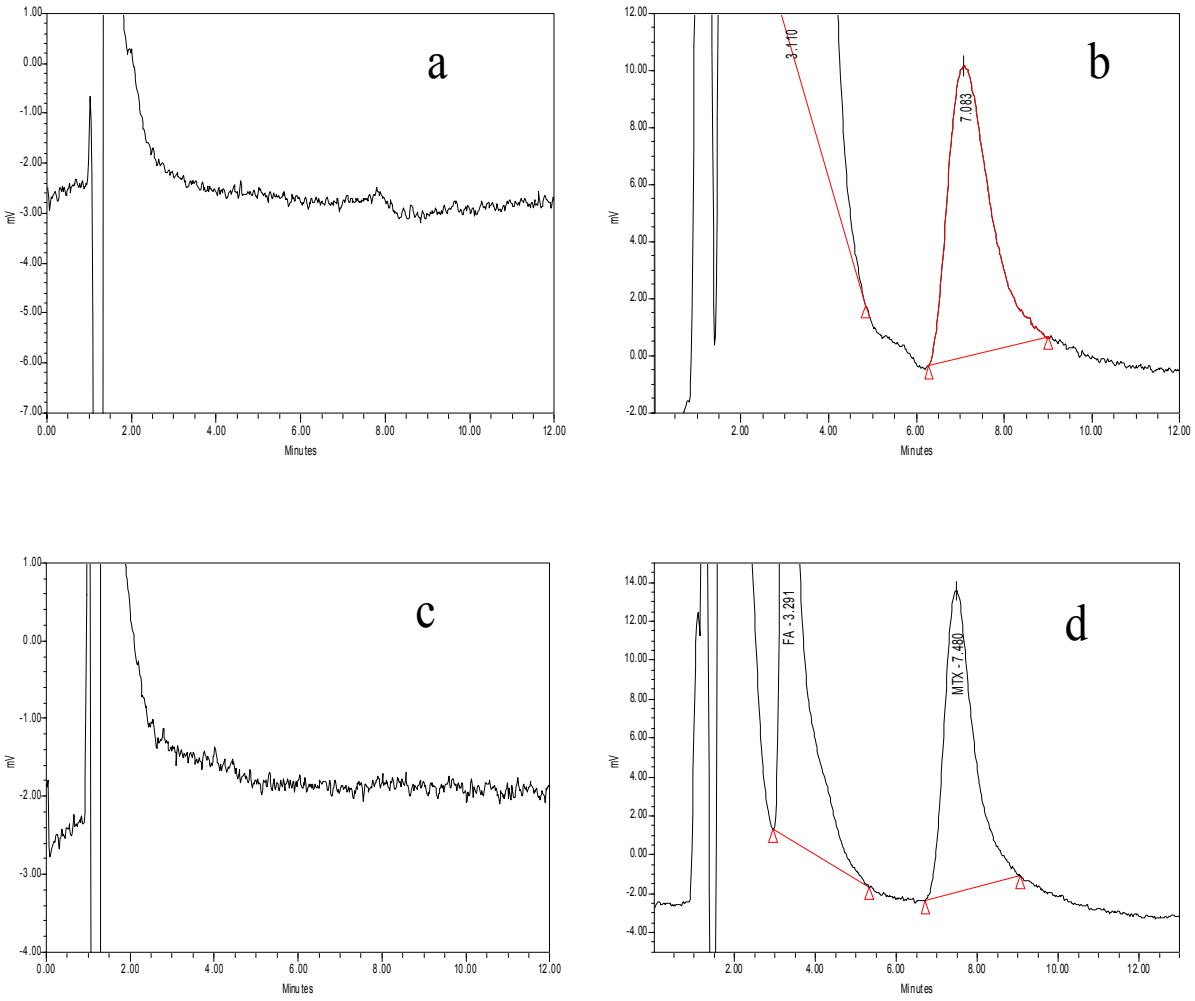

Fig. 4

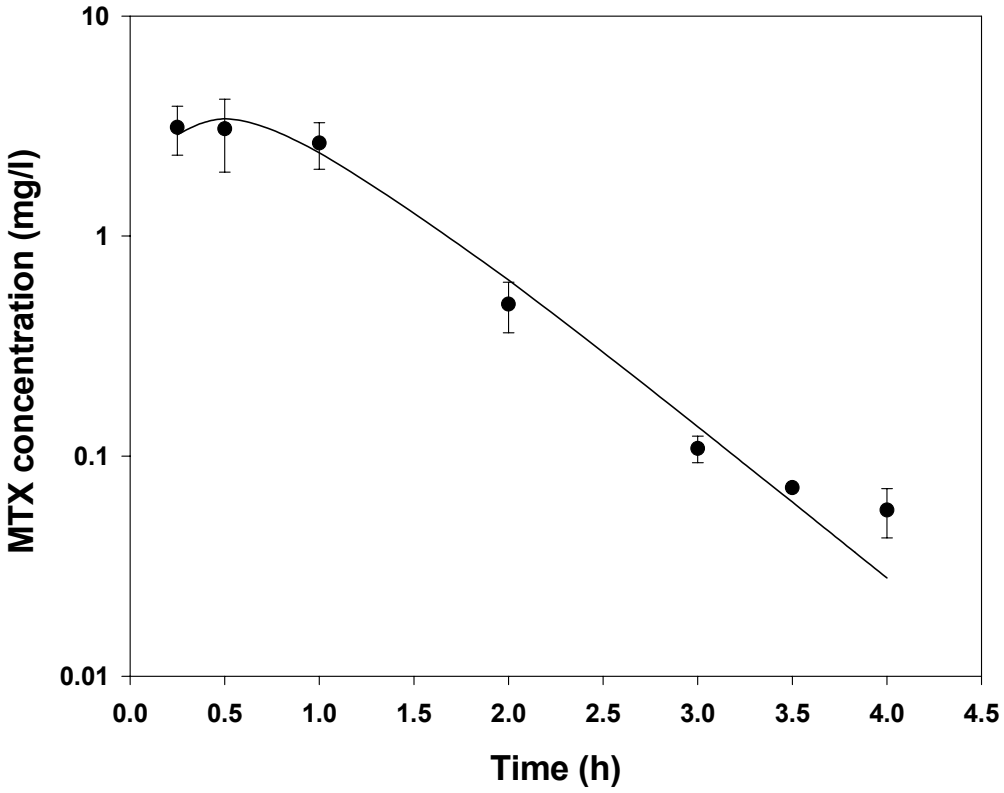
10
1
0.1
0.01
MTX concentration (mg/l)
0.0
0.5
1.0
1.5
2.0
2.5
3.0
3.5
4.0
4.5
Time (h)

Fig. 5

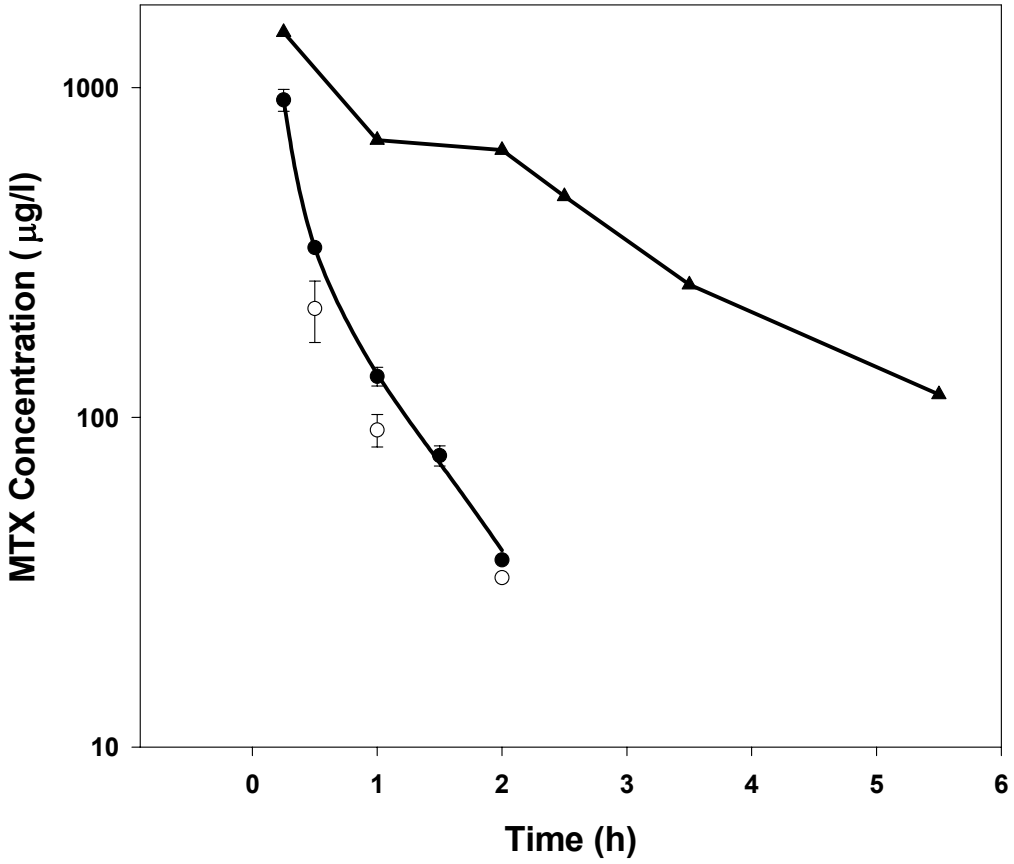

CHAPTER THREE

Pharmacokinetic pharmacodynamic modeling of methotrexate toxicity in mice

ABSTRACT

The prediction of chemotherapeutic efficacy is complicated by 'protocol dependencies' in dose-effect and dose-toxicity relationships. It has been proposed that pharmacokinetic-pharmacodynamic (PKPD) mathematical models may allow characterization of chemotherapeutic protocol dependencies, and may facilitate the prediction of chemotherapeutic efficacy; however, few demonstrations exist in the literature. The present study examines the pharmacokinetics and toxicodynamics of methotrexate (MTX), a commonly used anti-cancer agent, following intraperitoneal administration to mice. MTX was administered via bolus or infusion (24h, 72h and 168h), at doses of 2.5–1000 mg/kg. MTX plasma and peritoneal pharmacokinetics were characterized through standard non-compartmental and compartmental techniques. Body weight loss was utilized as a measure of MTX-induced toxicity. We found that MTX pharmacokinetics were independent of dose (over a range of 3 – 600 mg/kg) and independent of dosing mode (i.e., i.p. bolus v. i.p. infusion). However, MTX-induced toxicity was shown to be highly dependent on the dosing protocol employed. For example, the maximally tolerated dose (MTD, i.e., the dose related to a mean body weight loss of 10%) was 200-fold greater following bolus administration relative to that observed for 72h infusion (760 mg/kg vs. 3.8 mg/kg). This profound protocol dependence in the relationship between MTX-induced toxicity and MTX exposure was characterized through the use of a new time-dissociated PKPD model (median prediction error: 3.9 %). In future studies, this model will be employed to

predict effects of anti-MTX antibody therapy on MTX toxicity, in a drug targeting strategy designed to improve the therapeutic selectivity of i.p. chemotherapy.

We are investigating a drug targeting strategy that attempts to optimize the intraperitoneal chemotherapy of peritoneal tumors (Balthasar and Fung, 1994; Balthasar and Fung, 1996). Our approach combines peritoneal drug administration with systemic (i.e., intravenous or intraarterial) administration of anti-drug antibodies (ADAb). We hypothesize that the presence of ADAb in the systemic circulation will lead to a rapid complexation of drug diffusing out of the peritoneum and entering the blood, reducing peak plasma free (unbound) drug concentrations and reducing the extravascular distribution of the chemotherapeutic. In addition, we have hypothesized that ADAb may allow reductions in the cumulative systemic exposure to free drug through elimination of the drug as the drug-antibody complex. We consider our approach to be an 'inverse targeting strategy' in that the intent is to increase the selectivity of drug therapy by decreasing the efficiency of drug delivery to sites associated with drug toxicities (i.e. as opposed to 'traditional targeting strategies' which attempt to increase the efficiency of drug delivery to sites associated with desired effects).

By reducing the delivery of drug to sites associated with systemic toxicity, we envision that our targeting strategy will allow dramatic increases in the MTD of chemotherapeutics, and thereby permit a large increase in peritoneal drug exposure. In earlier work, we tested our pharmacokinetic hypotheses using MTX as a model drug. Preliminary studies demonstrated that simultaneous peritoneal administration of MTX and systemic administration of anti-MTX antibodies (AMAb), (i.e. anti-MTX IgG and anti-MTX Fab) reduced peak plasma

concentrations of free MTX and decreased the systemic exposure to free drug, without altering peritoneal exposure (Balthasar and Fung, 1996). The pharmacokinetic results also indicated that anti-MTX Fab therapy limited the extravascular distribution of MTX, enhanced urinary elimination of MTX, and reduced cumulative systemic exposure to free (unbound) MTX.

These studies demonstrated that AMAb could reduce MTX systemic exposure, and consequently, it was envisioned that AMAb might decrease systemic toxicity resultant from i.p. MTX. However, we also observed that administration of AMAb altered the time course of MTX exposure, dramatically increasing the terminal half-life of MTX in rats. We feel that this finding is very significant, as chemotherapeutics often show a time-course dependency between chemotherapeutic exposure and toxicity. For example, preclinical and clinical studies of numerous cell cycle phase specific chemotherapeutics (e.g., arabinosyl cytosine, gemcitabine, topotecan, paclitaxel, methotrexate, etoposide) have shown that toxicity is dependent not only on the cumulative exposure (dose or AUC) but also on the duration of exposure (Braakhuis et al., 1995; Frei et al., 1969; Hutchison et al., 1971; Kohler and Goldspiel, 1994; Rowinsky and Verweij, 1997; Slevin et al., 1989). Although there has been no systematic study of the relationship of the time-course of MTX exposure to the degree of resultant toxicity, available literature data suggests that the cytotoxic effects of MTX are highly dependent on the time course of exposure, such that toxicity is increased with increases in the duration of drug administration (Goldie et al., 1972). We

were concerned that the beneficial reductions in cumulative systemic exposure allowed by AMAb would be offset by increases in the duration of MTX exposure.

Given the observed effects of AMAb on the time course of MTX disposition, and the likelihood of time-course dependencies in the relationships of MTX exposure and toxicity, we concluded that a systematic investigation of these relationships was essential to our efforts to develop our inverse targeting strategy. In this report, we present investigations of the relationship between MTX administration and MTX-induced weight loss in mice, investigations of protocol dependencies in MTX pharmacokinetics, and the mathematical modeling of the time course of MTX exposure to MTX-induced toxicity. The PKPD model for MTX-induced toxicity will be utilized in future experiments to evaluate the potential of AMAb to reduce MTX toxicity.

METHODS

Materials

MTX (>99.9% purity), folic acid (approximately 98.0% purity), sodium hydrosulfite and xylazine were obtained from Sigma (St Louis, MO). All solvents and chemicals used were of analytical grade. ALZET® micro-osmotic pumps 2001D, 1003D and 2007D were obtained from Alza Corporation (Palo Alto, CA). Pharmacokinetic and toxicity studies were conducted using 5-6 week-old (20-25 g) Swiss Webster male mice (Harlan Sprague-Dawley, Inc., Indianapolis, IN).

The animals were housed on a standard light-dark cycle, with continuous access to food and water.

HPLC Assay for MTX

MTX was analyzed by an HPLC assay utilizing pre-column derivatization and fluorescence detection, as previously reported (Lobo and Balthasar, 1999). Briefly, a solution of 50 μl of mouse plasma containing MTX, 25 μl of folic acid (5000 ng/ml, internal standard), 100 μl of phosphate saline buffer (pH 7.4), 75 μl of sodium acetate/acetic acid (2M/5M) buffer (pH 6.0) and 50 μl of freshly prepared sodium hydrosulfite solution (10 mg/ml) was heated to 92ºC for 30 min. Standard curves were prepared from blank mouse plasma and phosphate saline buffer containing known concentrations of MTX (15.6 to 500 ng/ml). After cooling, the samples were centrifuged at 5000 *g* for 4 min. The supernatant solution (200 μl) was injected on the column and analyzed with a fluorescence detector. The limit of quantitation for MTX was 1.25 ng (25 ng/ml).

MTX Pharmacokinetics

The pharmacokinetics of MTX were investigated following four i.p. administration protocols: (a) constant-rate infusion of 0.2 mg/kg/h (3 mg/kg), (b) constant-rate infusion of 1.0 mg/kg/h (12 mg/kg), (c) bolus injection of 10 mg/kg, and (d) bolus injection of 600 mg/kg.

Constant-rate i.p. infusions of MTX in sterile 0.9% sodium chloride were administered to 4-8 mice with the osmotic pumps. Pumps were equilibrated in sterile 0.9% sodium chloride for 4 h at 37ºC before implantation. The osmotic pumps were placed subcutaneously on the dorsal surface near the shoulder blade under ketamine (100 mg/kg, Fort Dodge Laboratories, Fort Dodge, IA) and xylazine (10 mg/kg) anesthesia. Cannulas were tunneled subcutaneously and inserted into the peritoneal cavity through a small opening made in the abdominal muscle. The abdominal opening was then sealed with glue and the abdominal skin was closed with sterile surgical sutures. Blood samples were either collected from the saphenous vein (10-40 μl) or the jugular vein (0.5-1.0 ml) at the end of the infusion (12-15 h). Peritoneal samples were collected immediately after the animals were sacrificed. Both plasma and peritoneal samples were analyzed for MTX concentration with the HPLC assay.

Bolus i.p. doses of 10 mg/kg and 600 mg/kg MTX in 1.0 ml sterile 0.9% sodium chloride were administered to two groups of 3 mice. Serial blood samples (10-60 μl) were withdrawn from the saphenous vein at 15, 30, 60, 120, 180 and 240 min. Plasma samples were obtained after centrifugation at 10,000 *g* for 2 min. When necessary, samples were diluted with blank mouse plasma prior to assay.

The peritoneal clearance, CL_d, was calculated using the following relationship $R = \frac{C_p}{C_{ss}} = 1 + \frac{CL}{CL_d}$, where C_p is the steady state concentration of MTX in the peritoneum, C_{ss} is the systemic steady state plasma concentration of MTX, CL

represents systemic clearance and CL_d is peritoneal clearance (Dedrick, 1986). Systemic clearance was calculated as the ratio of the infusion rate to the steady state MTX plasma concentration or as the quotient of the dose administered and the area under the concentration time curve, for data obtained following MTX administration by constant-rate i.p. infusion and by i.p. bolus, respectively. Additionally, MTX plasma concentration data were fitted to a one-compartment mammillary model with ADAPT II software (D'Argenio and Schumitzky, 1997).

Toxicity Studies

Four i.p. administration protocols were investigated: (a) bolus, (b) 24 h constant-rate infusion, (c) 72 h constant-rate infusion (d) 168 h constant-rate infusion. The MTD was defined as the dose that caused a mean 10% body weight loss relative to the saline-treated controls. Each dose was tested in a group of 5 mice. Constant-rate infusions of MTX in sterile 0.9% sodium chloride were delivered by micro-osmotic pumps, as described in the pharmacokinetic studies. The doses of MTX investigated for MTD determination were (a) bolus: 250 mg/kg, 500 mg/kg and 1000 mg/kg, (b) 24 h constant-rate infusion: 5 mg/kg, 10 mg/kg, 25 mg/kg and 50 mg/kg (c) 72 h constant-rate infusion: 2.5 mg/kg, 5 mg/kg and 10 mg/kg, (b) 168 h constant-rate infusion: 5 mg/kg, 6.5 mg/kg and 7.5 mg/kg. The body weight of the mice was monitored daily. Control animals implanted with osmotic pumps experienced body weight loss after surgery. The 24 h and 168 h osmotic pumps were of larger size (1.1 g) than the 72 h osmotic pumps (0.5 g). The mean percent nadir body weight loss in 24 h infusion controls (10.8 ± 4.5%) and 168 h

(9.2 ± 4.2%) infusion controls was observed to be greater than in 72 h infusion controls (4.4 ± 1.7%). The total body weight loss in MTX treated animal was a sum of surgery-related weight loss and MTX-induced weight loss. The nadir body weight loss for each MTX treated animal was estimated as, MTX treated nadir body weight loss - control mean nadir body weight loss. In cases where no weight loss was observed, a value of zero was used for determining the average percent weight loss for the group. In cases where death occurred, weight loss was defined as the maximal percent weight loss of the expired animal. The MTD was determined by linear interpolation between administered doses.

PKPD Modeling

Three time-dissociated models, based on those proposed by Karlsson et al., were evaluated to characterize the relationship between the time course of MTX plasma concentration and the mean percent nadir body weight loss (Karlsson et al., 1998). In the time-dissociated model paradigm, drug concentration is related to an unobserved 'direct effect', and the time-integral of this 'direct effect' is related to the observed effect. The general time-dissociated model can be described as follows,

$$E_{dir} = \frac{E_{max} C(t)^{\gamma_1}}{EC_{50}{}^{\gamma_1} + C(t)^{\gamma_1}}$$

$$E_{obs} = \int_0^{\infty} E_{dir} dt = \int_0^{\infty} \frac{E_{max} C(t)^{\gamma_1}}{EC_{50}{}^{\gamma_1} + C(t)^{\gamma_1}} dt$$

where E_{dir} is the 'direct effect' related to drug concentration, C(t) is the drug concentration at time t, E_{obs} is the observed or measured effect, E_{max}, maximal

direct (or unobserved) effect, $EC_{50,}$ is the drug concentration causing 50% of the maximal direct effect and γ describes the steepness of the relationship between drug concentration and direct effect.

In our application of this modeling strategy, the mean percent nadir weight loss was set as the 'observed effect'. Model 1, with three fit parameters, utilized a simple sigmoidal relationship between MTX plasma concentration and the unobserved effect. The basic time-dissociated model was further modified to allow complete characterization of the toxicity data. Model 2 and Model 3 included a second sigmoidal term, with 5 and 6 parameters, respectively. The time course of plasma MTX exposure following i.p. administration was related to the mean percent nadir body weight loss.

Model 1

$$\% \text{ Nadir body weight loss} = \int_0^{\infty} \frac{E_{max} M(t)^{\gamma_1}}{EC_{50}{}^{\gamma_1} + M(t)^{\gamma_1}} dt$$

Model 2

$$\% \text{ Nadir body weight loss} = \int_0^{\infty} \left(\frac{E_{max} M(t)^{\gamma_1}}{EC1_{50}{}^{\gamma_1} + M(t)^{\gamma_1}} + \frac{E_{max} M(t)^{\gamma_2}}{EC2_{50}{}^{\gamma_2} + M(t)^{\gamma_2}} \right) dt$$

Model 3

$$\% \text{ Nadir body weight loss} = \int_0^{\infty} \left(\frac{E1 M(t)^{\gamma_1}}{EC1_{50}{}^{\gamma_1} + M(t)^{\gamma_1}} + \frac{E2 M(t)^{\gamma_2}}{EC2_{50}{}^{\gamma_2} + M(t)^{\gamma_2}} \right) dt$$

where M(t) is MTX plasma concentration at time t; E_{max}, E1, E2 are the maximal direct effect produced with MTX; EC_{50}, $EC1_{50}$, $EC2_{50}$, are MTX concentration

causing 50% of the maximal direct effect; and γ_1 and γ_2 relate the steepness of the relationship between MTX concentration and direct effect.

Doses that caused 100% mortality or no weight loss were not included in the evaluation of the models. Mean nadir body weight loss data from nine MTX doses were fitted simultaneously. Models were evaluated based on their Akiake Information Criterion, and median prediction error. Prediction error was calculated as |mean observed percent nadir weight loss - predicted percent nadir weight loss|/ mean observed percent nadir weight loss $\times$ 100). Pharmacokinetic parameters were obtained from the pharmacokinetic studies and were fixed during fitting. The pharmacokinetic model predicted the time course of plasma MTX concentration following i.p. MTX dose. ADAPT II software was utilized for model development and evaluation. The software was unable to solve the differential equations for all doses simultaneously unless the exponents γ_1, and γ_2 were fixed as integers.

RESULTS

MTX Pharmacokinetics

Results of the non-compartmental analysis of MTX pharmacokinetics are summarized in Table 1. Systemic clearances following MTX administration at: 3 mg/kg, 10 mg/kg, 12 mg/kg, and 600 mg/kg were compared and were not found to be statistically different ($p>0.05$). Mean systemic clearance was calculated to be 2.4 ± 0.4 l/kg/h, and the mean half-life of MTX was found to be 33.8 ± 6.5 min.

Fig. 1. presents MTX concentration-time data following i.p bolus administration of 10 mg/kg and 600 mg/kg and following i.p. constant-rate infusion of 3 mg/kg and 12 mg/kg. Mean concentration data were fitted simultaneously to a one-compartment mammillary model with first-order (peritoneal) absorption. The data were weighted by 1/variance using ADAPT II software. Estimated parameters were the first order absorption constant, ka = 4.5 ± 1.5 h^{-1}, systemic clearance, CL = 2.9 ± 0.2 l/kg/h, and volume of distribution, Vd = 2.2 ± 0.2 l/kg.

MTX Toxicity

The time courses of MTX induced body weight loss are shown in Fig. 2. The data demonstrated a time delay between MTX plasma exposure and the time of nadir body weight. Within a given administration protocol, there appeared to be a rightward shift in the time to reach peak effect (i.e. nadir body weight) with increasing MTX dose. The nadir percent weight loss observed for all doses tested are presented in Table 2. Dose-dependent increases in body weight loss were observed for each administration protocol. Interestingly, the MTD showed profound dependence on the administration protocol (Fig. 3), ranging from 760 mg/kg (bolus administration) to 3.8 mg/kg bolus (72 h infusion).

PKPD Modeling

Each time-dissociated model allowed simultaneous fitting of all data. Model 3 demonstrated the lowest AIC values and the lowest median percent prediction error, and was therefore concluded to be superior to Model 1 and Model 2 (Table

3). Model 3 predictions of the nadir percent weight loss are shown in Fig. 4. Fit values of the pharmacodynamic parameters were γ_1 = 4, γ_2 = 2, $EC1_{50}$ = 0.022 mg/l (CV% = 2.7), $EC2_{50}$ = 130.9 mg/l (CV% = 9.2), $E1_{max}$ = 0.41 (CV% = 3.2), and $E2_{max}$ = 8.6 (CV% = 7.2).

DISCUSSION

The outgrowth of peritoneal micrometastates often occurs in the course of ovarian, colo-rectal, and gastro-intestinal cancer (Cintron and Pearl, 1996; Markman et al., 1993; Patel and Benjamin, 2000). In most cases, chemotherapy of these tumors is not curative, as systemic toxicity prevents the administration of sufficient quantities of drug to eradicate the diseased cells (Howell et al., 1984; Speyer et al., 1990). Intraperitoneal chemotherapy has been predicted to allow increases in the ratio of peritoneal : systemic drug exposure (Dedrick et al., 1978), and has been investigated for utility in improving the therapeutic selectivity of the chemotherapy of peritoneal tumors (Alberts et al., 1996). Unfortunately, for most patients, systemic toxicity continues to be dose limiting, and only modest therapeutic benefit is provided by the increased peritoneal drug exposure provided by ‘standard’ i.p. chemotherapy (Gadducci et al., 2000).

We have proposed a drug targeting strategy that attempts to optimize i.p. chemotherapy by decreasing the efficiency of drug delivery to sites associated with systemic toxicity (Balthasar and Fung, 1994; Balthasar and Fung, 1996). Our approach, which combines peritoneal chemotherapy with simultaneous

systemic administration of ADAb, allows reductions in systemic concentrations of unbound drug (fCmax, peak unbound plasma drug concentration and fAUC, area under the unbound plasma drug concentration). In most cases, it is expected that drug binding to ADAb will lead to an increase in the plasma half-life of the target drug, and consequently, extend the duration of chemotherapeutic exposure. This phenomenon, which has been observed with our model drug, MTX, is of significance as effects and toxicities are dependent on the time course of MTX exposure. As such, AMAb-mediated extension in duration of MTX exposure could potentially lead to increased systemic toxicity (i.e., as opposed to the desired reduction in systemic toxicity). No systematic study had been previously conducted to investigate protocol-dependencies in MTX pharmacokinetics and pharmacodynamics; consequently, the impact of AMAb on MTX toxicity could not be predicted.

Pharmacokinetic investigations in the present study assessed MTX disposition following MTX administration via i.p. bolus injection, and by i.p. infusion, at doses ranging from 3 – 600 mg/kg. Non-compartmental analyses of the plasma concentration data showed no statistically significant differences in MTX clearance in this dose range. Mean clearance was found to be 2.4 $\pm$ 0.4 l/kg/h with a half-life of 33.8 $\pm$ 6.5 min. These results are consistent with reports of linear MTX pharmacokinetics in CD4 male mice following constant-rate subcutaneous infusions for 10 h to 48 h in the dose range of 125 μg/kg to 240 mg/kg (Pinedo et al., 1976). Our estimated values for clearance and half-life are similar to those reported in female Swiss albino mice (clearance: 1.85 $\pm$ 0.07

l/kg/h, half life: 28.4 ± 2.4 min) following an i.p. bolus of 50 mg/kg (Osman et al., 1994). In our study, the mean peritoneal MTX concentration to plasma MTX concentration ratio (R) was 75, which is similar to the value reported for humans (R = 92, peak peritoneal concentration : peak plasma concentration) (Markman et al, 1993).

Investigations of MTX pharmacodynamics in mice have shown that the intestinal epithelium is more sensitive to MTX than the bone marrow tissue (Zaharko et al., 1974), and that MTX damage to the intestinal epithelium leads to malabsorption and reductions in body weight (Nakamaru et al., 1998). Therefore, in our toxicity studies, we measured changes in body weight to assess the degree of MTX-induced toxicity in mice. Four intraperitoneal administration protocols were investigated: bolus, 24 h constant-rate infusion, 72 h constant-rate infusion and 168 h constant-rate infusion. For each administration protocol, we observed dose dependent increases in body weight loss, steep dose-toxicity relationships, substantial delays between the time-course of drug administration and the time-course of MTX-induced weight-loss, and dose-dependent increases in the time associated with nadir body weight. This study also demonstrated that relationships between MTX dose and toxicity are highly dependent on the time course of drug administration; the dose associated with 10% nadir body weight loss (i.e., the MTD) differed tremendously for the tested administration protocols (Fig. 3), ranging from 760 mg/kg (following bolus administration) to 3.8 mg/kg (following 72 h constant-rate infusion).

Our pharmacodynamic findings may be explained based on the known pharmacology of MTX. The tremendous differences observed in MTD between the bolus protocol and the infusion protocols may be due to saturable cellular uptake of MTX via the reduced-folate transporter (Goldman et al., 1968), saturable generation of active poly-glutamated metabolites of MTX (Poser et al., 1981), or the cell-cycle phase specific nature of MTX cytotoxicity (Hryniuk et al., 1969). Each of these factors would be expected to lead to an increase in the degree of cytotoxicity with increases in duration of exposure, for a given AUC.

A primary goal of the present study was to develop an integrated PKPD model to facilitate predictions of MTX toxicity following alterations in MTX exposure (e.g., as expected following anti-MTX antibody therapy). The simplest models used to characterize chemotherapeutic effects relate chemotherapeutic endpoints (e.g., nadir white cell count, tumor response rate) to time-averaged parameters of drug exposure (e.g. C_{ave}, C_{ss}, AUC) or to time above a threshold concentration (Gianni et al., 1995; Jodrell et al., 1992; Karlsson et al., 1995). These models have been successfully applied for characterizing PKPD relationships for several chemotherapeutics (Galpin and Evans, 1993); however, such models would not be useful for our data, as we have found no unique relationship between MTX toxicity and systemic AUC, C_{ss}, or duration above a threshold concentration.

Time-delays in the development of effects have been predominantly characterized through the use of ‘effect-site’ models (Segre, 1968; Sheiner et al.,

1979) or through ‘indirect response models’ (Dayneka et al., 1993; Jusko and Ko, 1994). The effect-site model assumes first-order distribution of the drug from the central compartment to the effect site and first order elimination of drug from the effect site. Consequently, peak drug concentrations in the effect-site are predicted to occur at the same time, regardless of the dose administered. A direct relationship is assumed between drug concentration in the effect-site compartment and the effect produced; thus, peak effects are predicted to occur at the same time, regardless of increasing doses. Our data clearly showed a shift in the time to reach nadir body weight loss with increasing MTX doses, within each administration protocol. For example, following 168 h constant-rate infusion, the time for nadir body weight loss occurred at 144 h, 192 h, and 216 h at 5 mg/kg, 6.5 mg/kg and 7.5 mg/kg, respectively. Thus, the effect-site model predicted a time-course of MTX toxicity that was not consistent with our data.

Indirect response models have been applied successfully to characterize chemotherapeutic toxicity (Friberg et al., 2000; Minami et al., 1998; Minami et al., 2001). Given the indirect nature of MTX effects, it was reasonable to attempt to fit our data to mechanistically - relevant indirect effect models. Several indirect response models were evaluated (data not shown). These models were able to fit some individual data well, but numerical integration errors prevented ADAPT II from simultaneously fitting all of the data sets.

Due to difficulties associated with the development of a model capable of characterizing the time course of MTX-induced toxicity, we proceeded to relate the time course of MTX exposure to the peak MTX effect (i.e., mean body weight loss at nadir) using derivatives of the time-dissociated model presented by Karlsson et al. (Karlsson et al, 1998). Pharmacokinetic parameters for MTX were obtained from fitting the bolus and infusion data with a linear one-compartment model with first order absorption from the peritoneum. The time course of MTX concentration was related to the unobserved, direct effect (E_{dir}) with a sigmoid E_{max} relationship. The time-dissociated models were shown to provide accurate, simultaneous fitting of our data, with the superior model (Model 3) showing a median prediction error of 3.9%. This robust model is expected to allow prediction of MTX toxicity following alterations of MTX disposition resultant from AMAb therapy.

There are only a handful of reports of modeling chemotherapeutic toxicity following different administration protocols. For example, Zhou et al. conducted population PKPD analyses of data from a phase 1 clinical study, and related neutrophil nadir count to AUC with an inhibitory Emax model following drug administration via continuous infusion for 3 – 120 h (Zhou et al., 2000). In this work, protocol dependency was not an issue, as a unique relationship between AUC and effect was identified. Gianni et al. and Ohtsu et al. characterized paclitaxel-induced myelosuppression following 3 h and 24 h paclitaxel infusions with a sigmoid Emax model relating the duration above a threshold concentration

(0.05 μM) to the percent decrease in neutrophil or granulocyte count (Gianni et al, 1995; Ohtsu et al., 1995). Goh et al. developed a population pharmacodynamic model to characterize the protocol-dependent hematological toxicity of rhizoxin following administration by continuous infusion for 3 h, 8 h, 24 h, 48 h, or 72 h protocols. In this study, pharmacokinetic data were neither collected nor modeled; consequently, the modeling approach developed may have little utility in cases where pharmacokinetic variability contributes substantially to variability in drug response (Goh et al., 2000). Lastly, Karlsson et al. introduced a general time-dissociated PKPD model to characterize the paclitaxel toxicity following continuous infusions of 3 h and 24 h (Karlsson et al, 1998). In this work, a single set of parameters was determined to relate drug administration to the survival fraction of neutrophils at nadir.

In this report, we have investigated the protocol dependence of MTX pharmacokinetics and toxicity. We found no protocol dependencies in MTX pharmacokinetics, and profound protocol dependencies in MTX dose – toxicity relationships. A PKPD model was developed to relate the entire time course of drug exposure to nadir weight-loss following different administration protocols. The present model will be of great value for our work, in that it allows the prediction of optimal AMAb dosing strategies to reduce 'peak' systemic toxicity (i.e., nadir body weight loss). Future work will present the simulations of AMAb effects, and in vivo experiments providing further validation of the PKPD model.

REFERENCES:

Alberts DS, Liu PY, Hannigan EV, R OT, Williams SD, Young JA, Franklin EW, Clarke Pearson DL, Malviya VK and DuBeshter B (1996) Intraperitoneal cisplatin plus intravenous cyclophosphamide versus intravenous cisplatin plus intravenous cyclophosphamide for stage III ovarian cancer [see comments]. *N Engl J Med* **335**:1950-1955.

Balthasar JP and Fung HL (1994) Utilization of antidrug antibody fragments for the optimization of intraperitoneal drug therapy: studies using digoxin as a model drug. *J Pharmacol Exp Ther* **268**:734-739.

Balthasar JP and Fung HL (1996) Inverse targeting of peritoneal tumors: selective alteration of the disposition of methotrexate through the use of anti-methotrexate antibodies and antibody fragments. *J Pharm Sci* **85**:1035-1043.

Braakhuis BJ, Ruiz van Haperen VW, Boven E, Veerman G and Peters GJ (1995) Schedule-dependent antitumor effect of gemcitabine in in vivo model system. *Semin Oncol* **22**:42-46.

Cintron JR and Pearl RK (1996) Colorectal cancer and peritoneal carcinomatosis. *Semin Surg Oncol* **12**:267-278.

D'Argenio DZ and Schumitzky A (1997): ADAPT II User's Guide: Pharmacokinetic/Pharmacodynamic Systems Analysis Software. Los Angeles: Biomedical Simulations Resource.

Dayneka NL, Garg V and Jusko WJ (1993) Comparison of four basic models of indirect pharmacodynamic responses. *J Pharmacokinet Biopharm* **21**:457-478.

Dedrick RL (1986) Interspecies scaling of regional drug delivery. *J Pharm Sci* **75**:1047-1052.

Dedrick RL, Myers CE, Bungay PM and DeVita VT, Jr. (1978) Pharmacokinetic rationale for peritoneal drug administration in the treatment of ovarian cancer. *Cancer Treat Rep* **62**:1-11.

Frei Ed, Bickers JN, Hewlett JS, Lane M, Leary WV and Talley RW (1969) Dose schedule and antitumor studies of arabinosyl cytosine (NSC 63878). *Cancer Res* **29**:1325-1332.

Friberg LE, Freijs A, Sandstrom M and Karlsson MO (2000) Semiphysiological model for the time course of leukocytes after varying schedules of 5-fluorouracil in rats. *J Pharmacol Exp Ther* **295**:734-740.

Gadducci A, Carnino F, Chiara S, Brunetti I, Tanganelli L, Romanini A, Bruzzone M and Conte PF (2000) Intraperitoneal versus intravenous cisplatin in combination with intravenous cyclophosphamide and epidoxorubicin in optimally cytoreduced advanced epithelial ovarian cancer: a randomized trial of the Gruppo Oncologico Nord-Ovest. *Gynecol Oncol* **76**:157-162.

Galpin AJ and Evans WE (1993) Therapeutic drug monitoring in cancer management. *Clin Chem* **39**:2419-2430.

Gianni L, Kearns CM, Giani A, Capri G, Vigano L, Lacatelli A, Bonadonna G and Egorin MJ (1995) Nonlinear pharmacokinetics and metabolism of paclitaxel and its pharmacokinetic/pharmacodynamic relationships in humans. *J Clin Oncol* **13**:180-190.

Goh BC, Fleming GF, Janisch L, Vogelzang NJ, Stadler WM and Ratain MJ (2000) Development of a schedule-dependent population pharmacodynamic model for rhizoxin without quantitation of plasma concentrations. *Cancer Chemother Pharmacol* **45**:489-494.

Goldie JH, Price LA and Harrap KR (1972) Methotrexate toxicity: correlation with duration of administration, plasma levels, dose and excretion pattern. *Eur J Cancer* **8**:409-414.

Goldman ID, Lichtenstein NS and Oliverio VT (1968) Carrier-mediated transport of the folic acid analogue, methotrexate, in the L1210 leukemia cell. *J Biol Chem* **243**:5007-5017.

Howell SB, Pfeifle CE and Olshen RA (1984) Intraperitoneal chemotherapy with melphalan. *Ann Intern Med* **101**:14-18.

Hryniuk WM, Fischer GA and Bertino JR (1969) S-phase cells of rapidly growing and resting populations. Differences in response to methotrexate. *Mol Pharmacol* **5**:557-564.

Hutchison DJ, Shimoyama M and Schmid FA (1971) Quinazoline antifolates: dosage schedules and toxicity. *Cancer Chemother Rep* **55**:123-132.

Jodrell DI, Egorin MJ, Canetta RM, Langenberg P, Goldbloom EP, Burroughs JN, Goodlow JL, Tan S and Wiltshaw E (1992) Relationships between carboplatin exposure and tumor response and toxicity in patients with ovarian cancer. *J Clin Oncol* **10**:520-528.

Jusko WJ and Ko HC (1994) Physiologic indirect response models characterize diverse types of pharmacodynamic effects [see comments]. *Clin Pharmacol Ther* **56**:406-419.

Karlsson MO, Molnar V, Bergh J, Freijs A and Larsson R (1998) A general model for time-dissociated pharmacokinetic-pharmacodynamic relationship exemplified by paclitaxel myelosuppression. *Clin Pharmacol Ther* **63**:11-25.

Karlsson MO, Port RE, Ratain MJ and Sheiner LB (1995) A population model for the leukopenic effect of etoposide. *Clin Pharmacol Ther* **57**:325-334.

Kohler DR and Goldspiel BR (1994) Paclitaxel (taxol). *Pharmacotherapy* **14**:3-34.

Lobo ED and Balthasar JP (1999) Highly sensitive high-performance liquid chromatographic assay for methotrexate in the presence and absence of anti-methotrexate antibody fragments in rat and mouse plasma. *J Chromatogr B Biomed Sci Appl* **736**:191-199.

Markman M, Reichman B, Hakes T, Curtin J, Jones W, Lewis JL, Barakat R, Rubin S, Mychalczak B, Saigo P and et al. (1993) Intraperitoneal chemotherapy in the management of ovarian cancer. *Cancer* **71**:1565-1570.

Minami H, Sasaki Y, Saijo N, Ohtsu T, Fujii H, Igarashi T and Itoh K (1998) Indirect-response model for the time course of leukopenia with anticancer drugs. *Clin Pharmacol Ther* **64**:511-521.

Minami H, Sasaki Y, Watanabe T and Ogawa M (2001) Pharmacodynamic modeling of the entire time course of leukopenia after a 3-hour infusion of paclitaxel. *Jpn J Cancer Res* **92**:231-238.

Nakamaru M, Masubuchi Y, Narimatsu S, Awazu S and Horie T (1998) Evaluation of damaged small intestine of mouse following methotrexate administration. *Cancer Chemother Pharmacol* **41**:98-102.

Ohtsu T, Sasaki Y, Tamura T, Miyata Y, Nakanomyo H, Nishiwaki Y and Saijo N (1995) Clinical pharmacokinetics and pharmacodynamics of paclitaxel: a 3-hour infusion versus a 24-hour infusion. *Clin Cancer Res* **1**:599-606.

Osman AM, Saad SF, Saad SY, el Aaser AB and el Merzabani MM (1994) Pharmacokinetic profile of methotrexate and 5-fluorouracil in normal and bilharzial-infested mice. *Chemotherapy* **40**:227-231.

Patel SR and Benjamin RS (2000) Management of peritoneal and hepatic metastases from gastrointestinal stromal tumors. *Surg Oncol* **9**:67-70.

Pinedo HM, Zaharko DS and Dedrick RL (1976) Device for constant Sc infusion of methotrexate: plasma results in mice. *Cancer Treat Rep* **60**:889-893.

Poser RG, Sirotnak FM and Chello PL (1981) Differential synthesis of methotrexate polyglutamates in normal proliferative and neoplastic mouse tissues in vivo. *Cancer Res* **41**:4441-4446.

Rowinsky EK and Verweij J (1997) Review of phase I clinical studies with topotecan. *Semin Oncol* **24**:S20-23-S20-10.

Segre G (1968) Kinetics of interaction between drugs and biological systems. *II Farmaco* **23**:906-918.

Sheiner LB, Stanski DR, Vozeh S, Miller RD and Ham J (1979) Simultaneous modeling of pharmacokinetics and pharmacodynamics: application to d-tubocurarine. *Clin. Pharmacol. Ther.* **25**:358-371.

Slevin ML, Clark PI, Joel SP, Malik S, Osborne RJ, Gregory WM, Lowe DG, Reznek RH and Wrigley PF (1989) A randomized trial to evaluate the effect of schedule on the activity of etoposide in small-cell lung cancer. *J Clin Oncol* **7**:1333-1340.

Speyer JL, Beller U, Colombo N, Sorich J, Wernz JC, Hochster H, Green M, Porges R, Muggia FM, Canetta R and et al. (1990) Intraperitoneal carboplatin: favorable results in women with minimal residual ovarian cancer after cisplatin therapy. *J Clin Oncol* **8**:1335-1341.

Zaharko DS, Dedrick RL, Peale AL, Drake JC and Lutz RJ (1974) Relative toxicity of methotrexate in several tissues of mice bearing Lewis lung carcinoma. *J Pharmacol Exp Ther* **189**:585-592.

Zhou H, Choi L, Lau H, Bruntsch U, Vries EE, Eckhardt G, Oosterom AT, Verweij J, Schran H, Barbet N, Linnartz R and Capdeville R (2000) Population pharmacokinetics/toxicodynamics (PK/TD) relationship of SAM486A in phase I studies in patients with advanced cancers. *J Clin Pharmacol* **40**:275-283.

CAPTIONS FOR FIGURES

Fig. 1. MTX pharmacokinetics. Mean plasma MTX concentration time profiles following i.p. MTX bolus administration (10 mg/kg (▼) and 600 mg/kg (▽)) and i.p, constant-rate infusion ((3 mg/kg (●) and 12 mg/kg (o)) were simultaneously fitted to a one-compartment mammillary pharmacokinetic model. The mean and the standard deviations of MTX concentration (n= 3-9) are represented with symbols and the error bars. Solid lines represent the computer best-fit values. Data were weighted by 1/variance using ADAPT II software.

Fig. 2. MTX-induced changes in body weight. Shown are data following i.p MTX administration via: (A) bolus, (B) 24 h constant-rate infusion, (C) 72 h constant-rate infusion, and (D) 168 h constant-rate infusion. Control animals received sterile 0.9% sodium chloride solution. Symbols and error bars represent the mean and the standard deviations of the percent body weight (n=4-5 per dose). MTX was administered on 'day zero'. Percent body weight was calculated with respect to the body weight on day zero, prior to MTX treatment.

Fig. 3. Protocol-dependence in the maximally tolerated MTX dose. The MTD of MTX was found to be dependant on the time course of drug administration. MTD, indicative of a mean body weight loss of 10%, was found to range from 760 mg/kg (bolus administration) to 3.8 mg/kg (72 h infusion).

Fig. 4. Accuracy of PKPD model. The prediction accuracy of Model 3 is shown following simultaneous fitting of nine MTX administration protocols. Data represent the observed and model-predicted values for mean nadir percent body weight loss following i.p administration of MTX via bolus, 24 h constant-rate infusion, 72 h constant-rate infusion and 168 h constant-rate infusion. The median prediction error by the model was 3.9% (correlation coefficient, r for observed v. predicted percent nadir body weight loss was 0.981). Doses for each protocol were in mg/kg.

Fig. 1

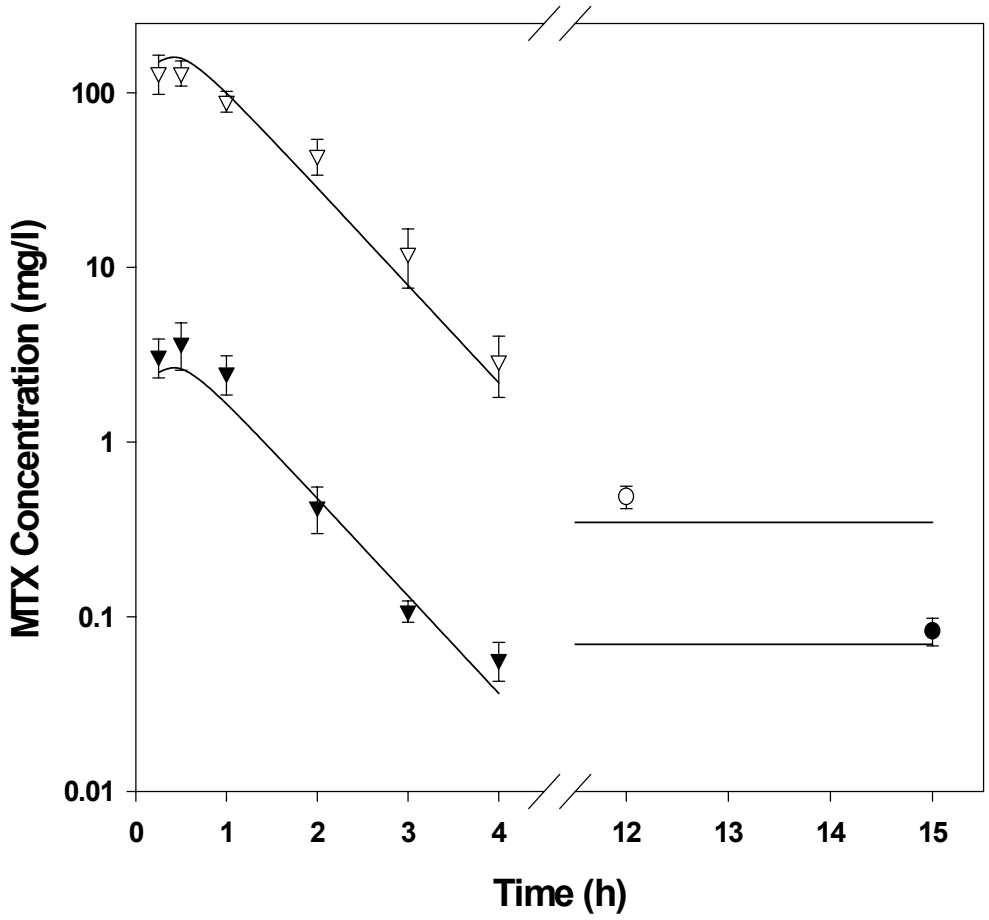

Fig. 2

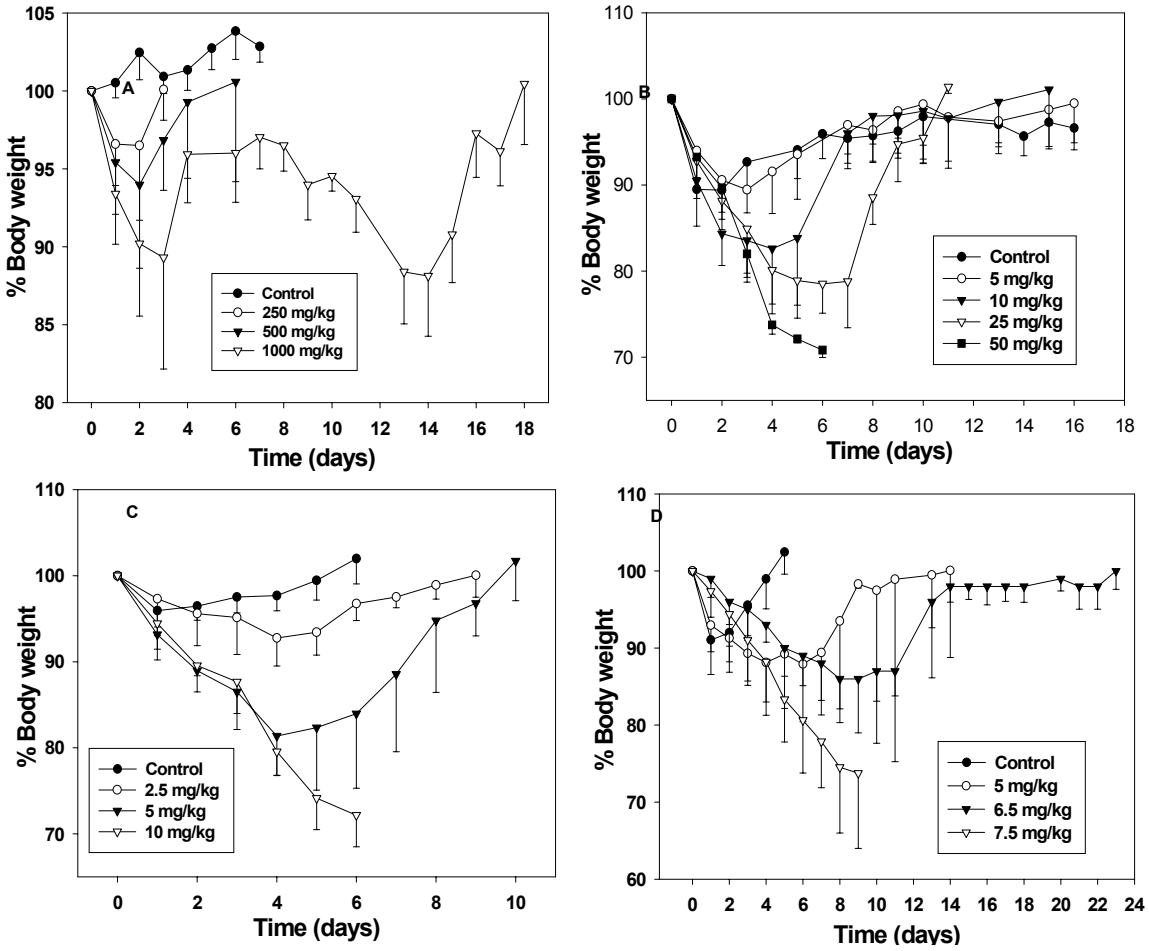
A
% Body weight
Time (days)
Control
250 mg/kg
500 mg/kg
1000 mg/kg
B
% Body weight
Time (days)
Control
5 mg/kg
10 mg/kg
25 mg/kg
50 mg/kg
C
% Body weight
Time (days)
Control
2.5 mg/kg
5 mg/kg
10 mg/kg
D
% Body weight
Time (days)
Control
5 mg/kg
6.5 mg/kg
7.5 mg/kg

Fig. 3

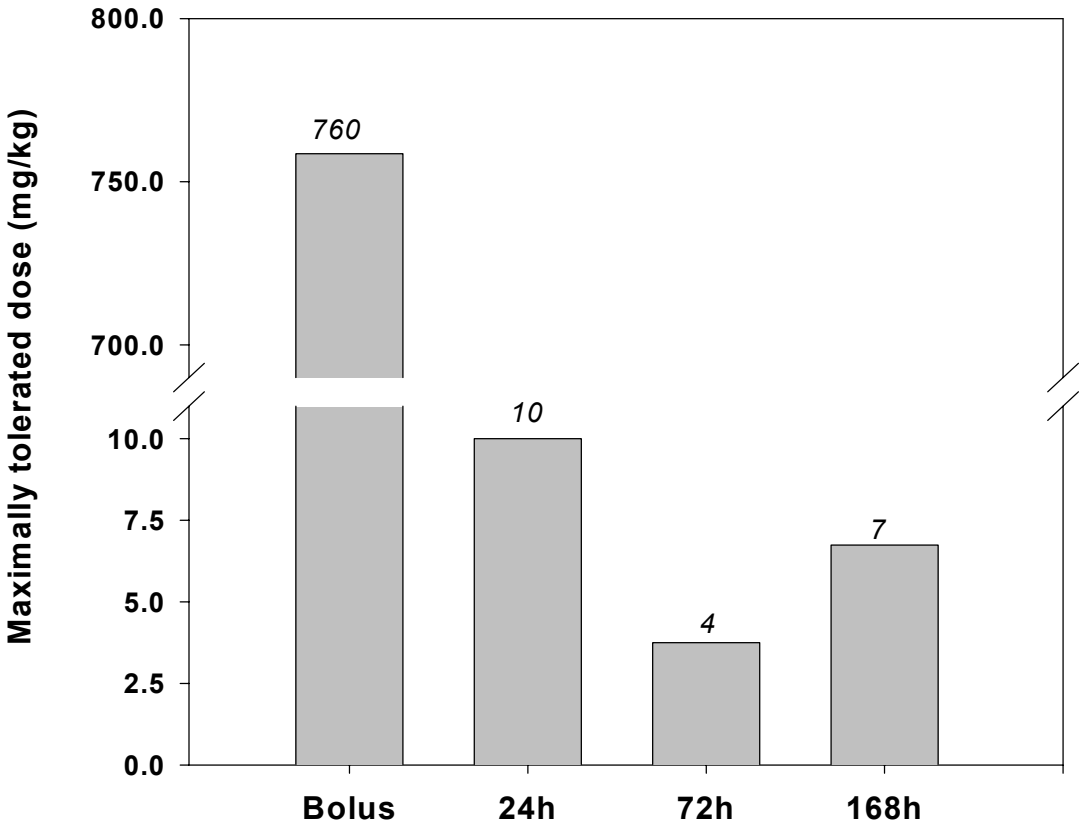
Maximally tolerated dose (mg/kg)
800.0
750.0
700.0
10.0
7.5
5.0
2.5
0.0
760
10
4
7
Bolus
24h
72h
168h

Fig. 4

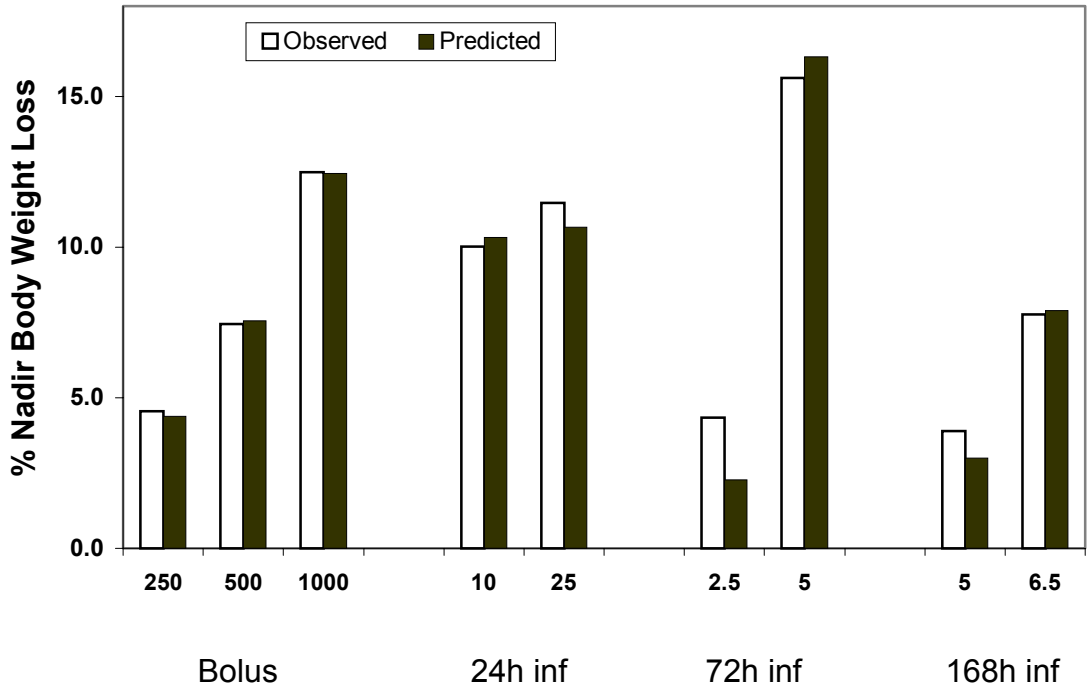
Observed
Predicted
% Nadir Body Weight Loss
15.0
10.0
5.0
0.0
250
500
1000
10
25
2.5
5
5
6.5
Bolus
24h inf
72h inf
168h inf

Table 1—MTX pharmacokinetics: Non-compartmental analyses[a]

	10 mg/kg Bolus	600 mg/kg Bolus	0.2 mg/kg/h (3 mg/kg) Infusion	1 mg/kg/h (12mg/kg) Infusion
AUC (mg/L.h)[b]	267 ± 50	12,500 ± 1,500	-	-
CL (L/kg/h)[c]	2.3 ± 0.4	2.9 ± 0.3	2.5 ± 0.4	2.1 ± 0.3
$t_{1/2}$ (min)	36.8 ± 7.6	30.7 ± 4.4	-	-
CLd (L/kg/h)	-	-	0.03 ±0.04	-
R	-	-	75.6 ± 49.8	-

[a] The results were expressed as mean±SD. The number of animals for 10, 600, 3, and 12 mg/kg were 3, 3, 9 and 4 respectively. [b] AUC, the area under the MTX plasma concentration time profile from time zero to infinity; CL, systemic clearance; $t_{1/2}$, half-life of MTX obtained from the terminal slope; CLd, peritoneal clearance; R, ratio of peritoneal concentration to systemic concentration at steady state. [c] Systemic clearance was not found to be significantly different (i.e., $p > 0.05$) in the dose range of 3 to 600 mg/kg.

Table 2—Mean percent body weight loss at nadir following i.p. MTX

	Bolus			24h Infusion				72h Infusion			168h Infusion		
Dose (mg/kg)	250	500	1000	5	10[a]	25[b]	50[c]	2.5	5	10[c]	5	6.5[b]	7.5[c]
Mean[d]	4.6	7.4	12.5	0.1	10.0	11.5	18.6	4.4	15.6	23.8	3.5	7.8	17.0
SD	4.4	6.6	6.2	3.0	6.2	4.0	1.4	2.4	5.3	3.3	9.7	9.3	8.3

[a] One of 5 animals died of toxicity. [b] Two of 4 animals died of toxicity. [c] All animals died of toxicity. [d] The mean percent nadir body weight loss corrected for 'surgical' weight loss, estimated as the mean percent weight-loss observed for respective controls (n= 4 or 5).

Table 3—Evaluation of the three time-dissociated models relating the time course of MTX administration to the percent nadir body weight loss[a]**.**

	Parameters	AIC[b]	% MPE
Model 1	3	51.2	23.5
Model 2	5	48.0	17.5
Model 3	6	27.9	3.9

[a] The observed mean percent nadir body weight loss from nine administration protocols was simultaneously fitted to each model. [b] AIC, Akaike's information criterion; % MPE, median prediction error calculated as |observed nadir weight loss-predicted nadir weight loss| / observed nadir weight loss x 100.

CHAPTER FOUR

Application of pharmacokinetic – pharmacodynamic modeling to predict the kinetic and dynamic effects of anti-methotrexate antibodies in mice.

Abstract

We have shown that i.v administration of anti-methotrexate antibodies (AMAb) reduces the systemic exposure of i.p. methotrexate (MTX) therapy, and we have proposed that AMAb effects on MTX systemic exposure would allow a reduction in MTX-induced systemic toxicity (i.e., producing a desirable antagonistic effect). However, many literature reports have shown that anti-toxin antibodies occasionally demonstrate unexpected agonist-like activity, increasing the extent of toxicity induced by their ligand. In this report, we have developed a pharmacokinetic-pharmacodynamic (PKPD) model to predict the potential of AMAb to increase or decrease the magnitude of MTX-induced body weight loss in mice. Murine monoclonal anti-MTX IgG (AMI) and anti-MTX Fab fragments (AMF) were produced, purified, and characterized. Simulations were conducted to identify administration protocols most likely to produce agonistic or antagonistic effects, and these model predictions were tested in vivo in mice. Agonistic effects were tested following 24h infusion of i.p. MTX (10mg/kg) and i.v. administration of an equimolar dose of AMI. Antagonistic effects were tested following 72h infusion of i.p. MTX (5mg/kg) and i.v. infusion of an equimolar dose of AMF. Consistent with model predictions of agonist-like activity, AMI significantly increased animal mortality rate (all animals died, $p<0.005$) and mean nadir weight loss ($p<0.005$). Also consistent with the predictions of the PKPD model, AMF significantly decreased animal mortality and mean nadir body weight loss ($p<0.01$). Thus, these studies demonstrate that agonistic and antagonistic effects of anti-toxin antibodies may be predicted through the use of an integrated PKPD model.

Our laboratory is investigating the potential use of anti-drug antibodies (ADAb) to reduce systemic toxicities that arise following the intraperitoneal chemotherapy of peritoneal cancers (Balthasar and Fung, 1994; Balthasar and Fung, 1996). Our approach combines i.p. chemotherapy with systemic administration of ADAb, where ADAb are employed to produce regio-selective alterations in drug disposition. We have shown that systemic administration of ADAb allows reductions in peak blood concentrations of unbound drug, and limits the extent of drug distribution to systemic tissues, following i.p. drug administration (Balthasar and Fung, 1994; Balthasar and Fung, 1996). Additionally, we have shown that systemic administration of AMF leads to a significant reduction in the cumulative systemic exposure to unbound MTX (fAUC), and significantly increases the renal elimination of MTX, presumably through direct renal elimination of MTX-AMF complexes (Balthasar and Fung, 1996).

Given the above pharmacokinetic effects, it may be reasonable to project that ADAb would act as an antagonist to allow reductions in systemic drug toxicities. However, several examples appear in the literature to show that antibodies directed against drugs, toxins, or endogenous substances (e.g., cytokines) occasionally demonstrate unexpected agonistic activity, increasing the magnitude of effects produced by their ligand (Faulstich et al., 1988; Fisher et al., 1996; May et al., 1993; Sato et al., 1993). As such, it has been difficult to predict the influence that antibodies will have on the pharmacodynamics of ligands, both

in terms of the direction of effect (agonistic or antagonistic) as well as in terms of magnitude of effect.

The present study describes the development of an integrated PKPD model, which allows prediction of antibody effects on ligand disposition and on ligand effects. This model combines the PKPD model of MTX induced body weight loss with a pharmacokinetic model that predicts the influence of AMAb on the disposition of MTX. The model has been applied to conduct computer simulations that predict the effects of monoclonal AMAb (intact IgG and fab fragments) on MTX pharmacokinetics and MTX-induced weight loss in mice. To our knowledge, this is the first model that predicts in vivo effects of anti-drug or anti-toxin antibodies. Additionally, we present the development of a new hybridoma secreting AMAb, as well as the production, purification, and characterization of monoclonal AMI and AMF. Lastly, in vivo experiments have been conducted to allow assessment of the predictions of the PKPD model.

Methods

Computer Simulations

The pharmacokinetic model employed to predict MTX disposition mice in the presence of AMAb is shown schematically in Fig. 1. The following differential equations define the model:

$$\frac{dMp}{dt} = -k_a \cdot Mp \quad (1)$$

$$\frac{dM}{dt} = \frac{k_a}{V} \cdot Mp - \frac{CL}{V} \cdot M - k_{on} \cdot M \cdot A \cdot \frac{VA}{V} + k_{off} \cdot MA \cdot \frac{VA}{V} + \frac{CLA}{V} \cdot MA \cdot R_f \quad (2)$$

$$\frac{dA}{dt} = -\frac{CLA}{VA} \cdot A - k_{on} \cdot M \cdot A + k_{off} \cdot MA \quad (3)$$

$$\frac{dMA}{dt} = -\frac{CLA}{VA} \cdot MA + k_{on} \cdot M \cdot A - k_{off} \cdot MA \quad (4)$$

Mp represents the amount of MTX in the peritoneum; M, A, MA are the concentrations of unbound MTX, anti-MTX antibody (AMI or AMF) and MTX-anti-MTX antibody complex in the central compartment. CL represents the elimination clearance of MTX; CLA is the elimination clearance of anti-MTX antibody and MTX-anti-MTX antibody complex. V and VA are the volumes of distribution of MTX and anti-MTX antibody, respectively. Ka is the first order rate constant for MTX absorption from the peritoneum, k_{on} is the second order rate constant for MTX-anti-MTX antibody association, and k_{off} is the first order rate constant for MTX-anti-MTX antibody dissociation. Rf represents the fraction of MTX-anti-MTX antibody complex that undergoes catabolism and recycles MTX back into the central compartment.

Pharmacokinetic parameters for MTX were obtained from pharmacokinetic studies conducted in our laboratory (Lobo and Balthasar, 2002). The equilibrium affinity constant of MTX - anti-MTX antibody complexes, Keq, was assumed to lie between 10^7 and 10^9 M^{-1}. The volumes of distribution for AMI and AMF were assumed to be equal to the plasma volume in mice. Antibody clearance values were estimated based on literature reports of IgG and Fab elimination rates

(Holton et al., 1987; Pimm et al., 1987). Table 1 summarizes the pharmacokinetic parameters utilized for the simulations.

MTX induced weight loss was related to the time course of MTX exposure with a toxicodynamic model developed in our laboratory (Lobo and Balthasar, 2002).

$$\%\ \text{Nadir Body Weight Loss} = \int_0^{\infty} \left(\frac{E1_{max}\, M(t)^{\gamma_1}}{EC1_{50}{}^{\gamma_1} + M(t)^{\gamma_1}} + \frac{E2_{max}\, M(t)^{\gamma_2}}{EC2_{50}{}^{\gamma_2} + M(t)^{\gamma_2}} \right) dt$$

where M(t), is MTX plasma concentration at time t, $E1_{max}$ = 0.41, $EC1_{50}$ = 0.022 mg/L, γ_1 = 4, $E2_{max}$= 8.6, $EC2_{50}$ = 130.9 mg/L, γ_2 = 2.

Simulations were conducted to investigate the influence of the time course of drug and antibody administration, antibody type (i.e., intact IgG or Fab), the molar dose ratio (antibody:MTX), the binding equilibrium constant, and the recycling fraction on the disposition of unbound MTX and on the extent of MTX-induced weight loss. Simulations were evaluated through comparison of the following outputs: the time course of unbound MTX exposure, the maximal unbound MTX concentration in plasma (C_{maxf}), the area under the unbound MTX concentration time profile (AUC_f), and the magnitude of MTX induced weight loss.

The effect of the time course of MTX and antibody administration on MTX toxicity were investigated via simulations conducted at the maximally tolerated dose of

MTX (i.e., the dose causing 10% body weight loss in mice) as determined from previous studies of MTX toxicity. The four i.p. dosing protocols included bolus (760 mg/kg), 24 h constant-rate infusion (10 mg/kg), 72 h constant-rate infusion (3.8 mg/kg) and 168 h constant-rate infusion (6.8 mg/kg). The molar dose ratio for the antibody and MTX was set to 1, Keq was 10^8 M^{-1}, Rf was 1 for AMI and 0.25 for AMF for all simulations. The effect of Keq and Rf were on MTX toxicity was determined following simulated administration of 72 h infusions of i.p. MTX (5 mg/kg) and equimolar dose of i.v. AMF. Simulations investigated antibody affinity constant of: 10^7, 10^8, or 10^9 M^{-1} at fixed Rf of 0.5 and the recycled fraction for AMF between 0 and 0.5 at fixed Keq of 10^8 M^{-1}.

Hybridoma Development

A MTX immunogen was synthesized by covalently linking MTX to keyhole limpet hemacyanin (KLH, Pierce, Rockford, IL) through the formation of amide bonds catalyzed by 1-ethyl-3-(3-dimethylamino-propyl)carbodiimide (EDC, Sigma Chemical, St. Louis, MO) using an approach similar to that described previously (Balthasar and Fung, 1995). Briefly, MTX (18 mg), KLH (20 mg), and EDC (15 mg) were dissolved into 5 ml of a 1:5 v/v solution of distilled water / pyridine, and stirred for 1 h at room temperature. MTX-KLH was precipitated and washed with methanol (2 × 10 ml). The pale yellow conjugate was dried under a stream of nitrogen gas under room temperature (× 2 h), and then stored at –20ºC until used. Additionally, a MTX – bovine serum albumin (BSA, Sigma Chemical) conjugate was prepared using a similar strategy.

The MTX-KLH conjugate, emulsified in Freund's incomplete adjuvant (Sigma Chemical), was used to repetitively immunize six Balb/c mice (Harlan, Indianapolis, IN). Animals were bled from the saphenous vein 7-10 days following immunization, and AMI were detected with an antigen capture enzyme linked immunosorbant assay (ELISA) using the BSA-MTX conjugate. The animal with the highest ELISA response was selected for use as a splenocyte donor, and fusion was performed with murine SP20 myeloma cells (ATCC, Manassas, VA). Briefly, the mouse was sacrificed with ketamine (150 mg/kg) and xylazine (30 mg/kg), and the spleen was rapidly removed using aseptic technique. Splenocytes were teased out of spleen tissue with the use of sterile 22 ga needles, suspended in RPMI 1640, and fused with SP20 cells by centrifugation with polyethylene glycol, using standard techniques (Harlow and Lane, 1988). Fused cells were selected through application of HAT selection medium (Sigma Chemical), and tissue culture supernatant was assayed for AMI by evaluating ELISA response against MTX-BSA.

Hybridoma Characterization

Following identification of hybridomas as secretors of AMI via ELISA, additional screening was conducted to assess growth characteristics in serum free media, assess the affinity of secreted antibodies for MTX, and to determine the isotype of secreted antibodies. Antibody affinity was determined following Protein–G purification of tissue culture supernatant (described below). Purified antibody, at a fixed concentration, was co-incubated for 2 h at 4ºC with a range of MTX

concentrations, where MTX was tracer-labeled with ^{3}H-MTX (Amhersham, Piscataway, NJ). Unbound MTX was separated from antibody-bound MTX through the use of ultrafiltration tubes (Centrifree, Millipore, Bedford, MA). Unbound MTX concentrations in the ultrafiltrate were determined as the product of the free fraction of ^{3}H-MTX (assessed by liquid scintillation counting) and the total MTX concentration in the incubation solution. Bound MTX concentrations were calculated as the difference between the total MTX concentration and the assayed unbound concentration in the ultrafiltrate. Previous work conducted in this laboratory has demonstrated that ^{3}H-MTX does not bind to the ultrafiltration tubes (Balthasar and Fung, 1996). Parameter estimates of the equilibrium affinity constant of MTX-antibody complexes (Keq) and of the concentration of MTX binding sites (nPt) were determined by ADAPT II (D'Argenio and Schumitzky, 1997) fitting of the collected data to the following binding isotherm: $B/F = \frac{nPt}{1/Keq + F}$, where F and B represent the measured free and calculated bound concentrations of MTX, respectively. Antibody isotype was determined through the use of a commercial assay kit (ISO-1, Sigma Chemical).

AMI Production

Gram quantities of AMI were produced through the use of a hollow fiber bioreactor (Cell Pharm, 10 ft^{2}, 10 K, Biovest International, Minneapolis, MN). Briefly, 'seed' hybridoma cells were grown within 1 l spinner flasks containing serum free hybridoma media (Hybridoma SFM, Invitrogen, Grand Island, NY). Approximately 10^{9} hybridoma cells in 60 ml serum free hybridoma media were

loaded aseptically into the extracapillary space of the hollow fiber cartridge. Intracapillary feed media consisted of RPMI 1640 (Fisher Scientific, Pittsburgh, PA) containing glucose, 5 g/l, and gentamicin, 5 mg/l. The system was maintained at pH 7.0 and at 37^{o}C. Media feed rates were adjusted to maintain glucose concentrations of 2.5 – 3.0 g/l. Extracapillary media, which contained the secreted antibody, was collected at a rate of 30 - 75 ml/day and was replaced with fresh serum free hybridoma media.

AMI Purification

AMI was purified from serum free media via Protein-G affinity chromatography (HiTrap Protein-G, Pharmacia Biotech Inc., Piscataway, NJ), through the use of an automated medium-pressure system (BioLogic, Bio-Rad, Hercules, CA). Sodium phosphate, 20 mM (pH 7), was used for column washing; elution was accomplished with 100 mM glycine HCl (pH 2.8). Column eluate was immediately neutralized with 1 M Tris base to pH 7. IgG concentrations were estimated via uv absorbance at 280 nm, assuming that 1 mg/ml corresponds to 1.35 AU (Harlow and Lane, 1988).

AMF Production

Purified AMI was concentrated to 5 mg/ml in sodium acetate buffer (pH 5.5). Cysteine HCL, EDTA, and papain were added to the AMI solution and the mixture was incubated at 37ºC for 6 h with occasional stirring. After 6 h, iodoacetamide was added (75 mM) to stop the reaction. Following 30 min

incubation at room temperature, the digest was dialyzed overnight against 5 mM $KHPO_4$ (pH 6). Fab fragments were purified from the dialysate (which may be expected to contain Fab fragments, undigested IgG, Fc fragments, and secondary digest products) through hydroxyapatite chromatography (BioRad Laboratories, Hercules, CA). Concentrated AMI and AMF in PBS (pH 7.4) were passed through Detoxi endotoxin removing gel (Pierce, Rockford, IL) 3 times, and tested for endotoxin using the Limulus Amebocyte Lysate test (Charles River Endosafe, Charleston, SC). Endotoxin concentration in antibody solutions was lower than 20 ng/ml; as such, animals were exposed to doses of endotoxin that were well below those associated with toxicity in mice (Khan et al., 2000).

Assessment of Antibody Purity

Antibody purity was assessed via sodium dodecyl sulfate–polyacrylamide gel electrophoresis (SDS-PAGE) under non-reducing conditions, using a 10% gel with 4% stacking gel. The molecular weights of AMI and AMF were estimated through the use of molecular weight standards (MW-SDS-200, Sigma Chemical). The gel was stained with Coomasie Brillant Blue R-250 (Bio-Rad Laboratories) for 45 min, and destained overnight with 40% methanol / 10% acetic acid.

Toxicity Studies

Male Swiss Webster mice weighing 20-25 g (Harlan) had their jugular veins cannulated at least 3 days prior to experimentation to allow convenient and reliable i.v. access for administration of treatments. Briefly, using aseptic

technique, a short length of Micro-Renathane Tubing-Type MRE-025 was implanted into the right external jugular vein of mice under ketamine (90 mg/kg) / xylazine (9 mg/kg) anesthesia. Peritoneal infusions were performed through the use of osmotic pumps (Alza Corporation, Palo Alta, CA), which were attached to peritoneal cannulas and implanted subcutaneously. Briefly, animals were anesthesized with i.p. ketamine / xylazine (100 / 10 mg/kg), and pre-equilibrated osmotic pumps (37°C, 0.9% sterile sodium chloride) were placed subcutaneously near the shoulder blade on the dorsal side. Cannulas were inserted into the peritoneal cavity through a small opening made in the abdominal muscle.

Investigation of predicted agonist effect. Computer simulations predicted that co-administration of AMI (11 μmol [22 μmol binding sites], i.v. over 24 h) with an equimolar dose of MTX (i.p. over 24 h) would lead to increase in toxicity relative to that observed following administration of MTX alone (22 μmol, i.p. over 24 h). This simulation result was tested using three groups of 4 mice that received simultaneous administration of: (a) i.v. 24 h constant-rate infusion of AMI (1.65 g/kg, 22 μmol binding sites) delivered through the use of an infusion pump (Harvard pump model 22, 66.7μl/h) and i.p. 24 h constant-rate infusion of 0.9% sterile sodium chloride; (b) i.v. 24 h constant-rate infusion of AMI (1.65 mg/kg, 22 μmol MTX binding sites) and i.p. 24 h infusion of MTX (10 mg/kg, 22 μmol); (c) i.v. 24h infusion of 0.9% sterile sodium chloride and i.p. 24 h infusion of MTX (22 μmol).

Investigation of predicted antagonist effect. Computer simulations predicted that co-administration of AMF (11 μmol, i.v. over 72 h) with an equimolar dose of MTX (i.p. over 72 h) would lead to a decrease in toxicity relative to that observed following administration of MTX alone (11 μmol, i.p. over 72 h). This simulation result was tested using three groups of mice that received simultaneous administration of: (a) 72 h i.v. infusion of 0.9% sterile sodium chloride and 72 h i.p. infusion of MTX (5 mg/kg, 11 μmol); (b) 72 h i.v. infusion of AMF (550 mg/kg, 11 μmol) and 72 h i.p. infusion of MTX (11 μmol); (c) 72 h i.v. infusion of 0.9% sterile sodium chloride and 72 h i.p. infusion of 0.9% sterile sodium chloride.

Animals were monitored daily and body weight was recorded. Percent body weight was calculated to be the percentage of animal weight on the day before the implantation of the pumps. In cases where death occurred, nadir weight loss was defined as the maximal percent weight loss of the expired animal (i.e., prior to death).

Statistics

Data are expressed as mean and the standard deviation. Unpaired two-tailed student's *t*-tests were applied to compare the mean nadir body weight loss following various treatments. Probability of less than 0.05 was considered to be significant. Mortality rates were compared using the Binomial proportion test.

Results

Computer Simulations

Simulations were conducted at the maximally tolerated dose of MTX as determined from previous studies evaluating MTX toxicity resulting from four dosing protocols (i.e., i.p. administration via bolus, 24 h constant-rate infusion, 72 h constant-rate infusion and 168 h constant-rate infusion). Model predictions for the time course of unbound MTX, following simulated MTX dosing with or without simulated co-administration of i.v. AMI (Rf = 1, Keq = 10^8 M^{-1}) or AMF (Rf = 0.25, Keq = 10^8 M^{-1}), are shown in Fig. 2A. For all dosing combinations, AMI and AMF were predicted to reduce the peak unbound plasma concentrations of MTX. However, AMI and AMF also increased the duration of MTX exposure following all dosing combinations. Predictions for MTX-induced weight loss are shown in Fig. 2B. Increases in MTX-induced weight loss (agonistic effect) were predicted following bolus administration of MTX with AMI or AMF and also following 24 h administration of MTX with co-infusion of AMI. Decreases in MTX-induced weight loss (antagonistic effect) were predicted following simulated administration of MTX with AMI or AMF over 72 h and 168 h.

The magnitude of MTX-induced weight loss also depended on the affinity of MTX-antibody binding and on the extent of 'recycling' of MTX (i.e., following elimination as MTX-antibody complexes). Predicted effects of AMF on the time courses of unbound MTX concentration are shown in Fig. 3A, where Keq is set at 10^8 M^{-1} and where the recycling fraction is adjusted to be 0, 0.25, and 0.5,

respectively. The magnitude of MTX-induced nadir body weight loss was predicted to increase with increases in Rf (Fig. 3B). As shown in Fig. 3C, predictions of unbound MTX concentrations varied with Keq (10^7, 10^8, and 10^9 M^{-1}), following 72 h co-infusion of i.v. AMF (Rf = 0.5) and i.p. MTX. The magnitude of MTX induced weight loss was predicted to decrease with increases in antibody binding affinity (Fig. 3D).

Hybridoma Development and Characterization

Several hybridomas were found to secrete AMI (as determined by ELISA). Hybridoma W8 was selected for further development, as this hybridoma demonstrated good growth in serum free media, and secreted IgG1 antibodies with good affinity for MTX ($5.46 \pm 0.23 \times 10^8$ M^{-1}).

Antibody Production and Purification

Following loading of W8 hybridoma cells in the hollow fiber bioreactor, AMI production rate increased rapidly, reaching approximately 500 mg/week by the 3rd week. Two pools of protein were collected during the course of Protein-G chromatography (Fig. 4). Proteins that did not bind to the column eluted at the beginning of the run, and bound proteins were collected following elution with 0.1 M glycine buffer. The method yielded highly concentrated IgG (typically 2.0 to 3.3 mg/ml), and allowed purification of IgG at a rate of approximately 60 mg/h.

Fab fragments were purified from papain digest solution, which might be expected to contain Fab, Fc fragments, undigested IgG, and low molecular weight contaminants (e.g., products of secondary digestion). SDS-PAGE mobility patterns for purified AMI and AMF are shown in Fig. 5. As demonstrated by the gel, the purified AMF preparation was free of undigested IgG, and largely contained protein with an estimated molecular weight consistent with that expected for Fab (i.e., 50 kDa), as well as additional lower molecular weight protein contaminants.

Agonistic Effect

MTX, 22 μmol i.p. over 24 h, induced reductions in animal body weight as shown in Fig. 6. Nadir body weight loss for animals receiving MTX i.p. with saline i.v. was 8.2 ± 2.4%. When the same dose of MTX (22 μmol i.p. over 24 h) was given with co-administration of an equimolar dose of i.v. AMI, a dramatic increase in animal toxicity was observed. Nadir body weight loss increased by 142% to 19.9 ± 4.3% ($p<0.005$). Additionally, AMI also dramatically increased animal mortality rate (all animals died, n=4) as compared to MTX with i.v. saline (all animals survived treatment and regained weight, n=4, $p<0.005$). Animals cotreated with a non-specific mouse IgG i.v (same dose as AMI) and MTX (22 μmol i.p. over 24 h) i.p. had a nadir body weight loss of 7.1 ± 4.0% (n=4) similar to MTX/saline treatment and all animals survived. The observed percent mean nadir body weight loss data were similar to values predicted by the PKPD model (Fig. 7). Animals treated with AMI alone had a mean nadir percent body weight of 6.2 ±

4.3 (n=3), which is similar to that observed following administration of saline alone (4.2 ± 1.9, n=6).

Antagonistic Effect

The time courses of MTX-induced weight loss following 72 h i.p. infusion of MTX (11 μmol) with i.v. infusion of saline or AMF (11 μmol) are shown in Fig. 8. Mean percent nadir body weight loss was reduced by 56% in animals receiving i.v. AMF and i.p. MTX relative to weight loss observed in animals receiving i.v. saline and i.p. MTX ($p<0.01$). Additionally, AMF increased animal survival rate from 33% (following i.p. MTX with i.v. saline, n = 6) to 100% (following i.p. MTX with i.v. AMF, n = 4, $p<0.05$). Again, these results were consistent with the predictions of the PKPD model (Fig. 9).

Discussion

Antibodies have been widely investigated as antagonists to prevent or reverse the deleterious effects of drugs (e.g., digoxin, colchicine, phencyclidine), venoms, endotoxins, and cytokines (Sabouraud et al., 1991; Smith et al., 1976; Sullivan, 1987; Teng et al., 1985; Valentine et al., 1996). ADAb have also been evaluated for use in minimizing the systemic toxicity (e.g., mucositis and bone marrow toxicities) arising from administration of chemotherapeutics (Balsari et al., 1994; Kroll et al., 1994; Morelli et al., 1997; Sardini et al., 1992). In our laboratory, we are investigating the potential of ADAb to reduce systemic toxicities associated

with intraperitoneal chemotherapy (Balthasar and Fung, 1994; Balthasar and Fung, 1996).

Although anti-toxin antibodies typically produce desired antagonistic effects, several literature reports have shown that anti-toxin antibodies may produce unexpected agonistic effects (enhancement of toxicities). For example, May et al. demonstrated that administration of anti-interleukin-6 antibodies led to a 30% increase in the extent of interleukin-6 induction of fibrinogen levels in mice (May et al, 1993). Similarly, Sato et al. found a five-fold increase in IgE production in mice treated with IL-4 binding protein as compared to IL-4 alone (Sato et al, 1993). Anti-IL-3 monoclonal antibodies were found to increase mucosal mast cell number by 16-fold as compared to results observed in mice treated with IL-3 alone (Finkelman et al., 1993), and monoclonal anti-amantin antibodies were found to decrease the survival rate of mice receiving amanitin (a mushroom toxin) (Faulstich et al, 1988). In a septic shock canine model, administration of monoclonal anti-endotoxin antibodies increased animal mortality rate from 43% (where no antibody administered) to 85% (Quezado et al., 1993). Lastly, in a clinical study of an anti-TNF fusion protein in septic shock, mortality increased dose-dependently with the anti-TNF therapy, increasing from 30% in placebo-treated patients to 53% in patients receiving the highest dose of the fusion protein (Fisher et al, 1996). Clearly, the development of many antibody-based therapies has been impeded by difficulties associated with the prediction of antibody effects.

In an attempt to improve the predictability of the effects of ADAb in our drug targeting strategy, we collected data that allowed PKPD modeling of the relationship between MTX exposure and MTX-induced toxicity (Lobo and Balthasar, 2002). This model of MTX toxicity was merged with a pharmacokinetic model that allows prediction of the effects of AMAb on MTX disposition. By merging the PKPD model that characterizes the relationship of MTX exposure to MTX-induced weight loss with the kinetic model that allows prediction of antibody effects on MTX disposition, we anticipated that we might accurately predict effects of AMAb on MTX-induced toxicity.

Data were available to allow estimation of many of the parameters of the integrated model; however, several assumptions were necessary. For example, the fate of MTX-AMAb complexes is uncertain. It is logical to assume that some fraction of MTX that is eliminated as MTX-complexes may return to the systemic circulation following AMAb catabolism. Although data are not yet available to allow determination of the fraction of MTX that is released back into the systemic circulation, the present model attempts to account for drug recycling through the parameter Rf (i.e., the recycling fraction, Fig. 1). Intact IgGs are primarily cleared by catabolism within tissues (Covell et al., 1986); as such, the recycling fraction for MTX-AMI complexes was assumed to be between 0.75 and 1. On the other hand, Fab fragments are primarily cleared via filtration through the kidneys; consequently, the recycling fraction of MTX-AMF complexes was assumed to be between 0 and 0.5. The model assumes linear pharmacokinetics for MTX and for

the antibodies, that AMAb does not affect the distribution or elimination of unbound MTX, and that AMAb does not produce any toxicity (directly).

Simulations with the integrated PKPD model predicted that AMI and AMF would increase total MTX concentrations (simulated data not shown) and decrease peak free (unbound) MTX concentrations. AMF also reduced the cumulative exposure to free MTX by providing an additional pathway for the clearance of MTX (i.e., via elimination of MTX-AMF). AMI and AMF were predicted to extend the terminal half-life of MTX and to extend the duration of exposure to free MTX. As shown in Fig. 2, the PKPD model predicted that AMF and AMI could lead to both increases and decreases in MTX toxicity. The direction and magnitude of simulated effects were dependent on the dosing protocol employed, the value of Rf, and on the value of Keq.

Model predictions were tested in vivo, using dosing protocols that were selected due to predictions of antagonistic and agonistic effects, and based on feasibility issues (e.g., antibody dose, solubility, feasible injection volume, etc.). For example, the model predicted that the greatest increases in MTX toxicity would result from bolus administration of MTX and AMAb. However, the dose of antibody required to test this dosing mode was prohibitive (i.e., 250 g/kg AMI or 84 g/kg AMF). On the other hand, the model predicted that a sizable agonistic effect could be produced by co-infusion of MTX (10 mg/kg, 22 μmol/kg, over 24 h i.p.) and a more feasible quantity of AMI (1.65 g/kg, 22 μmol/kg binding sites,

over 24 h i.v.). As such, the 24 h infusion of equimolar doses of MTX and AMI was selected over the bolus protocol. Antagonistic effects were predicted with both AMI and AMF following 72 h and 168 h infusion dosing protocol; however, 72 h dosing of AMF provided the best compromise in terms of predicted antagonistic effect, antibody dose, and convenience of administration.

As predicted by the integrated model, agonistic effects were observed in vivo with AMI following 24 h constant-rate infusion. AMI administration led to highly significant increases in nadir body weight loss and in mortality rate (Fig. 6). Interestingly, the time of nadir body weight loss was increased in animals receiving AMI (144 h) relative to that found following administration of i.p. MTX with i.v. saline (24 h); this difference may be due to an effect of AMI on the duration of MTX exposure (i.e., extension in MTX duration, as predicted by the model). Although we found that administration of AMI alone leads to modest weight loss (nadir % body weight loss = 6.2 ± 4.3), this is similar to that observed following administration of saline alone (nadir % body weight loss = 4.2 ± 1.9), and cannot account for the dramatic increases in toxicity observed in animals receiving AMI and MTX. Also increase in MTX toxicity was observed with AMI and not with non-specific mouse IgG.

Again, as predicted by the PKPD model, AMF was found to reduce MTX toxicity, following 72 h co-infusion (i.v. AMF 11 μmol/kg and i.p. MTX 11 μmol/kg , Fig. 8). AMF decreased the extent of MTX-induced body weight loss at nadir (21.4 ± 4.8

vs. 9.3 ± 5.1, $p < 0.01$), and also improved the survival from 33% (MTX i.p. with saline i.v.) to 100% (MTX i.p. with AMF i.v., $p < 0.05$).

There have been very few attempts to investigate approaches that may allow predictions regarding the influence of antibody on ligand effects. Ramanathan proposed a pharmacokinetic approach utilizing relative exposure index to predict the agonistic or antagonistic effects of cytokine binding proteins (Ramanathan, 1996). The model assumed steady state conditions for cytokine and reversible binding of cytokine to the binding proteins. While this model is interesting, it may not be suitable for use in predicting in vivo effects of anti-toxin antibodies, where steady-state assumptions may not be appropriate.

In this paper, we have applied a PKPD model to predict dosing protocols in the presence of the antibody that would produce agonistic or antagonistic effects. Hybridomas producing anti-MTX monoclonal antibodies were developed, and secreted antibodies and antibody Fab fragments were produced, purified, and characterized. Predictions of the integrated PKPD model were tested in animals, and experimental results were found to agree well with model simulations. We believe that integrated PKPD models, such as the model presented in this report, will be of great value in attempts to predict in vivo effects of antibodies. The integrated PKPD model will be applied to guide the development of our inverse targeting strategy for optimization of intraperitoneal chemotherapy.

References

Balsari AL, Morelli D, Menard S, Veronesi U and Colnaghi MI (1994) Protection against doxorubicin-induced alopecia in rats by liposome- entrapped monoclonal antibodies. *Faseb J* **8**:226-230.

Balthasar JP and Fung HL (1994) Utilization of antidrug antibody fragments for the optimization of intraperitoneal drug therapy: studies using digoxin as a model drug. *J Pharmacol Exp Ther* **268**:734-739.

Balthasar JP and Fung HL (1995) High-affinity rabbit antibodies directed against methotrexate: production, purification, characterization, and pharmacokinetics in the rat. *J Pharm Sci* **84**:2-6.

Balthasar JP and Fung HL (1996) Inverse targeting of peritoneal tumors: selective alteration of the disposition of methotrexate through the use of anti-methotrexate antibodies and antibody fragments. *J Pharm Sci* **85**:1035-1043.

Covell DG, Barbet J, Holton OD, Black CD, Parker RJ and Weinstein JN (1986) Pharmacokinetics of monoclonal immunoglobulin G1, F(ab')2, and Fab' in mice. *Cancer Res* **46**:3969-3978.

D'Argenio DZ and Schumitzky A (1997): ADAPT II User's Guide: Pharmacokinetic/Pharmacodynamic Systems Analysis Software. Los Angeles: Biomedical Simulations Resource.

Faulstich H, Kirchner K and Derenzini M (1988) Strongly enhanced toxicity of the mushroom toxin alpha-amanitin by an amatoxin-specific Fab or monoclonal antibody. *Toxicon* **26**:491-499.

Finkelman FD, Madden KB, Morris SC, Holmes JM, Boiani N, Katona IM and Maliszewski CR (1993) Anti-cytokine antibodies as carrier proteins. Prolongation of in vivo effects of exogenous cytokines by injection of cytokine-anti-cytokine antibody complexes. *J Immunol* **151**:1235-1244.

Fisher CJ, Agosti JM, Opal SM, Lowry SF, Balk RA, Sadoff JC, Abraham E, Schein RM and Benjamin E (1996) Treatment of septic shock with the tumor necrosis factor receptor:Fc fusion protein. The Soluble TNF Receptor Sepsis Study Group. *N Engl J Med* **334**:1697-1702.

Harlow E and Lane D (1988) *Antibodies A laboratory manual* Cold Spring Harbor Laboratory, New York.

Holton OD, 3rd, Black CD, Parker RJ, Covell DG, Barbet J, Sieber SM, Talley MJ and Weinstein JN (1987) Biodistribution of monoclonal IgG1, F(ab')2, and Fab' in

mice after intravenous injection. Comparison between anti-B cell (anti-Lyb8.2) and irrelevant (MOPC-21) antibodies. *J Immunol* **139**:3041-3049.

Khan AA, Slifer TR, Araujo FG, Suzuki Y and Remington JS (2000) Protection against lipopolysaccharide-induced death by fluoroquinolones. *Antimicrob Agents Chemother* **44**:3169-3173.

Kroll RA, Pagel MA, Langone JJ, Sexton GJ and Neuwelt EA (1994) Differential permeability of the blood-tumour barrier in intracerebral tumour-bearing rats: antidrug antibody to achieve systemic drug rescue. *Ther Immunol* **1**:333-341.

Lobo ED and Balthasar JP (2002) Pharmacokinetic-pharmacodynamic modeling of methotrexate toxicity in mice. *J Pharm Pharmacol, for submission.* :Thesis Chapter 3, pg 71-107.

May LT, Neta R, Moldawer LL, Kenney JS, Patel K and Sehgal PB (1993) Antibodies chaperone circulating IL-6. Paradoxical effects of anti-IL-6 "neutralizing" antibodies in vivo. *J Immunol* **151**:3225-3236.

Morelli D, Menard S, Cazzaniga S, Colnaghi MI and Balsari A (1997) Intratibial injection of an anti-doxorubicin monoclonal antibody prevents drug-induced myelotoxicity in mice. *Br J Cancer* **75**:656-659.

Pimm MV, Caten JE, Clegg JA, Jacobs E and Baldwin RW (1987) Comparative biodistribution of methotrexate and monoclonal antibody- methotrexate complexes in mice. *J Pharm Pharmacol* **39**:764-767.

Quezado ZM, Natanson C, Alling DW, Banks SM, Koev CA, Elin RJ, Hosseini JM, Bacher JD, Danner RL and Hoffman WD (1993) A controlled trial of HA-1A in a canine model of gram-negative septic shock. *Jama* **269**:2221-2227.

Ramanathan M (1996) A pharmacokinetic approach for evaluating cytokine binding macromolecules as antagonists. *Pharm Res* **13**:84-90.

Sabouraud A, Urtizberea M, Grandgeorge M, Gattel P, Makula ME and Scherrmann JM (1991) Dose-dependent reversal of acute murine colchicine poisoning by goat colchicine-specific Fab fragments. *Toxicology* **68**:121-132.

Sardini A, Villa E, Morelli D, Ghione M, Menard S, Colnaghi MI and Balsari A (1992) An anti-doxorubicin monoclonal antibody modulates kinetic and dynamic characteristics of the drug. *Int J Cancer* **50**:617-620.

Sato TA, Widmer MB, Finkelman FD, Madani H, Jacobs CA, Grabstein KH and Maliszewski CR (1993) Recombinant soluble murine IL-4 receptor can inhibit or enhance IgE responses in vivo. *J Immunol* **150**:2717-2723.

Smith TW, Haber E, Yeatman L and Butler VP, Jr. (1976) Reversal of advanced digoxin intoxication with Fab fragments of digoxin- specific antibodies. *N Engl J Med* **294**:797-800.

Sullivan JB, Jr. (1987) Past, present, and future immunotherapy of snake venom poisoning. *Ann Emerg Med* **16**:938-944.

Teng NN, Kaplan HS, Hebert JM, Moore C, Douglas H, Wunderlich A and Braude AI (1985) Protection against gram-negative bacteremia and endotoxemia with human monoclonal IgM antibodies. *Proc Natl Acad Sci U S A* **82**:1790-1794.

Valentine JL, Mayersohn M, Wessinger WD, Arnold LW and Owens SM (1996) Antiphencyclidine monoclonal Fab fragments reverse phencyclidine- induced behavioral effects and ataxia in rats. *J Pharmacol Exp Ther* **278**:709-716.

CAPTIONS FOR FIGURES

Fig. 1. Pharmacokinetic model. The model was employed in computer simulations to predict the effects of anti-MTX IgG and anti-MTX Fab fragments on the disposition of MTX in mice. Parameters are described in the methods.

Fig. 2. Computer simulation of the influence of the time-course of MTX and AMAb administration on unbound MTX concentrations and on the degree of MTX-induced toxicity. A. Predicted time course of unbound (free) MTX concentrations in the presence of MTX alone (—), anti-MTX IgG (…) and anti-MTX Fab fragments (---). For each simulated protocol, the i.p. MTX dose was set as the maximally tolerated dose determined from earlier in vivo studies (i.e., bolus: 760 mg/kg; 24 h infusion: 10 mg/kg; 72 h infusion: 3.8 mg/kg; 168 h infusion: 6.7 mg/kg). AMAb was simulated as i.v. equimolar dose (relative to the MTX dose used for each protocol). Keq was set as 10^8 M^{-1} for AMI and AMF, while Rf was set as 1 and 0.25 for AMI and AMF, respectively. B. Predicted extent of MTX-induced weight loss for each protocol described above.

Fig. 3. Computer simulation of the influence of MTX recycling and AMF binding affinity on unbound MTX concentrations and on the degree of MTX-induced toxicity. Simulations were conducted with i.v. AMF (11 μmol) and i.p. MTX (11 μmol) via 72 h infusion. A. Influence of the recycling fraction, Rf, on unbound (free) MTX concentration. Predicted time course of unbound MTX concentration for MTX alone (no AMF) (—), in presence of AMF when Rf was set as 0 (–··–),

0.25 (….) and 0.5 (– –) with Keq fixed at 10^8 M^{-1}. B. Influence of Rf on MTX-induced toxicity. Rf was varied from 0 to 0.5, while Keq was fixed at 10^8 M^{-1}. C. Influence of AMF equilibrium affinity constant, Keq, on unbound (free) MTX concentration. Predicted time course of unbound MTX concentration for MTX alone (no AMF)(—), and in presence of AMF with Keq set as 10^7 M^{-1}(– –), 10^8 M^{-1} (….) and 10^9 M^{-1}(–··–) and Rf was fixed at 0.5. D. Influence of Keq on MTX-induced toxicity. Keq was varied as 10^7, 10^8 and 10^9 M^{-1} and Rf was fixed at 0.5.

Fig. 4. Protein-G purification of anti-MTX IgG. Media obtained from the bioreactor was loaded on the column and buffers were applied as described in the text. The affinity column procedure allowed for separation of purified IgG (pool 2) from other proteins present in media (pool 1).

Fig. 5. SDS-page of AMI and AMF. Electrophoresis was conducted on a SDS-page consisting of 10% resolving gel and 4% stacking gel. Migration patterns are shown for molecular weight standards, purified anti-MTX IgG, and purified anti-MTX Fab fragments, following staining with Coomasie blue. Lane 1 contains standards run under reducing conditions. Lane 2 and lane 3 contain Protein-G purified AMI and HAP purified AMF, run under non-reducing conditions. The molecular weight estimates for AMI and AMF bands were 164 kDa and 51 kDa, respectively.

Fig. 6. In vivo investigation of predicted agonistic effects. A. MTX-induced changes in body weight in mice following simultaneous administration of i.p. MTX (22 μmol) and i.v. AMI (11 μmol, 22 μmol binding sites) as 24 h infusion. B. Mean nadir percent body weight loss was significantly increased in animals receiving AMI (**$p<0.01$, n=4).

Fig. 7. Comparison of predicted and observed MTX-induced toxicity following administration of MTX or MTX with AMI. MTX-induced changes in body weight in mice following simultaneous administration of i.p. MTX (22 μmol) and i.v. AMI (11 μmol, 22 μmol binding sites) via 24 h infusion. Nadir body weight loss in animals receiving MTX + saline was observed to be 8.2 ± 2.4%, and predicted by simulation to be 10.3%. Following administration of MTX + AMI, nadir body weight loss was observed to be 19.9 ± 4.3%, and predicted to be 24.8%.

Fig. 8. In vivo investigation of predicted antagonistic effects. A. MTX induced changes in body weight following simultaneous administration of i.v. saline + i.p. MTX (11 μmol), i.v. AMF (11 μmol) + i.p. MTX (11 μmol), or i.v. saline + i.p. saline via 72 h infusion. B. Mean nadir percent body weight loss in presence of AMF (n=4) was significantly (*$p<0.05$) different from MTX treated animals (n=6). The mean nadir body weight loss in animals receiving i.v. AMF and i.p. MTX was not significantly (#$p>0.05$) different from animals infused with i.v. saline and i.p. MTX.

Fig. 9. Comparison of predicted and observed MTX-induced toxicity following administration of MTX or MTX with AMF. MTX-induced changes in body weight in mice following simultaneous administration of i.v. saline + i.p. MTX (11 μmol) or i.v. AMF (11 μmol) + i.p. MTX (11 μmol) via 72 h infusion. Nadir body weight loss in animals receiving MTX + saline was observed to be 21.4 ± 4.8%, and predicted by simulation to be 21.3%. Following administration of i.v. AMF + i.p. MTX, nadir body weight loss was observed to be 9.3 ± 5.1%, and predicted to be 7.8%.

Fig. 1

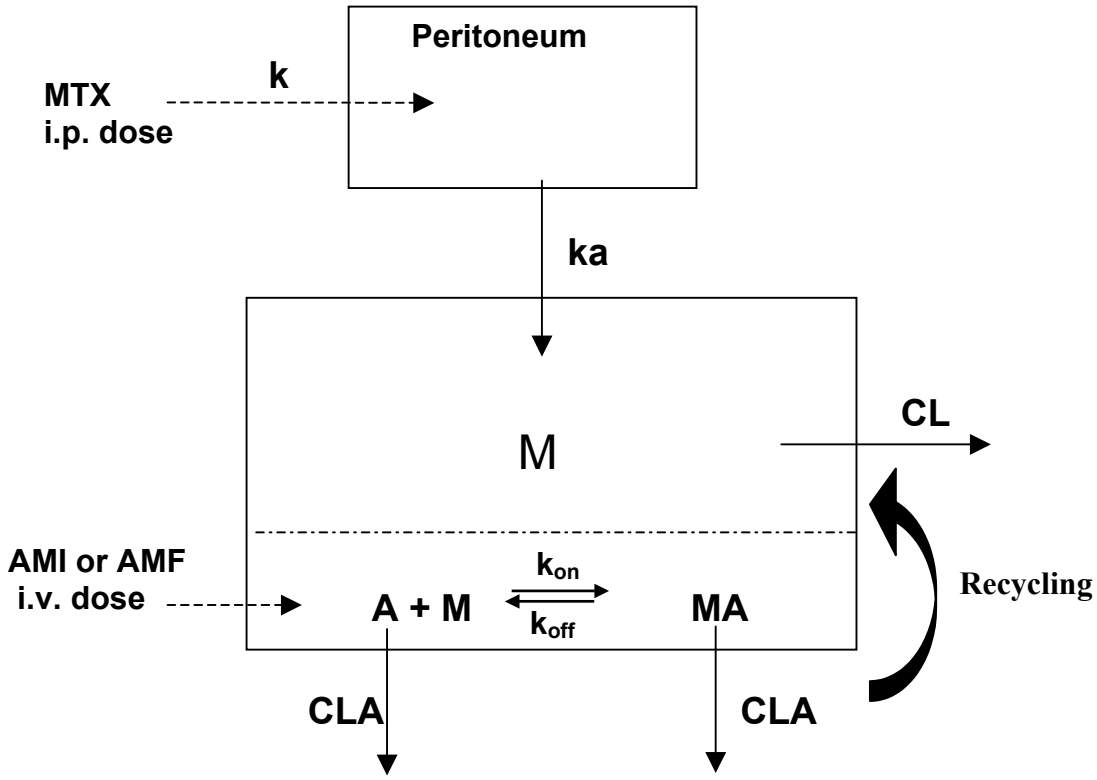
Peritoneum
k
MTX
i.p. dose
ka
M
CL
AMI or AMF
i.v. dose
A + M
k_{on}
k_{off}
MA
Recycling
CLA
CLA

Fig. 2

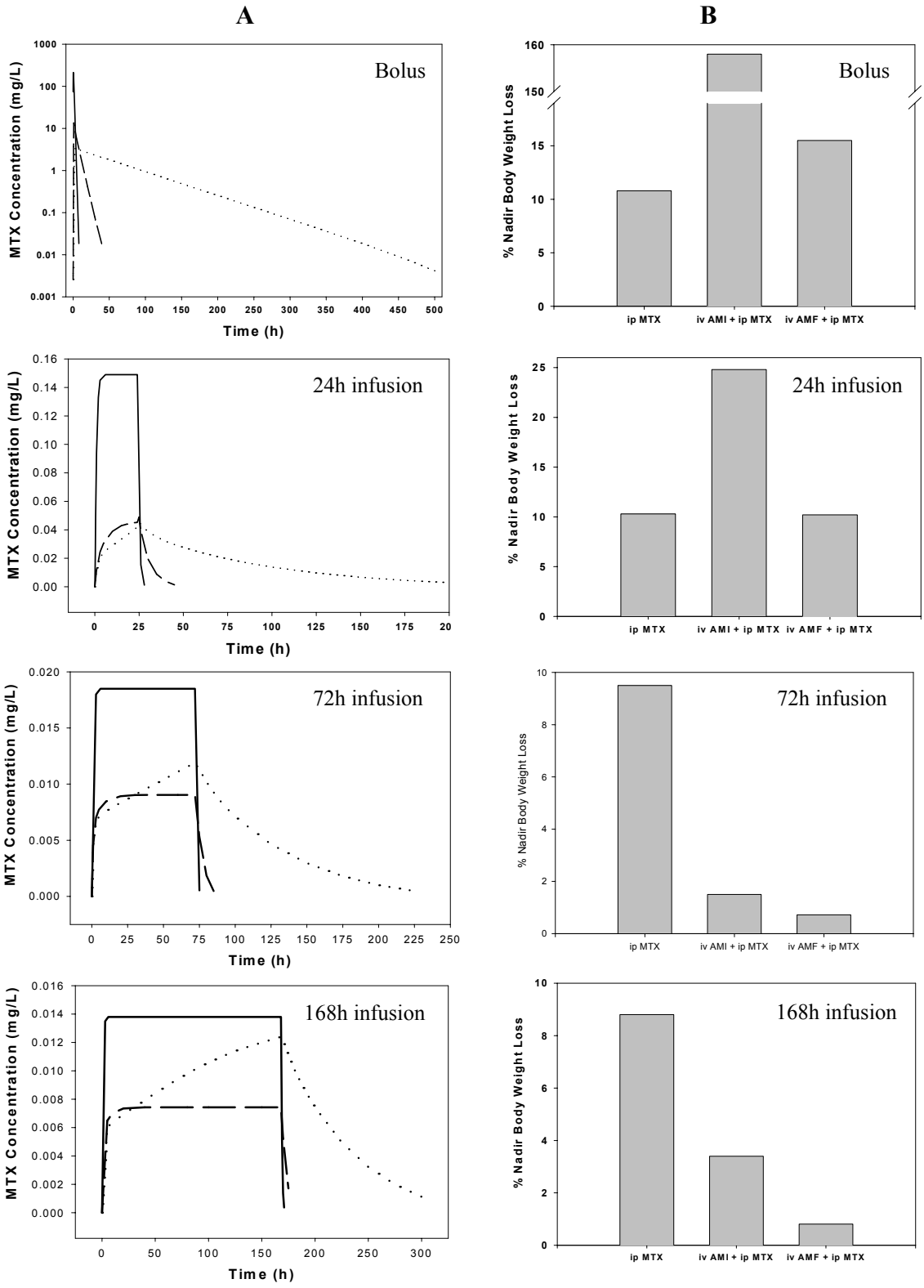
A
B
Bolus
24h infusion
72h infusion
168h infusion
MTX Concentration (mg/L)
Time (h)
% Nadir Body Weight Loss
ip MTX
iv AMI + ip MTX
iv AMF + ip MTX

Fig. 3

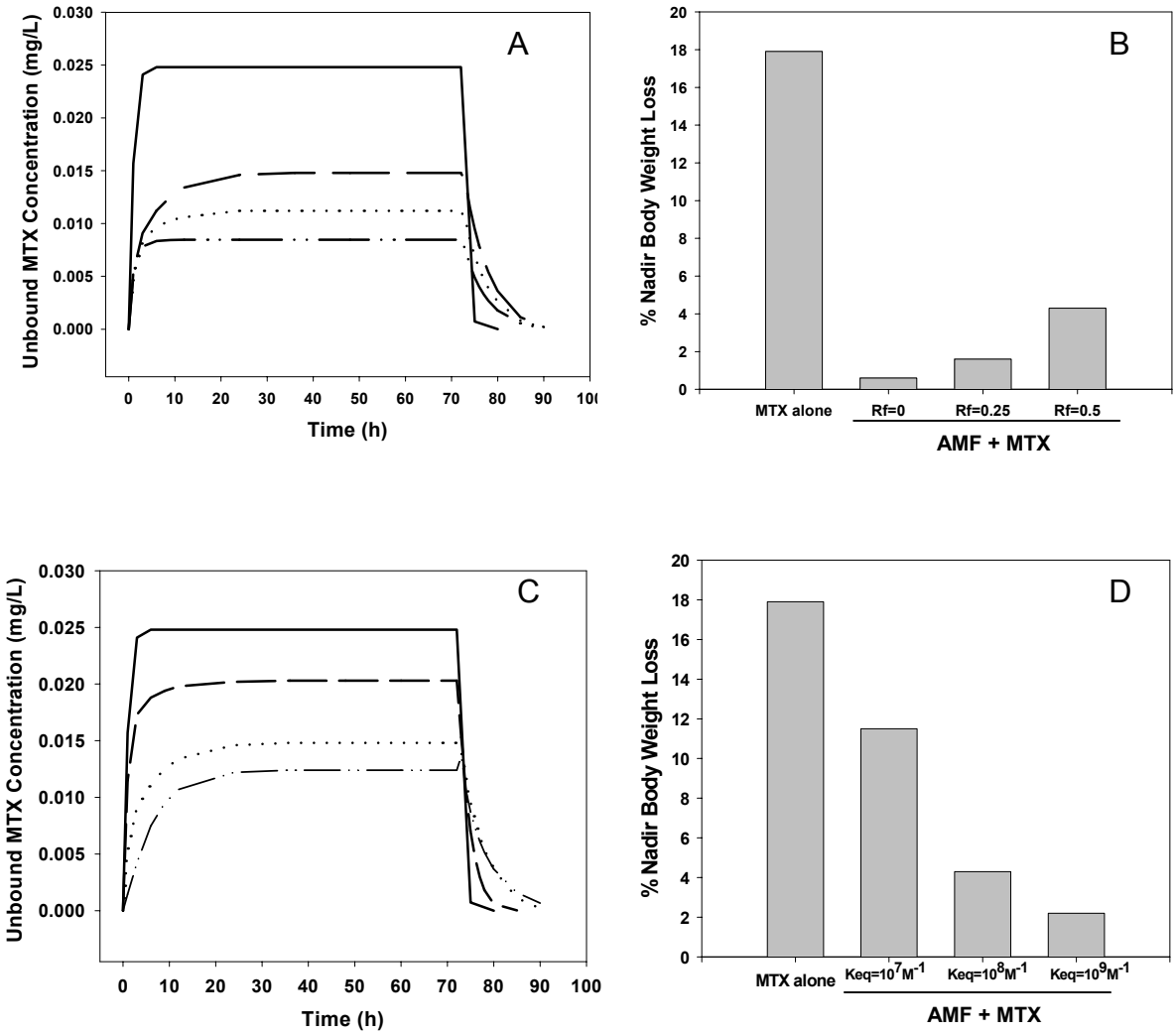
A
Unbound MTX Concentration (mg/L)
0.030
0.025
0.020
0.015
0.010
0.005
0.000
0 10 20 30 40 50 60 70 80 90 100
Time (h)
B
% Nadir Body Weight Loss
20 18 16 14 12 10 8 6 4 2 0
MTX alone
Rf=0
Rf=0.25
Rf=0.5
AMF + MTX
C
Unbound MTX Concentration (mg/L)
0.030
0.025
0.020
0.015
0.010
0.005
0.000
0 10 20 30 40 50 60 70 80 90 100
Time (h)
D
% Nadir Body Weight Loss
20 18 16 14 12 10 8 6 4 2 0
MTX alone
Keq=10^7 M^-1
Keq=10^8 M^-1
Keq=10^9 M^-1
AMF + MTX

Fig. 4

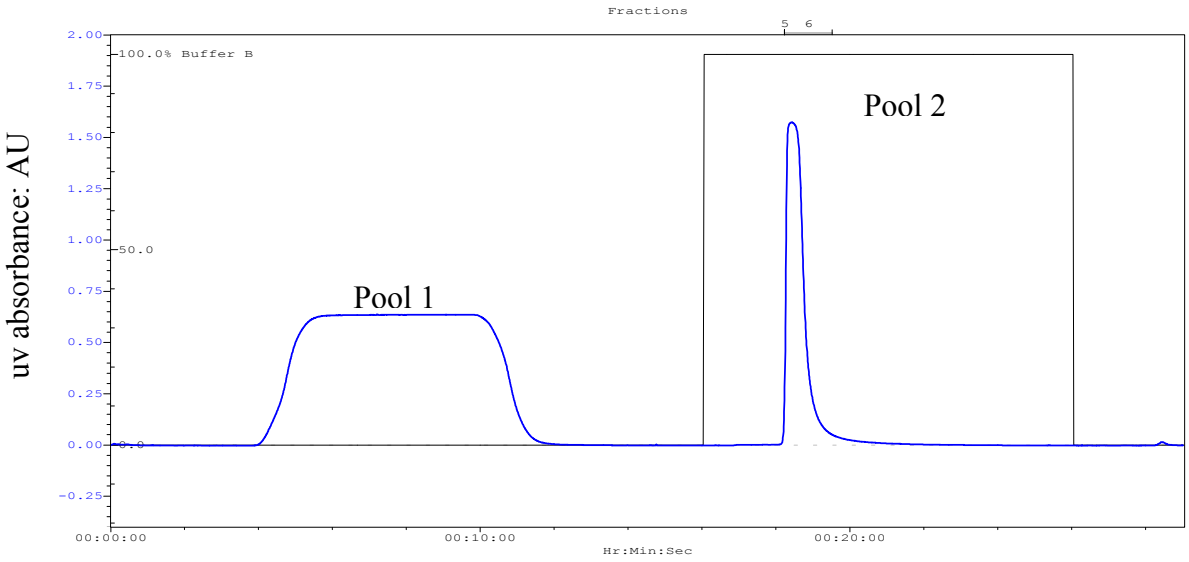
Fractions
5 6
100.0% Buffer B
50.0
0.0
Pool 1
Pool 2
uv absorbance: AU
2.00
1.75
1.50
1.25
1.00
0.75
0.50
0.25
0.00
-0.25
00:00:00
00:10:00
00:20:00
Hr:Min:Sec

Fig. 5.

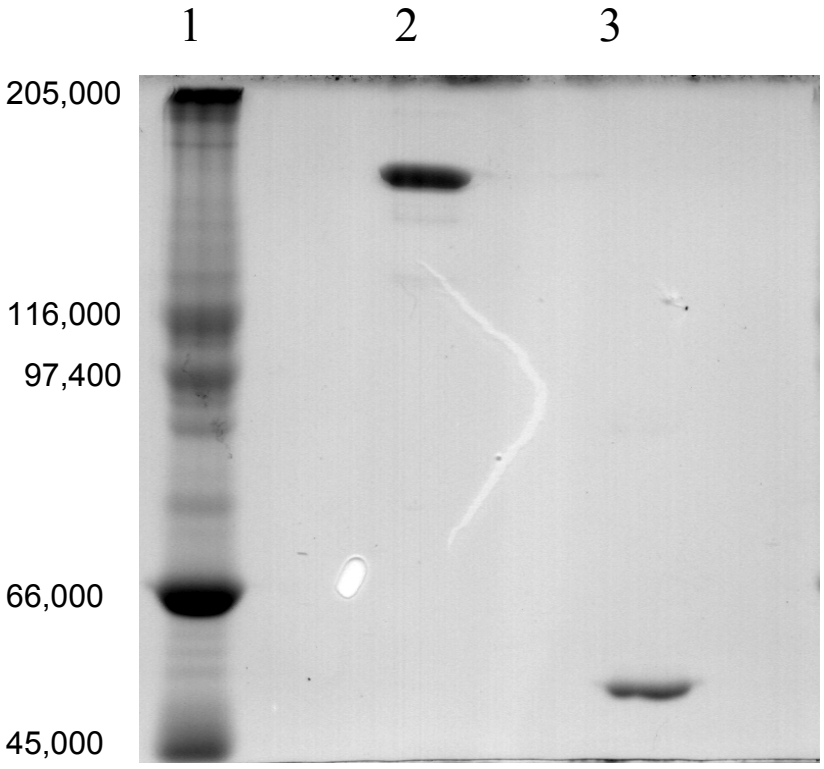

Fig. 6

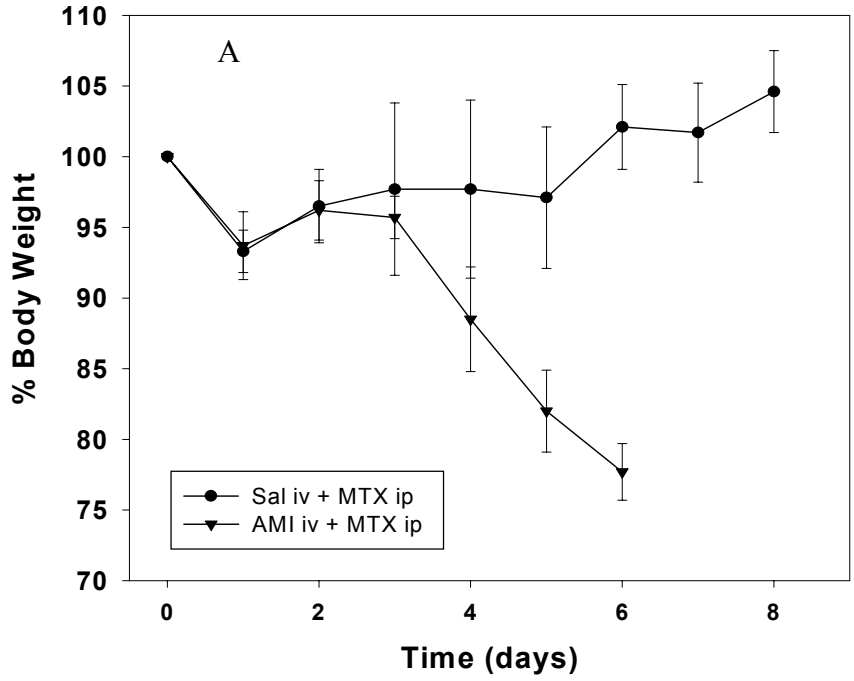
A
% Body Weight
110
105
100
95
90
85
80
75
70
0
2
4
6
8
Time (days)
Sal iv + MTX ip
AMI iv + MTX ip

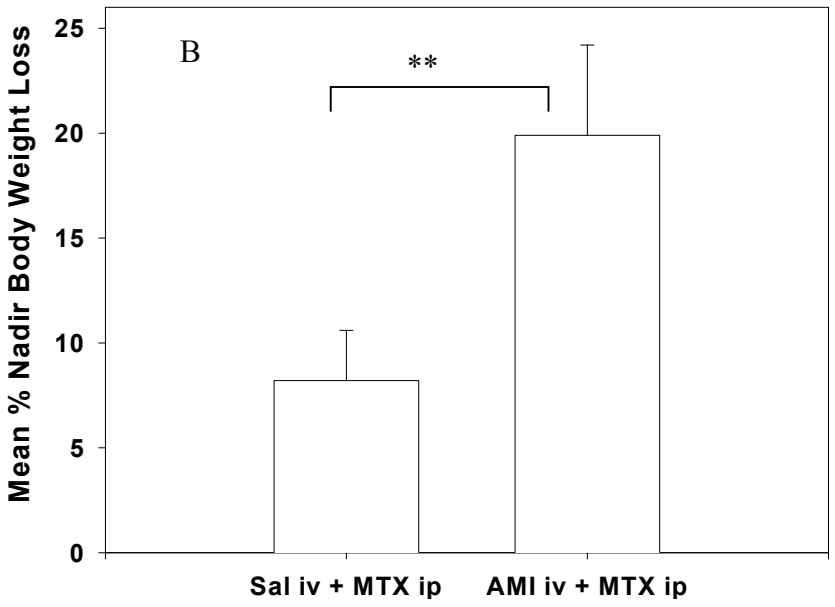
B
**
Mean % Nadir Body Weight Loss
25
20
15
10
5
0
Sal iv + MTX ip
AMI iv + MTX ip

Fig. 7

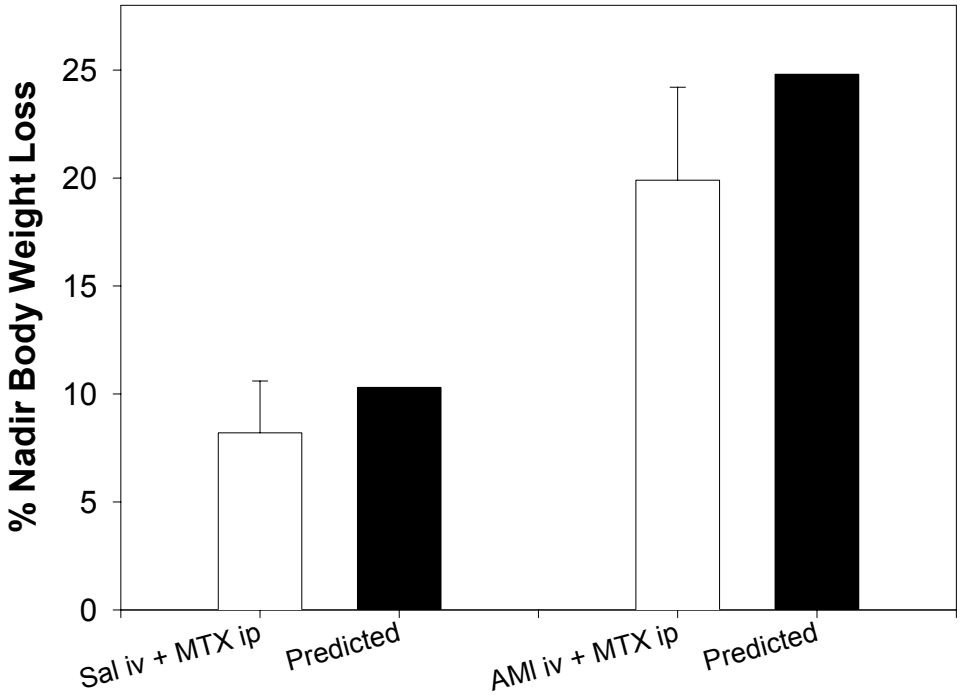
% Nadir Body Weight Loss
25
20
15
10
5
0
Sal iv + MTX ip
Predicted
AMI iv + MTX ip
Predicted

Fig. 8

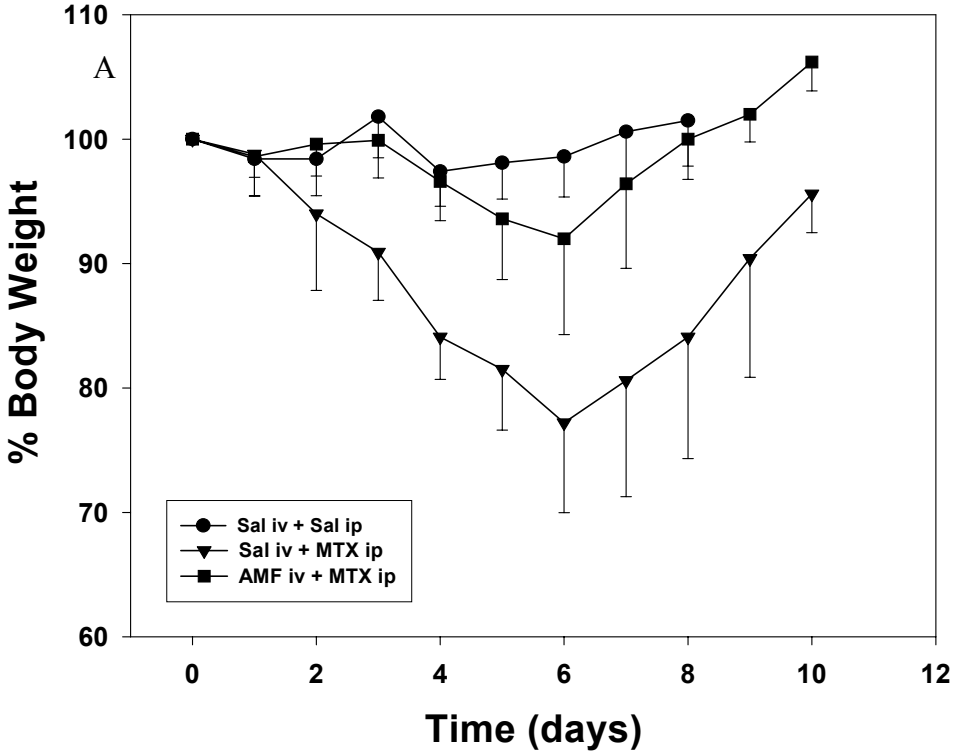
A
% Body Weight
Time (days)
Sal iv + Sal ip
Sal iv + MTX ip
AMF iv + MTX ip

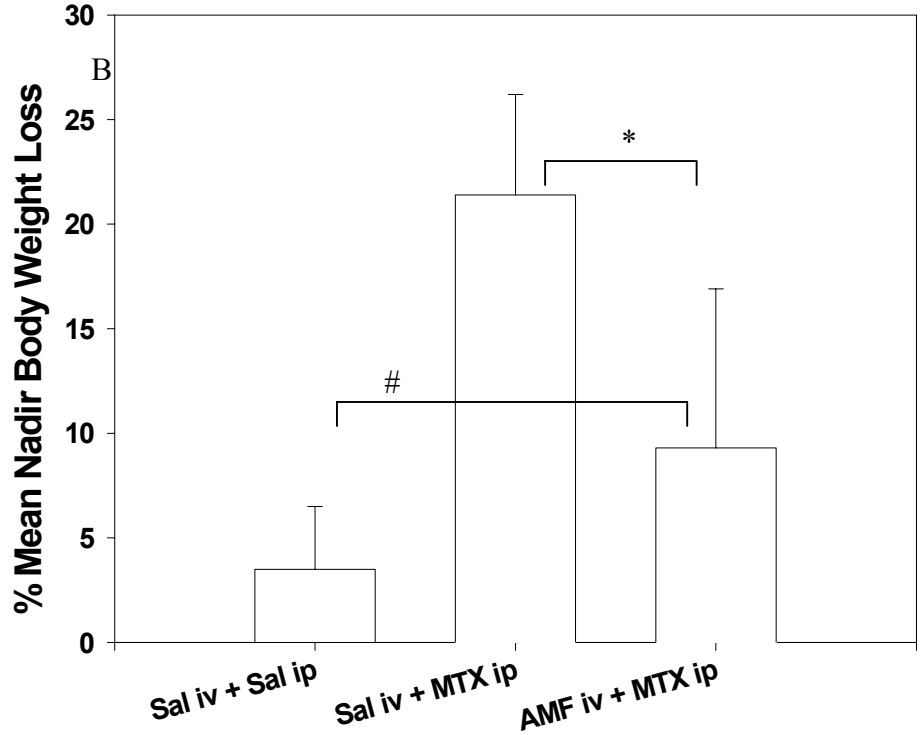
B
% Mean Nadir Body Weight Loss
*
#
Sal iv + Sal ip
Sal iv + MTX ip
AMF iv + MTX ip

Fig. 9.

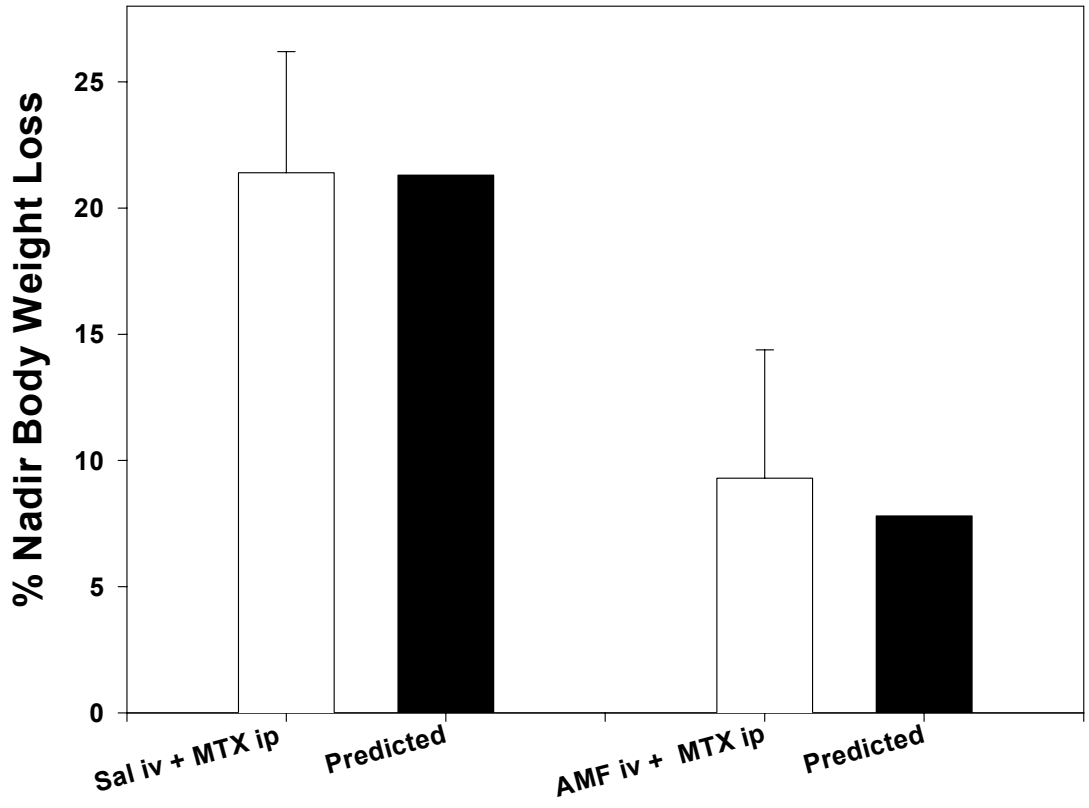
% Nadir Body Weight Loss
25
20
15
10
5
0
Sal iv + MTX ip
Predicted
AMF iv + MTX ip
Predicted

Table 1

Pharmacokinetic parameters utilized in the simulations with the PKPD model.

	MTX	AMI	AMF
Ka (h^{-1})	5.3	-	-
CL (L/kg/h)	2.8	0.000695	0.008
V (L/kg)	2.2	0.05	0.05
Rf	-	0.75 to 1	0 to 0.5
k_{on} (M^{-1} h^{-1})	-	10^8 – 10^{10}	10^8 – 10^{10}
k_{off} (M^{-1})	-	10	10

Ka, CL, and V for MTX were obtained from pharmacokinetic modeling of MTX pharmacokinetic data in mice. CL and V for AMI and AMF were based on literature data. Rf values for AMI and AMF were selected as discussed in the text.

CHAPTER FIVE

Utility of anti-methotrexate Fab fragments to optimize intraperitoneal methotrexate therapy in a murine model of peritoneal cancer

Abstract

Anti-drug antibodies may be used to impart regio-specific alterations in drug disposition, potentially enhancing the therapeutic selectivity of intracavitary chemotherapy. In the present study, we tested the hypotheses that systemic therapy with anti-methotrexate antibodies would allow increases in the maximum tolerated dose of intraperitoneal methotrexate (MTX) and allow increases in the therapeutic efficacy of intraperitoneal MTX in a murine model of peritoneal cancer. Monoclonal anti-MTX Fab antibody fragments (AMF) were produced, purified, and characterized. AMF pharmacokinetics were determined following i.v. bolus injection (0.4g/kg) and s.c. bolus injection (0.4g/kg, 0.8g/kg, 2.2g/kg). MTX efficacy was investigated in mice bearing peritoneal sarcoma 180 tumors, following administration of MTX via 72h i.p. infusion at 1.9mg/kg, 2.8mg/kg, 3.8mg/kg, and following combination therapy of 7.5mg/kg or 10mg/kg i.p. MTX (72h infusion) and 4.2g/kg s.c. AMF. The mean terminal half-life of AMF was found to be 10.9±3.3 h and was not dose–dependent, and s.c. bioavailability was 28±7% at 2.2 g/kg. In mice bearing peritoneal tumors, the maximally tolerated dose of i.p. MTX increased from 1.9 mg/kg (following i.p. MTX alone) to 10 mg/kg (with co-administration of s.c. AMF). Median survival times for saline-treated control animals and animals receiving i.p. MTX (1.9 mg/kg, 2.8 mg/kg, 3.8 mg/kg) were 9, 12, 11, and 7 days, respectively. However, for animals receiving combination therapy with i.p. MTX 7.5mg/kg or 10 mg/kg and 4.2 g/kg s.c. AMF, median survival time increased to 18 and 14 days, respectively. As such, the present data suggest that systemic administration of AMF may allow increases in

the maximally tolerated dose of i.p. MTX, and allow increases the therapeutic efficacy of i.p. MTX chemotherapy of peritoneal tumors.

Introduction

This research group has been investigating a targeting approach that attempts to improve the selectivity of intraperitoneal chemotherapy for peritoneal tumors (Balthasar and Fung, 1994; Balthasar and Fung, 1996). The approach combines i.p. chemotherapy with systemic administration of anti-drug antibodies to impart site-selective alterations in drug disposition. It is hypothesized that the presence of anti-drug antibodies in the systemic circulation would lead to rapid complexation of the drug diffusing out of the peritoneum and entering the blood, potentially reducing systemic free drug exposure and minimizing extravascular drug distribution.

Previous studies in rats demonstrated that i.v. administration of anti-methotrexate antibody fragments with simultaneous i.p. administration of MTX led to reductions in peak plasma concentrations of unbound MTX and in the area under the unbound MTX plasma concentration v. time curve, without significantly altering peritoneal MTX exposure (Balthasar and Fung, 1996). Additionally, AMF enhanced the urinary elimination of MTX and decreased the apparent volume of MTX distribution. In more recent toxicity studies conducted in mice, i.v. AMF therapy was found to decrease MTX-induced body weight loss and MTX-related mortality, following i.p. MTX administration (Lobo and Balthasar, 2002).

In this report, we have tested the hypothesis that AMF will allow increases in the maximally tolerated dose of i.p. MTX, and we investigated the anti-tumor efficacy

of MTX and MTX/AMF combination therapy in a peritoneal tumor model in mice. Additionally, the pharmacokinetics of AMF were investigated in mice following i.v. and s.c. administration.

Methods

Materials

MTX (>99.9% purity), xylazine, Tween-20, bovine serum albumin and Fab specific goat anti-mouse-antibody-alkaline phosphatase were obtained from Sigma (St Louis, MO). ALZET® micro-osmotic pumps (1003D), for 3 day constant-rate infusion, were obtained from Alza Corporation (Palo Alto, CA). Swiss Webster male mice, 5-6 week-old, (20-25 g) were obtained from Harlan Sprague-Dawley Inc. (Indianapolis, IN), and housed on a standard light / dark cycle, with continuous access to food and water. Cell culture media (RPMI 1640), certified fetal bovine serum, and gentamicin were obtained from Invitrogen Corporation (Grand Island, NY). Sarcoma 180 cells were obtained from American Type Cell Culture (Manassas, VA).

AMF Production

AMF was produced, purified, and characterized as reported previously (Lobo et al., 2002). Briefly, anti-MTX IgG was produced from hybridoma cells (developed in this laboratory), purified by affinity chromatography, and digested with papain. AMF was purified from undigested IgG, Fc fragments, and secondary digestion products through hydroxyapatite chromatography (BioRad Laboratories, Hercules, CA). Concentrated AMF in PBS (pH 7.4) was passed through Detoxi endotoxin removing gel (Pierce, Rockford, IL) at least 3 times prior to use. Endotoxin concentrations in antibody solutions used in vivo were lower than 20

ng/ml; as such, animals were exposed to doses of endotoxin that were well below those associated with toxicity in mice (Khan et al., 2000).

ELISA Assay for AMF

Assays were conducted using Maxisorp 96-well microplates (Nunc, Rosklide, Denmark). Bovine serum albumin-methotrexate conjugates (10 μg/ml in 0.02 M Na_2HPO_4, no pH adjustment), 0.25 ml, was placed into each assay well, and assay plates were incubated overnight at 4°C. Following incubation, plates were washed three times with a phosphate buffer (PB-Tween) consisting of 0.05% Tween 20 and 0.02 M Na_2HPO_4 (no pH adjustment), and rinsed twice with distilled water. Diluted plasma samples and standards were added and plates were incubated 2 h at room temperature. Standards were made by diluting a stock concentration of purified AMF to concentrations of 0, 25, 50, 100, 250 and 350 ng/ml with phosphate buffered saline (pH 7.4) containing 1% blank mouse plasma (Hilltop Lab Animals, Inc., Scottdale, PA). After incubation, the plate was washed with PB-Tween, rinsed with distilled water, and a secondary antibody conjugate was applied (0.25 ml, Fab specific goat anti-mouse-antibody-alkaline phosphatase, diluted 1:500 in PB Tween and 1% bovine serum albumin). After incubating with the secondary antibody at room temperature for 1 h, plates were washed with PB-Tween, rinsed with distilled water, and p-nitro phenyl phosphate (Pierce) was applied (4 mg/ml, 0.2 ml, pH 9.8). Plates were analyzed with a microplate reader (Spectra Max 340PC, Molecular Devices), which assessed the change in absorbance at 405 nm with time (dA/dt). Standard curves, using

standards run on each assay plate (0-350 ng/ml), were created to relate AMF concentration to dA/dt. The limit of quantitation of this assay was 25 ng/ml; intra- and inter-assay variability were found to be less than 13%.

AMF Pharmacokinetics

AMF was administered via i.v. bolus injection (0.4 g/kg) or via s.c. bolus injection (0.4 g/kg, 0.8 g/kg and 2.2 g/kg) to groups of three Swiss Webster mice. Animals receiving i.v. AMF were instrumented with jugular vein cannulas 3 days prior to experimentation. Following i.v. bolus injection, blood samples (10-20 μl) were collected from the saphenous vein at 15, 30, 60, 120, 180, 360, 540, 1440, 2880 min. After s.c. bolus injection, blood samples were collected at 30, 60, 120, 180, 360, 720, 1440, 2880 min. Plasma was obtained after centrifuging the blood at 10,000 *g* for 2 min, and AMF concentration was determined using the ELISA. The area under the plasma concentration v. time curves, AUC, was determined by non-compartmental analysis with WinNonlin software (Pharsight Corporation), and bioavailability (F) was calculated as $F = \frac{AUC_{sc}}{AUC_{iv}} \bullet \frac{Dose_{iv}}{Dose_{sc}}$.

Toxicity studies

In previous investigations of MTX-induced toxicity in Swiss-Webster mice, the maximally tolerated i.p. dose of MTX, infused over 72 h, was 3.8 mg/kg (Lobo and Balthasar, 2002). In this same investigation, 72 infusion of 5 mg/kg and 10 mg/kg MTX led to a mean nadir weight-loss of 15.6 ± 5.3% and 23.8 ± 3.3%, respectively. In the present study, MTX-induced toxicity was investigated in two

groups of 4-5 animals treated with 10 mg/kg i.p. MTX, infused over 72 h, with or without coadministration of s.c. AMF (4.2 g/kg, administered as two injections of 2.1 g/kg, separated by 31 h). MTX infusions were delivered via osmotic pumps attached to peritoneal cannulas. Briefly, animals were instrumented with osmotic pumps (pre-equibrated overnight at 37ºC in 0.9% sodium chloride solution) under ketamine / xylazine (100/10 mg/kg) anesthesia. Pumps were placed on the dorsal side near the shoulder blade, cannulas were tunneled subcutaneously, and inserted into the peritoneal cavity through a small incision made through the abdominal muscle layer. Animal body weight was recorded daily. Weight loss at nadir is reported as a percentage of animal weight just prior to pump implantation. In cases of animal death, weight loss is reported as the maximal percent weight loss prior to expiration.

Efficacy studies

MTX efficacy was investigated in Swiss Webster mice inoculated i.p. with sarcoma 180 cells. Prior to injection, sarcoma 180 cells were maintained in culture with RPMI 1640 media supplemented with 20 nM folic acid, 10% fetal bovine serum and 100 μg/ml gentamicin. One day prior to the initiation of drug treatment, cells were washed, suspended in sterile 0.9% sodium chloride, and injected into animals i.p. (10^6 cells in 0.5 ml). MTX was administered via constant-rate i.p. infusion, as described above, at doses of 1.9 mg/kg, 2.8 mg/kg, and 3.8 mg/kg (n = 10 animals/group). Additionally, MTX/AMF combination therapy was investigated where MTX was administered i.p. over 72 h (7.5 mg/kg

or 10 mg/kg) with s.c. administration of AMF (4.2 g/kg, administered as two 2.1 g/kg s.c. doses separated by 31 h, n = 3-5). Animal weight was recorded daily, and animals were sacrificed when body weight increased to 120% of animal weight on the day of tumor inoculation. Following sacrifice, animals were inspected for evidence of peritoneal tumors. The maximally tolerated dose of MTX in tumor bearing mice was defined as the highest dose for which no deaths occurred prior to the first death of control animals (i.e., animals inoculated with tumor, but not treated with drug). The percent increase in life span (%ILS) was calculated as: %ILS = (median survival time in treated animals - median survival time in control animals) / median survival time in control animals x 100.

Statistics

Data are expressed as mean and the standard deviation. One-way analysis of variance with Bonferroni post-test was applied to compare half-lives. Unpaired two-tailed student's *t*-tests were applied to compare the mean nadir body weight loss. Mortality rates were compared using the Binomial proportion test. Survival curves were compared for significance with the logrank test and hazard ratio. Statistical analysis was performed using InStat and Prism software (Graph Pad Software Inc, San Diego, CA).

Results

AMF Pharmacokinetics

The AMF concentration time profile following intravenous and subcutaneous administration is shown in Fig. 1. Non-compartmental analysis of the data is summarized in Table I. The terminal half of AMF was found to be 10.9 ± 3.3 h, and was not dependent on dose (in the dose range of 0.4 to 2.2 g/kg, $p > 0.05$), or on the route of administration (i.v. or s.c., $p>0.05$). AMF s.c. bioavailability was low and variable, ranging from 0.09 ± 0.01 at 0.8 g/kg to 0.28 ± 0.07 at 2.2 g/kg.

Toxicity studies

Animal body weight v. time is shown in Fig. 2A. For animals receiving 10 mg/kg i.p. MTX with 4.2 g/kg AMF, mean weight loss at nadir was found to be (16.6 ± 5.8%, n=4), which was significantly different that observed for animals receiving 10 mg/kg i.p. MTX alone (25.8 ± 3.7%, n=5, $p<0.05$). Treatment-associated mortality was markedly different between the two treatment groups; all animals receiving MTX alone died, whereas all animals receiving MTX/AMF combination therapy survived ($p<0.01$).

MTX Efficacy in peritoneal tumor bearing mice

The survival curves for tumor bearing control animals and for tumor bearing animals treated with i.p. MTX (1.9 mg/kg, 2.8 mg/kg, and 3.8 mg/kg) are shown in Fig. 3. The median survival times and %ILS for all the treatment groups are summarized in Table II. The highest tolerated MTX dose was observed to be 1.9

mg/kg, and animal survival following this dose of MTX was significantly different from that observed for control animals ($p<0.0001$). Following 2.8 mg/kg MTX, animal survival was not significantly different compared to that of control animals ($p>0.05$), and after 3.8 mg/kg MTX, survival time was significantly reduced relative to controls ($p < 0.05$).

Following combination therapy with i.p. MTX (7.5 mg/kg or 10 mg/kg) and s.c. AMF (4.2 g/kg), median survival time was increased relative to the control group and the MTX treated groups (Fig. 4). Survival curves were found to be significantly improved relative to that observed for the control group (7.5 mg/kg i.p. MTX / s.c. AMF: $p<0.005$; 10 mg/kg i.p. MTX / s.c. AMF: $p<0.05$).

Discussion

Intraperitoneal chemotherapy has been investigated as a means of improving the selectivity of chemotherapy of intra-abdominal tumors (e.g., ovarian, gastro-intestinal, pancreatic and colorectal cancers) (Cintron and Pearl, 1996; Markman et al., 1993; Patel and Benjamin, 2000). Much of the interest in i.p. chemotherapy stems from predictions made by Dedrick and co-workers, which suggested that i.p. drug administration would allow much greater peritoneal drug exposure relative to systemic drug exposure (Dedrick et al., 1978). Although clinical pharmacokinetic studies supported the predictions of Dedrick et al., the extent of peritoneal drug exposure afforded by i.p. chemotherapy appears to be insufficient to alter the site-specificity of chemotherapeutic cytotoxicity, as systemic toxicity remains dose-limiting, and only modest improvement in therapeutic benefit has been observed following i.p. chemotherapy (Alberts et al., 1996).

Dedrick et al. also proposed that the selectivity of i.p. chemotherapy may be enhanced through systemic administration of antidotal agents capable of antagonizing drug that diffuses out of the peritoneal cavity (Dedrick et al, 1978). The combination of i.p. chemotherapy and i.v. administration of antidotes has been investigated with a few drugs, for example: cisplatin (with systemic administration of sodium thiosulfate), mafosfamide (with systemic administration of cysteiene), and neocarzinostatin (with systemic administration of tiopronin) (Hasuda et al., 1989; Howell and Taetle, 1980; Wagner et al., 1986). However, such combinations have found relatively little application in the clinical treatment of intra-abdominal cancers, perhaps due to slow rates of drug inactivation in vivo

(Howell, 1988; Howell et al., 1982), or perhaps due to observations of decreased drug efficacy (presumably owing to neutralization of drug in the peritoneum) (Wagner et al, 1986).

This research group has been interested in utilizing anti-drug antibodies and antibody fragments as neutralizing agents to reduce systemic toxicities associated with i.p. chemotherapy (Balthasar and Fung, 1994; Balthasar and Fung, 1996). Antibodies may be raised to bind many drugs with high affinity and with high rates of association; additionally, due to their polar nature and large molecular size, antibodies would be expected to exhibit low rates of entry into the peritoneal cavity. Several preclinical reports have shown that anti-chemotherapeutic antibodies may be used to reduce drug-related mortality and drug-induced body weight loss; however, the application of anti-drug antibodies to increase the selectivity or efficacy of i.p. chemotherapy of peritoneal tumors has not yet been investigated (Balsari et al., 1991; Gutowski et al., 1995; Sardini et al., 1992).

To develop this targeting strategy, initial pre-clinical pharmacokinetic studies were conducted with i.p. digoxin / i.v. anti-digoxin Fab and i.p. MTX / i.v. anti-MTX polyclonal antibodies. These studies demonstrated that systemic antibody administration could reduce systemic tissue exposure to drug, and reduce systemic toxicity, without altering peritoneal drug exposure (Balthasar and Fung, 1994; Balthasar and Fung, 1995; Balthasar and Fung, 1996). Murine anti-MTX monoclonal antibodies and Fab fragments were recently developed in this

laboratory, which has now allowed rapid generation of large quantities of antibody, and thereby enabled investigation of the hypotheses that systemic administration of anti-drug antibodies would increase the maximal tolerated i.p. chemotherapeutic dose, and increase the efficacy of i.p. chemotherapy of peritoneal tumors.

Testing these hypotheses required the administration of high doses of anti-MTX Fab. Due to technical difficulties associated with intravenous administration of large doses of antibody (e.g., limited solubility of antibody, limited capacity of infusion pumps, etc.), pharmacokinetic studies were conducted to assess AMF bioavailability following s.c. administration. AMF bioavailability was found to be similar after s.c. administration of 0.4 g/kg and 2.2 g/kg (27±7% and 28±8%), suggesting dose-independent bioavailability. Although s.c. AMF bioavailability was far from complete, it was deemed to be sufficiently high to allow testing AMF/MTX combination therapy with s.c. AMF administration. Notably, AMF bioavailability was found to be significantly lower following s.c. administration of 0.8 g/kg relative to that observed following doses of 0.4 g/kg and 2.2 g/kg. This apparent difference in bioavailability may be an artifact, perhaps related to the high variability observed in AMF disposition, and the small sample sizes used in this pilot study (n=3). Additional pharmacokinetic studies will be conducted to develop a comprehensive characterization of AMF disposition, and to assist in future optimization of AMF/MTX combination therapy.

Prior to in vivo investigation, dosing regimens for AMF/MTX combination therapy were evaluated via computer simulations conducted with a pharmacokinetic-pharmacodynamic model (data not shown) (Lobo et al, 2002). These simulations were used to predict reductions in MTX toxicity provided by feasible, convenient, AMF administration regiments. Predicted toxicity results suggested that two s.c. bolus doses of 2.1 g/kg AMF, separated by 31 - 36 h, would provide satisfactory reductions in MTX-induced weight loss.

A preliminary toxicity study was conducted in tumor-free mice. Intraperitoneal infusion of MTX, 10 mg/kg, over 72 h led to profound weight loss (nadir % weight loss = 25.8 ± 3.7%), and mortality in 100% of treated animals (n=5). Combination therapy of i.p. MTX, 10 mg/kg over 72 h, and s.c. AMF, 4.2 g/kg, led to significantly reduced weight loss and mortality (16.6 ± 5.8, and 0%, respectively; n = 4).

The efficacy of MTX was investigated in mice bearing sarcoma 180 tumor cells in the peritoneum. From MTX toxicity studies in non-tumor bearing mice, the maximally tolerated dose of MTX infused as i.p. 72 h constant-rate infusion was observed to be 3.8 mg/kg (Lobo and Balthasar, 2002). In tumor bearing mice, 3.8 mg/kg dose of MTX was found to be toxic to the animals causing early deaths in 80% of the animals (within 7 days). Similar enhancements of chemotherapeutic toxicity in mice bearing peritoneal tumors have been previously reported for MTX and cyclophosphamide (Graczyk, 1981). It was observed that in tumor bearing

mice, the LD_{10} for MTX was 27% of the LD_{10} determined in non-tumor bearing mice and for cyclophosphamide the LD_{10} was 50% of the LD_{10} determined in non-tumor bearing mice. In the current study, the maximally tolerated dose for i.p. MTX (administered as 72 h constant-rate infusion) in tumor bearing mice was 1.9 mg/kg. At this dose, MTX provided an increase in median survival time relative to that observed in control animals (i.e., 12 d v. 9 d, 33 %ILS), and the associated survival curve was significantly different from that of control animals ($p<0.001$)(Fig. 3).

MTX efficacy and toxicity was also assessed following combination therapy with AMF (Fig. 4). Following combination therapy with 7.5 mg/kg or 10 mg/kg i.p. MTX and 4.2 g/kg s.c. AMF, no toxic deaths were observed, and median survival time increased to 18 d and 14 d, respectively (v. 9 d in control animals). As such, administration of AMF increased the maximally tolerated dose of MTX by more than 5-fold in the tumor bearing mice (1.9 mg/kg v. 10 mg/kg). Additionally, combined AMF/MTX therapy %ILS increased from 33% (MTX alone, 1.9 mg/kg) to 100% (7.5 mg/kg MTX / 4.2 g/kg AMF).

In this report, we have demonstrated that systemic AMF therapy may be used in combination with i.p. MTX chemotherapy, to reduce MTX-induced toxicity and increase the maximally tolerated dose of MTX. Additionally, our data suggest that AMF/MTX combination therapy may allow for improved efficacy of MTX chemotherapy of peritoneal tumors. It is plausible that further optimization may

be achieved by increasing the dose of anti-MTX Fab, or, perhaps, by altering the MTX/AMF administration regimens. As such, further investigation of this targeting strategy is warranted.

References

Alberts DS, Liu PY, Hannigan EV, R OT, Williams SD, Young JA, Franklin EW, Clarke Pearson DL, Malviya VK and DuBeshter B (1996) Intraperitoneal cisplatin plus intravenous cyclophosphamide versus intravenous cisplatin plus intravenous cyclophosphamide for stage III ovarian cancer [see comments]. *N Engl J Med* **335**:1950-1955.

Balsari A, Menard S, Colnaghi MI and Ghione M (1991) Anti-drug monoclonal antibodies antagonize toxic effect more than anti- tumor activity of doxorubicin. *Int J Cancer* **47**:889-892.

Balthasar JP and Fung HL (1994) Utilization of antidrug antibody fragments for the optimization of intraperitoneal drug therapy: studies using digoxin as a model drug. *J Pharmacol Exp Ther* **268**:734-739.

Balthasar JP and Fung HL (1995) High-affinity rabbit antibodies directed against methotrexate: production, purification, characterization, and pharmacokinetics in the rat. *J Pharm Sci* **84**:2-6.

Balthasar JP and Fung HL (1996) Inverse targeting of peritoneal tumors: selective alteration of the disposition of methotrexate through the use of anti-methotrexate antibodies and antibody fragments. *J Pharm Sci* **85**:1035-1043.

Cintron JR and Pearl RK (1996) Colorectal cancer and peritoneal carcinomatosis. *Semin Surg Oncol* **12**:267-278.

Dedrick RL, Myers CE, Bungay PM and DeVita VT, Jr. (1978) Pharmacokinetic rationale for peritoneal drug administration in the treatment of ovarian cancer. *Cancer Treat Rep* **62**:1-11.

Graczyk J (1981) Acute toxicity of methotrexate and cyclophosphamide in mice inoculated with malignant neoplasms. *Pol J Pharmacol Pharm* **33**:73-80.

Gutowski MC, Fix DV, Corvalan JR and Johnson DA (1995) Reduction of toxicity of a vinca alkaloid by an anti-vinca alkaloid antibody. *Cancer Invest* **13**:370-374.

Hasuda K, Kobayashi H, Kuroiwa T, Aoki K, Taniguchi S and Baba T (1989) Efficacy of two-route chemotherapy using intraperitoneal neocarzinostatin and its antidote, intravenous tiopronin, for peritoneally disseminated tumors in mice. *Jpn J Cancer Res* **80**:283-289.

Howell SB (1988) Intraperitoneal chemotherapy for ovarian carcinoma. *J Clin Oncol* **6**:1673-1675.

Howell SB, Pfeifle CL, Wung WE, Olshen RA, Lucas WE, Yon JL and Green M (1982) Intraperitoneal cisplatin with systemic thiosulfate protection. *Ann Intern Med* **97**:845-851.

Howell SB and Taetle R (1980) Effect of sodium thiosulfate on cis-dichlorodiammineplatinum(II) toxicity and antitumor activity in L1210 leukemia. *Cancer Treat Rep* **64**:611-616.

Khan AA, Slifer TR, Araujo FG, Suzuki Y and Remington JS (2000) Protection against lipopolysaccharide-induced death by fluoroquinolones. *Antimicrob Agents Chemother* **44**:3169-3173.

Lobo ED and Balthasar JP (2002) Pharmacokinetic-pharmacodynamic modeling of methotrexate toxicity in mice. *J Pharm Pharmacol,* for submission :Thesis Chapter 3, 71-107.

Lobo ED, Soda DM and Balthasar JP (2002) Application of pharmacokinetic-pharmacodynamic modeling to predict the kinetic and dynamic effects of anti-methotrexate antibodies in mice. *J Pharm Exp Ther,* for submission :Thesis Chapter 4, 108-148.

Markman M, Reichman B, Hakes T, Curtin J, Jones W, Lewis JL, Barakat R, Rubin S, Mychalczak B, Saigo P and et al. (1993) Intraperitoneal chemotherapy in the management of ovarian cancer. *Cancer* **71**:1565-1570.

Patel SR and Benjamin RS (2000) Management of peritoneal and hepatic metastases from gastrointestinal stromal tumors. *Surg Oncol* **9**:67-70.

Sardini A, Villa E, Morelli D, Ghione M, Menard S, Colnaghi MI and Balsari A (1992) An anti-doxorubicin monoclonal antibody modulates kinetic and dynamic characteristics of the drug. *Int J Cancer* **50**:617-620.

Wagner T, Mittendorff F and Walter E (1986) Intracavitary chemotherapy with activated cyclophosphamides and simultaneous systemic detoxification with protector thiols in Sarcoma 180 ascites tumor. *Cancer Res* **46**:2214-2219.

Captions for Figures

Fig. 1. AMF pharmacokinetics in mice. Mean plasma concentration of AMF following i.v. 0.4 g/kg bolus injection (●), and following s.c. bolus injections of 0.4 g/kg (○), 0.8 g/kg (▼), and 2.2 g/kg (▽). The mean and standard deviations for AMF concentration (n=3) are represented as symbols and error bars.

Fig. 2. Dose escalation of i.p. MTX therapy with s.c. AMF. Animals were treated with 10 mg/kg of i.p. MTX over 72 h infusion with or without coadministration of 4.2 g/kg of AMF given as two s.c. bolus injections of 2.1 g/kg (separated by 31 h). A. MTX-induced changes in body weight without AMF (●) and with AMF (▼). All animals treated with MTX alone (n=5) died whereas all animals treated with MTX/AMF (n=4) survived. B. MTX-induced mean nadir body weight loss with and without AMF ($p<0.05$).

Fig. 3. MTX efficacy in mice bearing peritoneal tumors. Each animal was inoculated with 10^6 sarcoma 180 cells (in 0.5 ml of sterile 0.9% NaCL) in the peritoneum (day 0). Treatment was initiated the next day. Control animals were treated with i.p. bolus injection of sterile 0.9% NaCL (0.5 ml). MTX treated animals received MTX as i.p. 72 h constant-rate infusion at 1.9 mg/kg, 2.8 mg/kg and 3.8 mg/kg. The survival time was defined as the time to death or the time to reach 120% body weight. Survival curves for (●) control animals and MTX treated animals at (○) 1.9 mg/kg, (▼) 2.8 mg/kg and (▽) 3.8 mg/kg. Survival in animals treated with 1.9 mg/kg MTX was significantly different from the control

animals ($p<0.001$). Survival of animals treated with 3.8 mg/kg MTX was significantly reduced relative to the controls ($p<0.05$).

Fig. 4. Comparison of MTX efficacy with or without co-administration of anti-MTX Fab fragments. Each animal was injected with 10^6 sarcoma 180 cells (in 0.5 ml sterile 0.9% NaCL) into the peritoneum (day 0). Treatment was initiated the next day. MTX efficacy at the maximally tolerated dose of i.p. MTX (1.9 mg/kg) was compared to that observed following AMF/MTX combination therapy of i.p. MTX, 72 h infusion (7.5 mg/kg or 10 mg/kg), and s.c. AMF (given as two s.c. bolus injections of 2.1 g/kg). The percent surviving animals treated with (●) 1.9 mg/kg MTX alone, (▼) 7.5 mg/kg MTX + 4.2 g/kg AMF and (○) and 10 mg/kg MTX + 4.2 g/kg AMF.

Fig. 1

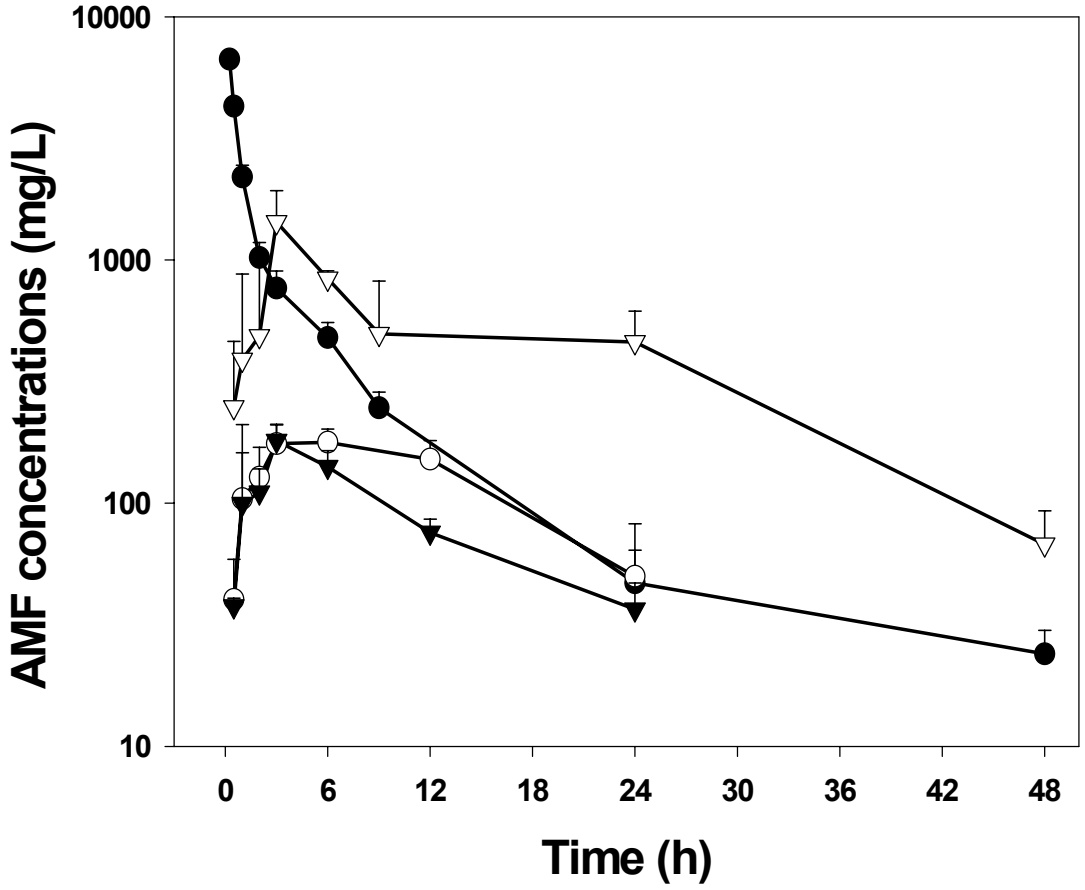
10000
1000
100
10
AMF concentrations (mg/L)
0
6
12
18
24
30
36
42
48
Time (h)

Fig. 2

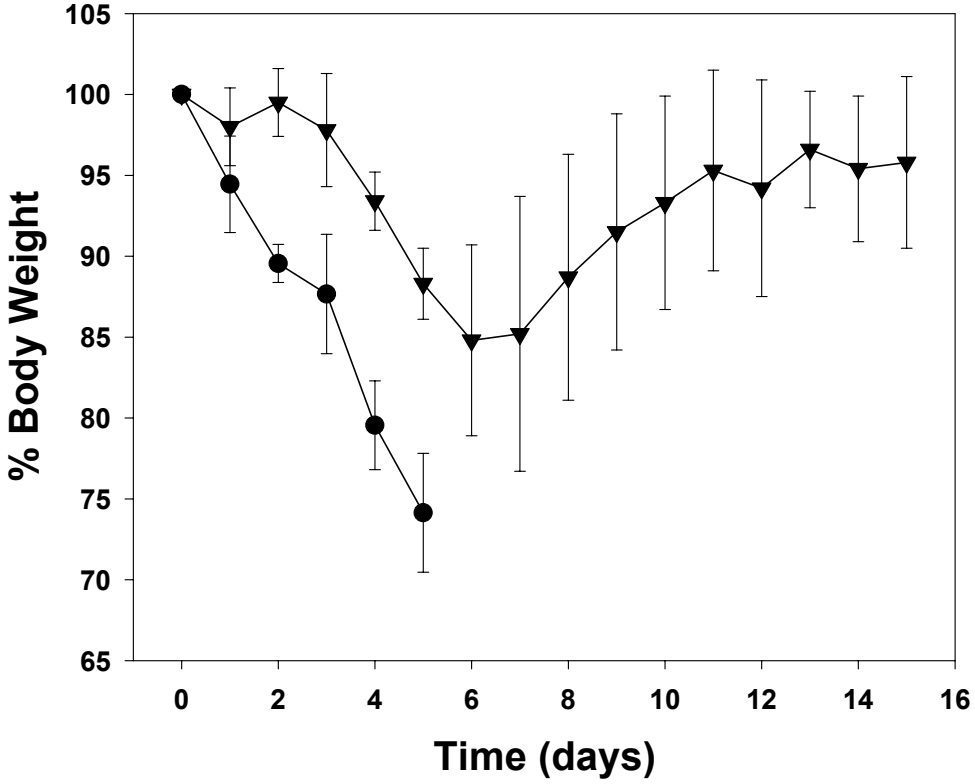
% Body Weight
105
100
95
90
85
80
75
70
65
0
2
4
6
8
10
12
14
16
Time (days)

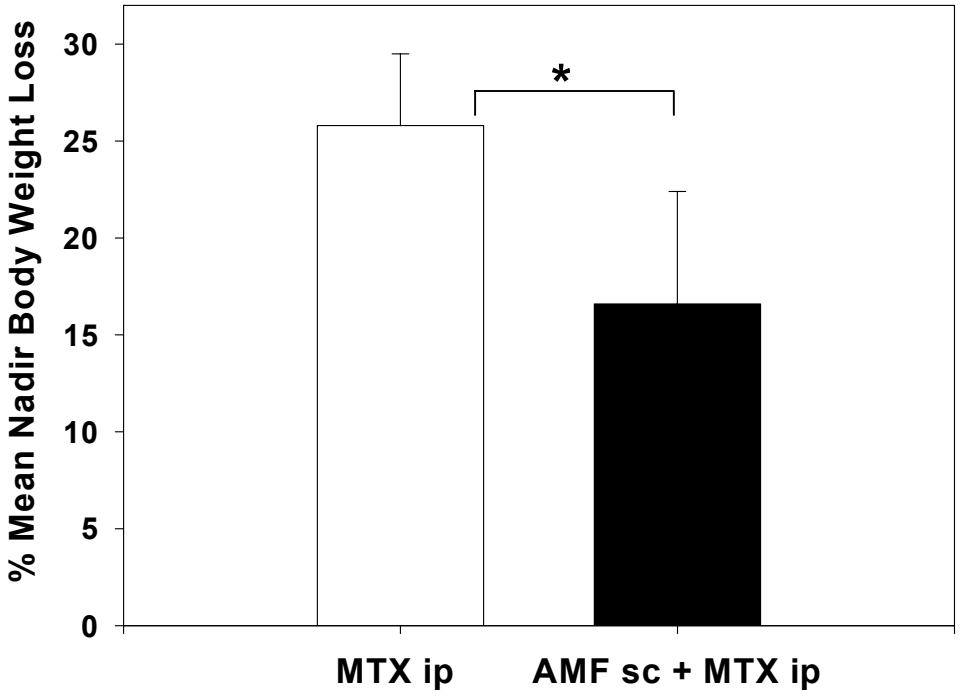
% Mean Nadir Body Weight Loss
30
25
20
15
10
5
0
*
MTX ip
AMF sc + MTX ip

Fig. 3

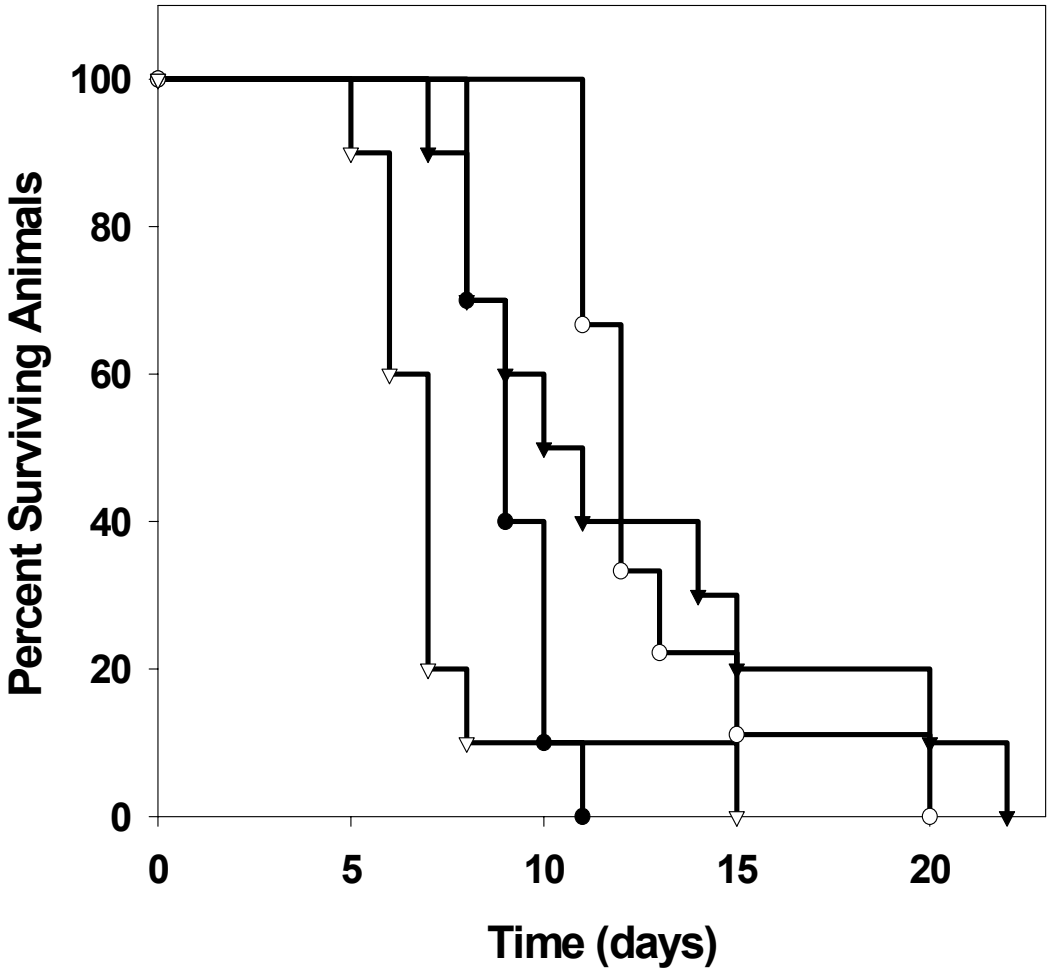
Percent Surviving Animals
100
80
60
40
20
0
0
5
10
15
20
Time (days)

Fig. 4

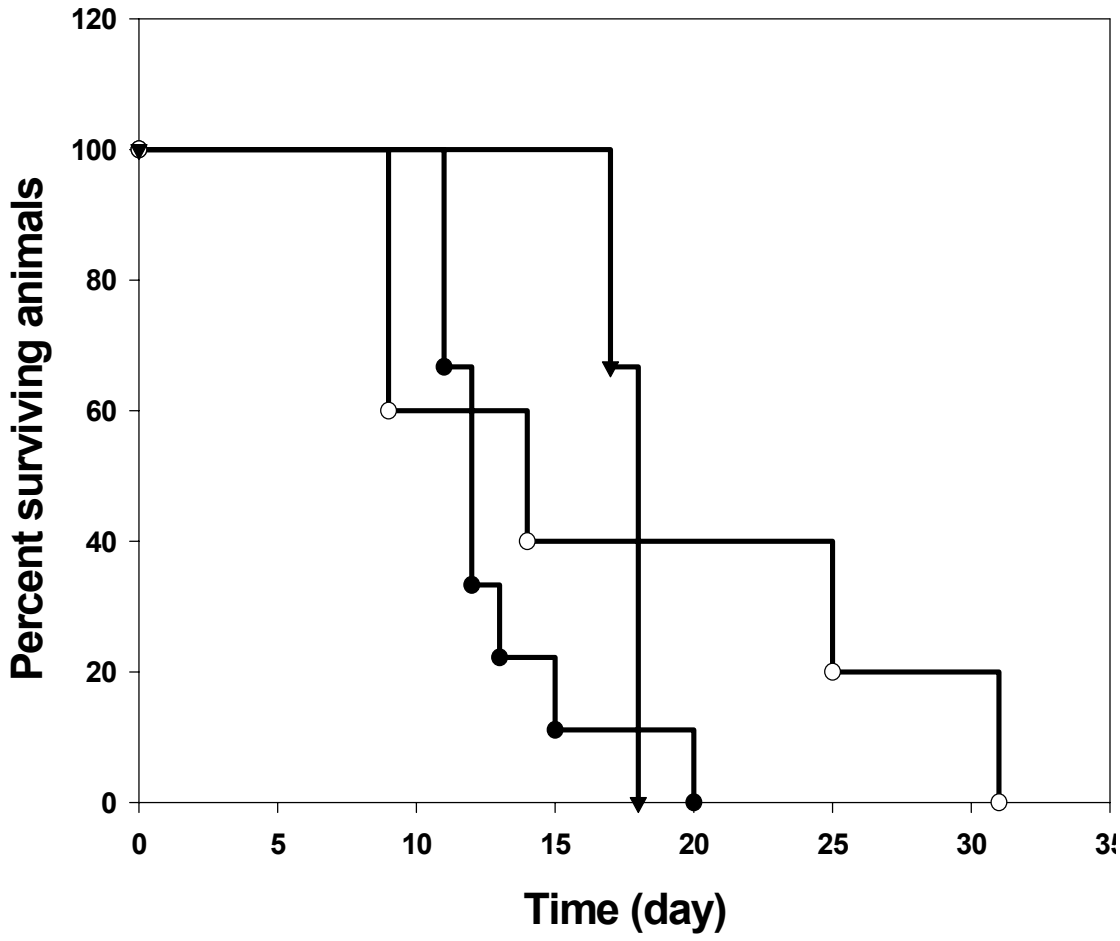
120
100
80
60
40
20
0
Percent surviving animals
0
5
10
15
20
25
30
Time (day)

Table 1. Non-compartmental analysis of AMF pharmacokinetics in mice[a]

	i.v. 0.4 g/kg	s.c. 0.4 g/kg	s.c. 0.8 g/kg	s.c. 2.2 g/kg
AUC (mg/L.min)	840,000 ± 2,600	225,000± 63,000	157,000 ± 14,300	1,300,000 ± 309,700
F	-	0.27 ± 0.07	0.09 ± 0.01	0.28 ± 0.07
$t_{1/2}$	8.8 ± 1.4	8.5 ± 3.7	9.5 ± 2.3	11.9 ± 2.6
CL (ml/kg/h)	28.6 ± 0.1	-	-	-
Vss (ml/kg)	191.6 ± 41.4	-	-	-

[a]AUC, area under the plasma concentration time curve from 0 to infinity; CL, systemic clearance; Vss, volume of distribution at steady-state; and λ, negative terminal slope of ln (AMF concentration) v time curve. Parameter values were obtained using WinNonlin. $t_{1/2}$, terminal half-life was estimated as 0.693/λ and F, the fraction absorbed on s.c. administration was calculated as (s.c. AUC/ i.v. AUC) x (i.v. dose/ s.c. dose).

Table II. Summary of MTX efficacy in mice bearing peritoneal tumors.

[a]Dosing protocol	N	MST (days)	% ILS	% Toxic deaths
Control	10	9	-	-
MTX 1.9 mg/kg	9	12	33	0
MTX 2.8 mg/kg	10	11	22	10
MTX 3.8 mg/kg	10	7	-	80
sc AMF+MTX 10 mg/kg	5	14	55	0
sc AMF+MTX 7.5 mg/kg	3	18	100	0

a Dosing protocol, control animals received bolus injection of sterile 0.9% NaCL; MTX was infused at constant-rate over 72 h; AMF was given as two s.c. bolus injections of 2.2 g/kg at 31 h interval; N, number of animals; MST, median survival time; % ILS, percent increase in life span calculated as (Treated MST – Control MST) / Control MST x 100. Toxic deaths, percent of deaths in animals within a week.

CHAPTER SIX

Pharmacodynamic modeling of chemotherapeutic effects: Application of a transit-compartment model to characterize methotrexate effects in vitro.

Abstract

The time-course of chemotherapeutic effect is often delayed relative to the time-course of chemotherapeutic exposure. In many cases, this delay is difficult to characterize mathematically through the use of standard pharmacodynamic models. In the present work, we investigated the relationship between methotrexate (MTX) exposure and the time-course of MTX effects on tumor cell growth in culture. Two cancer cell lines, Ehrlich ascites cells and sarcoma 180 cells, were exposed for 24 h to MTX concentrations that varied more than 700-fold (0.19-140 μg/ml). Viable cells were counted on day 1, 3, 5, 7, 9, 11, 13, 15, 17, 20, 22, and 24 for Ehrlich ascites cells and on day 1, 2, 3, 5, 7, 9, 11, 13, 14, 15, 17, 19 and 21 for sarcoma 180 cells, through the use of a tetrazolium assay. Although MTX was removed 24 h after application, cell number reached nadir values more than 100 hours after MTX exposure. Data from each cell line were fitted to three pharmacodynamic models of chemotherapeutic cell-killing, including a cell cycle phase specific model, phase non-specific model, and a transit compartment model (based on the general model recently reported by Mager and Jusko, Clin Pharmacol Ther 70:210-216, 2001). The transit compartment model captured the data much more accurately than the standard pharmacodynamic models, with correlation coefficients ranging from 0.86–0.999. This report shows the successful application of a transit compartment model for characterization of the complex time-course of chemotherapeutic effects; such models may be very useful in the development of optimization strategies for cancer chemotherapy.

Keywords: methotrexate, cell growth inhibition, modeling, chemotherapeutic effect, transit-compartment model.

Introduction

Although several chemotherapeutics demonstrate short elimination half-lives (e.g., less than 12 h),[1,2] maximal clinical effects (and toxicities) often occur 14-21 days following drug administration.[3-5] As such, peak drug concentrations often precede peak drug effects by days or weeks, greatly complicating attempts to relate the time-course of drug exposure to the time-course of drug effect. Such pharmacokinetic – pharmacodynamic (PKPD) relationships may be of great value, as they may facilitate the individualization and optimization of chemotherapy.

Perhaps due to the inherent difficulties, relatively few PKPD modeling approaches have been developed to characterize the time-course of chemotherapeutic effects.[6-8] In lieu of time-course models, PKPD individualization efforts have largely attempted to relate a time-averaged value of drug exposure (e.g., the area under the plasma concentration – time curve, AUC) to peak effect or peak toxicity (e.g., nadir white blood cell count).[9-13] Unfortunately, such 'static' approaches are of limited value, as these models do not predict the time-course of effect and, thus, may not be used to predict optimal schedules of drug administration. Additionally, it is desirable to relate effects to the entire time-course of drug exposure, because chemotherapeutic effects are often found to be 'protocol-dependent' (i.e., dependent on the duration of drug administration and on the duration of drug exposure),[14-16] where identical AUCs produce markedly different effects.

Recently, a simple, robust approach has been introduced to model PKPD time delays through the use of transit compartments.[17] In the present study, we wished to evaluate the transit compartment model for use in relating the time-course of chemotherapeutic exposure to the time-course of chemotherapeutic effect. Representative data were collected following investigations of the cytotoxic effects of MTX, an established anti-cancer drug, against two cancer cell lines in vitro. Consistent with expectations, the peak effect (i.e., the time to reach the lowest cell number following MTX treatment) was delayed tremendously relative to the time-course of MTX exposure in this experimental system. These data were modeled with the transit compartment model and with two established PKPD models of chemotherapeutic effects (i.e., a phase specific model and a phase non-specific model).[17-20] Relative to the established models, the transit compartment model was found to provide superior fitting of the data; consequently, this model may find broad application in the characterization of chemotherapeutic effects.

METHODS

Materials

MTX and 3-[4,5-dimethylthiazol-2-yl]-2,5-diphenyl-tetrazolim bromide (MTT) were purchased from Sigma Chemical (St. Louis, MO). Sodium dodecyl sulfate (SDS) was obtained from Bio-Rad laboratories (Hercules, CA). Cell culture media (RPMI 1640), certified fetal bovine serum, and gentamicin were obtained from

Invitrogen Corporation (Grand Island, NY). Ehrlich ascites cells and sarcoma 180 cells were obtained from American Type Cell Culture (Manassas, VA).

In-vitro cell growth inhibition

The cancer cell lines were grown within a humidified, 5% CO_2 incubator at 37°C. RPMI 1640 media was prepared to contain approximately 10 ng/ml folic acid, and was supplemented with 10% fetal bovine serum and gentamicin (100 μg/ml). Cell suspensions containing 10,000 cells / ml and 5,000 cells / ml were prepared for Ehrlich ascites cell and sarcoma 180, respectively, and 0.1 ml of suspension (i.e., containing 1000 or 500 cells) was dispensed into wells of twelve 96-well plates. After allowing the cells to attach for 48 h, media was aspirated through a 25-gauge needle. Preliminary studies demonstrated that this method of aspirating media did not result in significant loss of cells (recovery was found to be 100.7 ± 6.3%, n = 12). Following aspiration, 100 μl of media containing MTX (0.19 μg/ml, 2.0 μg/ml, 14.0 μg/ml, or 140.0 μg/ml) was added. Each plate was prepared in identical fashion, with 4 wells used for each concentration of MTX. Cells were incubated with MTX for 24 h, and media was then aspirated. Each well was then washed 4 times with 100 μl MTX-free media. Cell number was determined on day: 1, 3, 5, 7, 9, 11, 13, 15, 17, 20, 22, and 24 for Ehrlich ascites cells and on day: 1, 2, 3, 5, 7, 9, 11, 13, 14, 15, 17, 19 and 21 for sarcoma 180 cells, using one plate per assay, via the tetrazolium assay.[21] Briefly, on the day of analysis, media was aspirated from all wells of the assay plate. 100 μl of fresh media and 25 μl of MTT solution (5 mg/ml in phosphate saline buffer, pH 7.4) were added to

each well, and the plate was then incubated for 4.5 h at 37°C in the incubator. After incubation, 100 μl of 10% SDS-HCL (0.01 M HCL) was added to each well, and the plate was incubated overnight at 37°C. Absorbance in each well was determined at 590 nm using a plate reader (Spectromax, Molecular Devices). Cell number was determined through the use of a standard curve (run on each plate) that related absorbance to cell count (linear ranges: 156 to 10,000 cells for sarcoma 180 and 156 to 12,500 for Ehrlich ascites cells).

Pharmacodynamic modeling

Three pharmacodynamic models were used to fit the time-course of MTX effects: (a) a cell-cycle phase non-specific model of cytotoxicity, (b) a phase specific model of cytotoxicity, and (c) a cell kill model that was based on the general transit compartment model of Mager and Jusko.[17] Schematic representations of the models are shown in Figure 1. Differential equations were as follows:

(a) Phase non-specific model

$$\frac{dC}{dt} = kng \cdot C - K \cdot C$$

$$K = \frac{K_{\max} M}{K_{50} + M}$$

Where C represents the cell number, kng is a first order rate constant of net growth (mathematically equivalent to a first order growth rate constant [kg] minus a first order death rate constant [kd]; i.e., kng = kg - kd), K is a non-linear function

of MTX cell-kill, which is dependent on the MTX concentration in media, M, the maximal MTX cell kill rate, K_{max}, and a Michaelis constant, K_{50}.

(b) Phase specific model

$$\frac{dCs}{dt} = kg \cdot Cs - ksr \cdot Cs + krs \cdot Cr - K \cdot Cs$$
$$\frac{dCr}{dt} = ksr \cdot Cs - krs \cdot Cr - kd \cdot Cs$$
$$K = \frac{K_{\max} M}{K_{50} + M}$$

Two cell populations are assumed: a sensitive population (where Cs refers to the number of sensitive cells), and a resistant population (where Cr refers to the number of resistant cells). The first order rate constants ksr and krs refer to rates of cell cycling between the populations; kg and kd refer to rates of cell growth and cell death, respectively. K is as defined above.

(c) Transit compartment model

$$\frac{dC}{dt} = kng \cdot C - K4 \cdot C$$
$$\frac{dK1}{dt} = \frac{1}{\tau}(K - K1)$$
$$\frac{dK2}{dt} = \frac{1}{\tau}(K1 - K2)$$
$$\frac{dK3}{dt} = \frac{1}{\tau}(K2 - K3)$$
$$\frac{dK4}{dt} = \frac{1}{\tau}(K3 - K4)$$
$$K = \frac{K_{\max} M}{K_{50} + M}$$

C, K_{max}, K_{50}, M, and K are as defined above; however, the operative rate constant of MTX induced cell killing, K4, is related to K via a series of transit compartments (i.e., K1 – K4). τ refers to the mean transit time in each transit compartment. As shown, the transit compartments function to delay the time-course of cell kill, relative to the time-course of drug exposure. Four transit compartments are employed in this model; however, only one parameter is used to describe transit kinetics (τ). As such, the model is both flexible (due to the number of transit compartments), but also highly stable (due to the use of a small number of parameters [kng, K_{max}, K_{50}, τ]).

Because K is a function of M, a time-dependent variable, each model is a dynamic model of drug effect. That is, the cell kill constant changes with time, as influenced by factors that control the time-course of drug exposure (e.g., the dosing regimen and / or the relevant pharmacokinetics of the system). Additionally, cell number is also a time-dependent variable. As such, each model allows dynamic characterization of cell growth and drug-induced cell killing. Models were fitted to mean cell number v. time data, for each cell line, with ADAPT II software.[22]

RESULTS

In vitro MTX cell inhibition

The time-courses of cell growth for the two tumor cell lines are shown in Figure 2, 3, and 4. In the absence of MTX, each cell line demonstrated exponential growth.

MTX induced concentration dependent inhibition in apparent cell growth; however, MTX effects were significantly delayed relative to the time-course of drug exposure. Little change in cell number was observed during the 24 h incubation of MTX (i.e., immediately following MTX removal, cell number was not significantly different from the untreated cells, $p > 0.05$ for each cell line). Cell number reached nadir values at 168 h for sarcoma 180 and at 264 h for Ehrlich ascites cells. The rate of cell growth after recovery from MTX treatment appeared to be similar to that of the untreated cells.

Pharmacodynamic modeling

Best-fit predictions of the phase non-specific model, following simultaneous fitting to the data, are shown in Figure 2. The model provided satisfactory characterization of cell growth for untreated cells (r^2=0.999, for each cell line). Model predictions are close to observed values of cell number in the 'recovery phase' (i.e., after 150 – 200 h); however, the model was unable to capture the observed increase in cell number that occurred during MTX incubation, severely under-predicting cell number between 24 h and 120 h for each cell line. Model predictions of cell number data following MTX treatment were generally poor (Fig. 2), with correlation coefficients (r^2) between predicted and observed values of cell number as low as 0.099 (e.g., for 2 μg / ml MTX applied to Ehrlich ascites cells). Additionally, parameter estimates were associated with high variability (e.g., EC_{50}= 0.21 [%CV= 89%] for Ehrlich ascites cells, EC_{50}= 0.84 [%CV= 35%] for sarcoma 180 cells).

Predictions of the phase specific model are shown in Figure 3. As with the non-specific model, the phase specific model provided poor predictions of the cell counts in MTX treated wells between 24 – 120 h. Correlation coefficients for the fitted curves were generally poor, ranging from 0.16 to 0.99, and parameter estimates were associated with high variability (i.e., %CV values and 95% confidence intervals were too large for estimation by ADAPT II). The phase-specific model, which had twice the number of fitted parameters of the phase non-specific model (i.e., 6 vs. 3 parameters), was found to have a superior Akaike criterion value (i.e., 480 v. 489 for fitting sarcoma 180 data, and 556 v. 574, for fitting to the Ehrlich ascites data), which suggests that this model may be superior to the phase non-specific model for fitting to these data.

Predictions of the transit compartment model are presented in Figure 4. As shown, the transit compartment model provided satisfactory characterization of the entire time-course of cell count data, for each cell line. Although not shown, we also evaluated models with 2, 3, and 5 transit compartments, and we found that the present model, with four transit compartments, provided superior fitting to the data. Estimated parameter values for fitting to the Ehrlich ascites cell line were τ = 34.1 h (%CV = 3.4), K_{max} = 0.29 h^{-1} (%CV = 5.8), EC_{50} = 0.1 µg / ml (%CV = 48.7%) and kng = 0.02 h^{-1} (%CV = 4.9). Doubling time for Ehrlich ascites cells was estimated from kng to be 34.6 h. Estimated parameter values following fitting to the sarcoma 180 data were τ = 30.0 h (%CV = 2.5), K_{max} = 0.34 h^{-1}

(%CV = 2.1), EC_{50} = 0.32 μg / ml (%CV = 14.2%) and kng = 0.035 h^{-1} (%CV = 1.9). The doubling time for sarcoma 180 was estimated to be 19.8 h.

Discussion

The pharmacodynamics of chemotherapeutics have been extensively investigated in vitro and in vivo. In most experimental settings, chemotherapeutic effects are significantly delayed relative to chemotherapeutic exposure. The time-course of drug effect is of high interest in the field of cancer chemotherapy; however, due to the lack of simple mathematical models capable of characterizing the time-course of effect, most analyses have reported relationships of drug exposure to drug effect at a fixed time point (e.g., often at the time of peak effect for in vivo studies, and often at an arbitrary time point for in vitro studies).[10,12,13,23,24] By focusing on drug effect at a fixed time point, exposure – effect relationships may be easily characterized through the use of simple, static relationships (e.g., the Hill function: $\text{Effect} = \frac{E_{max} \bullet C^{\gamma}}{EC_{50}^{\gamma} + C^{\gamma}}$, where E_{max}, EC_{50}, and γ are constants, and where C may refer to the chemotherapeutic dose, steady-state concentration, or, most commonly, area under the concentration v. time curve). Static exposure – effect relationships have been successfully applied for the optimization of chemotherapy in several cases;[9,25,26] however, characterization of the entire time-course of chemotherapeutic effect may provide additional information to allow further optimization. For example, modeling of the time-course of drug effect may facilitate the scheduling of subsequent courses of chemotherapy and may assist in the selection of optimal drug combinations.

In early 1970s, Jusko proposed two models to describe the kinetics of chemotherapeutic effects (as shown in Figure 1).[18,19] For each of these models, the kinetics of cell killing is defined to be directly related to drug concentrations in plasma. As such, these models are not well suited to characterize chemotherapeutic effects in cases where effect is substantially delayed relative to the time-course of drug exposure. Perhaps because chemotherapeutic effects often appear days or weeks following drug exposure, these models have not found wide use in the field of cancer chemotherapy.

Time delays between the time-course of drug exposure and the time-course of drug effects have been typically described through the use of 'effect site' models or 'indirect response' models. The effect site model attributes the delay in effect to the delay associated with drug distribution to the site of effect.[27] Indirect response models predict a delayed time-course of apparent drug response as a consequence of indirect mechanisms of drug action (e.g., where drug may act via stimulation or inhibition of the processes involved in the production or loss of the measured response).[28] Recently, Sun and Jusko proposed a transit compartment model to characterize delayed drug effects, where the time delay is captured through the use of a series of transit compartments.[20] The model, which was originally developed to describe the kinetics of signal transduction, was later shown to have general utility in characterizing effects that occur via a cascade.[17] We were interested in evaluating this model for utility in characterizing

chemotherapeutic effects, which often occur via a complicated cascade of events.

In the present work, the time-course of MTX effects on cancer cell growth was assessed in vitro, following 24 h MTX exposure to sarcoma 180 cells and Ehrlich ascites cells, grown in culture. Consistent with the results of studies investigating MTX effects in vivo,[29] we observed a significant delay between the time-course of MTX exposure and the time-course of MTX effects in this model system. For example, at the conclusion of MTX exposure (i.e., 24 h after the initiation of MTX treatment), no difference was found when comparing cell number in MTX-treated wells and untreated wells (Figure 4, $p>0.05$), and the apparent 'peak effect' (i.e., the nadir cell count) occurred at 168 h and at 264 h for sarcoma 180 and Ehrlich ascites cells, respectively.

Data were fitted to three pharmacodynamic models, including a cell-cycle phase specific model, a phase non-specific model, and a transit compartment model. In each model, MTX effect (i.e., cell killing) was related to MTX concentration through a non-linear function. However, in contrast to the phase specific and phase non-specific models, the transit-compartment model incorporates a series of first-order transfer steps to allow characterization of delays between drug exposure and cell killing. Because the phase non-specific model and phase specific model assume a direct relationship between MTX concentration and cell killing, these models predicted a rapid decrease in cell number during the course

of MTX exposure (Figure 2 and Figure 3). The cell cycle phase specific model appeared to characterize the data better than the phase non-specific model both visually and based on model fitting criteria; however, neither model provided predictions consistent with the observation of continued cell growth during the 24 h treatment with MTX.

We found that the transit compartment model could adequately describe the entire cell count v. time profile, for each cell line, for each treatment (i.e., without MTX exposure, or for 24 h MTX exposure at concentrations ranging from 0.19 – 140 μg/ml). Consistent with the observed data, this model predicted increases in cell number during the MTX treatment, with nadir cell counts occurring 100 – 200 h after MTX removal. Thus, the relatively complex time-course of cell growth was described with a simple model consisting of only four parameters. Perhaps because of the simplicity of the model, parameters were estimated with fair precision (%CV=2-49%). The transit time was found to be similar for the two cell lines and was estimated to be 30 h and 34 h for sarcoma 180 and Ehrlich ascites cells, respectively. The values of the parameters K_{max} and EC_{50} were dependent on the tumor cell lines. The EC_{50} for Ehrlich ascites cells (0.1 μg/ml) was three fold lower than the EC_{50} of sarcoma 180 (0.32 μg/ml) suggesting that Ehrlich ascites cell line was more sensitive to the cell killing effect of MTX.

In this work, we have investigated the usefulness of the transit compartment model to characterize MTX cytotoxic effects in vitro. We successfully

characterized the complex time-course of cell growth in the presence of MTX with a simple pharmacodynamic model. The transit compartment model may find utility as a general model to characterize chemotherapeutic effects that are delayed relative to chemotherapeutic exposure. Modeling the time-course of chemotherapeutic effects is desirable as it may facilitate the development of individualization and optimization strategies for chemotherapy.

References

1. Lokich J, Anderson N. Dose intensity for bolus versus infusion chemotherapy administration: review of the literature for 27 anti-neoplastic agents. Ann Oncol. 1997;8:15-25.

2. Aisner J, Van Echo DA, Whitacre M, Wiernik PH. A phase I trial of continuous infusion VP16-213 (etoposide). Cancer Chemother Pharmacol. 1982;7:157-60.

3. Frei Ed, Bickers JN, Hewlett JS, Lane M, et al. Dose schedule and antitumor studies of arabinosyl cytosine (NSC 63878). Cancer Res. 1969;29:1325-32.

4. Wiernik PH, Schwartz EL, Strauman JJ, Dutcher JP, et al. Phase I clinical and pharmacokinetic study of taxol. Cancer Res. 1987;47:2486-93.

5. O'Dwyer PJ, Hudes GR, Walczak J, Schilder R, et al. Phase I and pharmacokinetic study of the novel platinum analogue CI-973 on a 5-daily dose schedule. Cancer Res. 1992;52:6746-53.

6. Minami H, Sasaki Y, Saijo N, Ohtsu T, et al. Indirect-response model for the time course of leukopenia with anticancer drugs. Clin Pharmacol Ther. 1998;64:511-21.

7. Minami H, Sasaki Y, Watanabe T, Ogawa M. Pharmacodynamic modeling of the entire time course of leukopenia after a 3-hour infusion of paclitaxel. Jpn J Cancer Res. 2001;92:231-8.

8. Friberg LE, Freijs A, Sandstrom M, Karlsson MO. Semiphysiological model for the time course of leukocytes after varying schedules of 5-fluorouracil in rats. J Pharmacol Exp Ther. 2000;295:734-40.

9. Jodrell DI, Egorin MJ, Canetta RM, Langenberg P, et al. Relationships between carboplatin exposure and tumor response and toxicity in patients with ovarian cancer. J Clin Oncol. 1992;10:520-8.

10. Stewart CF, Baker SD, Heideman RL, Jones D, et al. Clinical pharmacodynamics of continuous infusion topotecan in children: systemic exposure predicts hematologic toxicity. J Clin Oncol. 1994;12:1946-54.

11. Cellarier E, Terret C, Labarre P, Ouabdesselam R, et al. Pharmacokinetic study of cystemustine, administered on a weekly schedule in cancer patients. Ann Oncol. 2002;13:760-9.

12. Van Kesteren C, Mathot RA, Raymond E, Armand JP, et al. Population pharmacokinetics and pharmacokinetic-pharmacodynamic relationships of the

novel anticancer agent E7070 in four phase I studies. Br J Clin Pharmacol. 2002;53:553P.

13. Zhou H, Choi L, Lau H, Bruntsch U, et al. Population pharmacokinetics/toxicodynamics (PK/TD) relationship of SAM486A in phase I studies in patients with advanced cancers. J Clin Pharmacol. 2000;40:275-83.

14. Gimmel S, Maurer HR. Growth kinetics of L1210 leukemic cells exposed to different concentration courses of methotrexate in vitro. Cancer Chemother Pharmacol. 1994;34:351-5.

15. Braakhuis BJ, Ruiz van Haperen VW, Boven E, Veerman G, et al. Schedule-dependent antitumor effect of gemcitabine in in vivo model system. Semin Oncol. 1995;22:42-6.

16. Kishi S, Goto N, Nakamura T, Ueda T. Evaluation of cell-killing effects of 1-beta-D-arabinofuranosylcytosine and daunorubicin by a new computer-controlled in vitro pharmacokinetic simulation system. Cancer Res. 1999;59:2629-34.

17. Mager DE, Jusko WJ. Pharmacodynamic modeling of time-dependent transduction systems. Clin Pharmacol Ther. 2001;70:210-6.

18. Jusko WJ. Pharmacodynamics of chemotherapeutic effects: dose-time-response relationships for phase-nonspecific agents. J Pharm Sci. 1971;60:892-5.

19. Jusko WJ. A Pharmacodynamic model for cell-cycle-specific chemotherapeutic agents. J. Pharmacokin. Biopharm. 1973;1:175-200.

20. Sun YN, Jusko WJ. Transit compartments versus gamma distribution function to model signal transduction processes in pharmacodynamics. J Pharm Sci. 1998;87:732-7.

21. Tada H, Shiho O, Kuroshima K, Koyama M, et al. An improved colorimetric assay for interleukin 2. J Immunol Methods. 1986;93:157-65.

22. D'Argenio DZ, Schumitzky A. ADAPT II User's Guide: Pharmacokinetic/Pharmacodynamic Systems Analysis Software. In: . Los Angeles: Biomedical Simulations Resource; 1997.

23. Levasseur LM, Slocum HK, Rustum YM, Greco WR. Modeling of the time-dependency of in vitro drug cytotoxicity and resistance. Cancer Res. 1998;58:5749-61.

24. Hassan SB, Jonsson E, Larsson R, Karlsson MO. Model for time dependency of cytotoxic effect of CHS 828 in vitro suggests two different mechanisms of action. J Pharmacol Exp Ther. 2001;299:1140-7.

25. Rodman JH, Relling MV, Stewart CF, Synold TW, et al. Clinical pharmacokinetics and pharmacodynamics of anticancer drugs in children. Semin Oncol. 1993;20:18-29.

26. Evans WE, Relling MV, Rodman JH, Crom WR, et al. Conventional compared with individualized chemotherapy for childhood acute lymphoblastic leukemia. N Engl J Med. 1998;338:499-505.

27. Sheiner LB, Stanski DR, Vozeh S, Miller RD, et al. Simultaneous modeling of pharmacokinetics and pharmacodynamics: application to d-tubocurarine. Clin. Pharmacol. Ther. 1979;25:358-71.

28. Dayneka NL, Garg V, Jusko WJ. Comparison of four basic models of indirect pharmacodynamic responses. J Pharmacokinet Biopharm. 1993;21:457-78.

29. Labat C, Mansour K, Malmary MF, Terrissol M, et al. Chronotoxicity of methotrexate in mice after intraperitoneal administration. Chronobiologia. 1987;14:267-75.

Captions for Figures

Figure 1. Schematic representation of the models evaluated for characterization of MTX cytotoxicity. A. Phase non-specific model: C, viable cells; kng, net growth rate constant; K, the cell kill constant. B. Phase specific model: Cs, cells sensitive to MTX; Cr, cells resistant to MTX; kg, cell-proliferation rate constant; kd, cell loss rate constant; ksr, krs, cell cycling rate constants. C. Transit compartment model: K1, K2, K3, K4 refer to the cell kill rate constants in the transit compartments; τ, transit time; kng, net growth rate constant; C, viable cell number. For each model, the cell kill constant is a non-linear function of MTX concentration: $K = \frac{K_{\max} M}{K_{50} + M}$, where K_{max} is the maximal value of the cell kill constant, K_{50} is a Michaelis constant, and M refers to the MTX concentration, which is a time-dependent variable.

Figure 2. Phase non-specific model predictions of MTX effects on the time-course of cell growth. Ehrlich ascites cells, panel A, and sarcoma 180 cells, panel B, were treated with MTX for 24 h (concentrations ranging from 0 – 140 μg / ml). After removal of MTX, cells were fed with fresh media every 48 h. Solid symbols and bars refer to the mean and standard deviation (n=4). Model predicted profiles are shown as solid lines.

Figure 3. Phase specific model predictions of MTX effects on the time-course of cell growth. Ehrlich ascites cells, panel A, and sarcoma 180 cells, panel B, were treated with MTX for 24 h (concentrations ranging from 0 – 140 μg / ml). After

removal of MTX, cells were fed with fresh media every 48 h. Solid symbols and bars refer to the mean and standard deviation (n=4). Model predicted profiles are shown as solid lines.

Figure 4. Transit compartment model predictions of MTX effects on the time-course of cell growth. Ehrlich ascites cells, panel A, and sarcoma 180 cells, panel B, were treated with MTX for 24 h (concentrations ranging from 0 – 140 μg / ml). After removal of MTX, cells were fed with fresh media every 48 h. Solid symbols and bars refer to the mean and standard deviation (n=4). Model predicted profiles are shown as solid lines.

Figure 1

A.

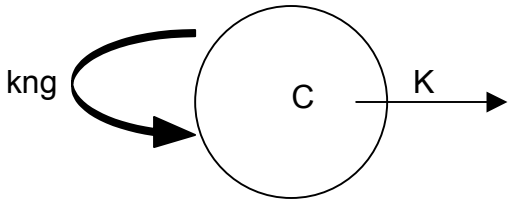

B.

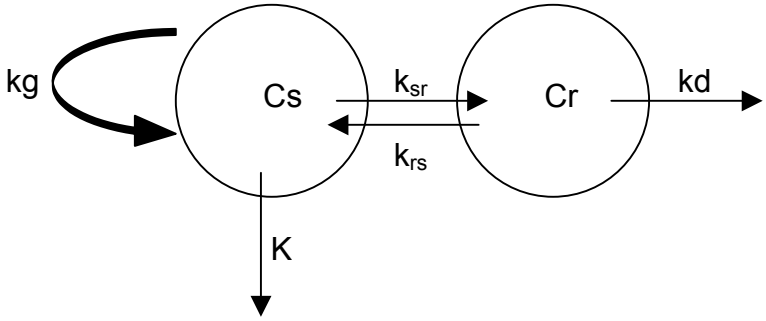

C.

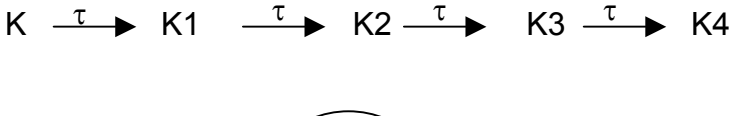

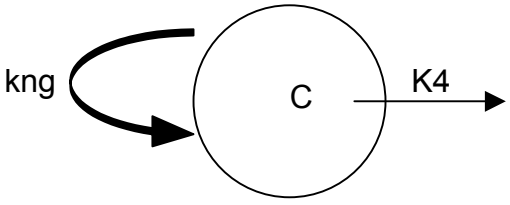

Figure 2

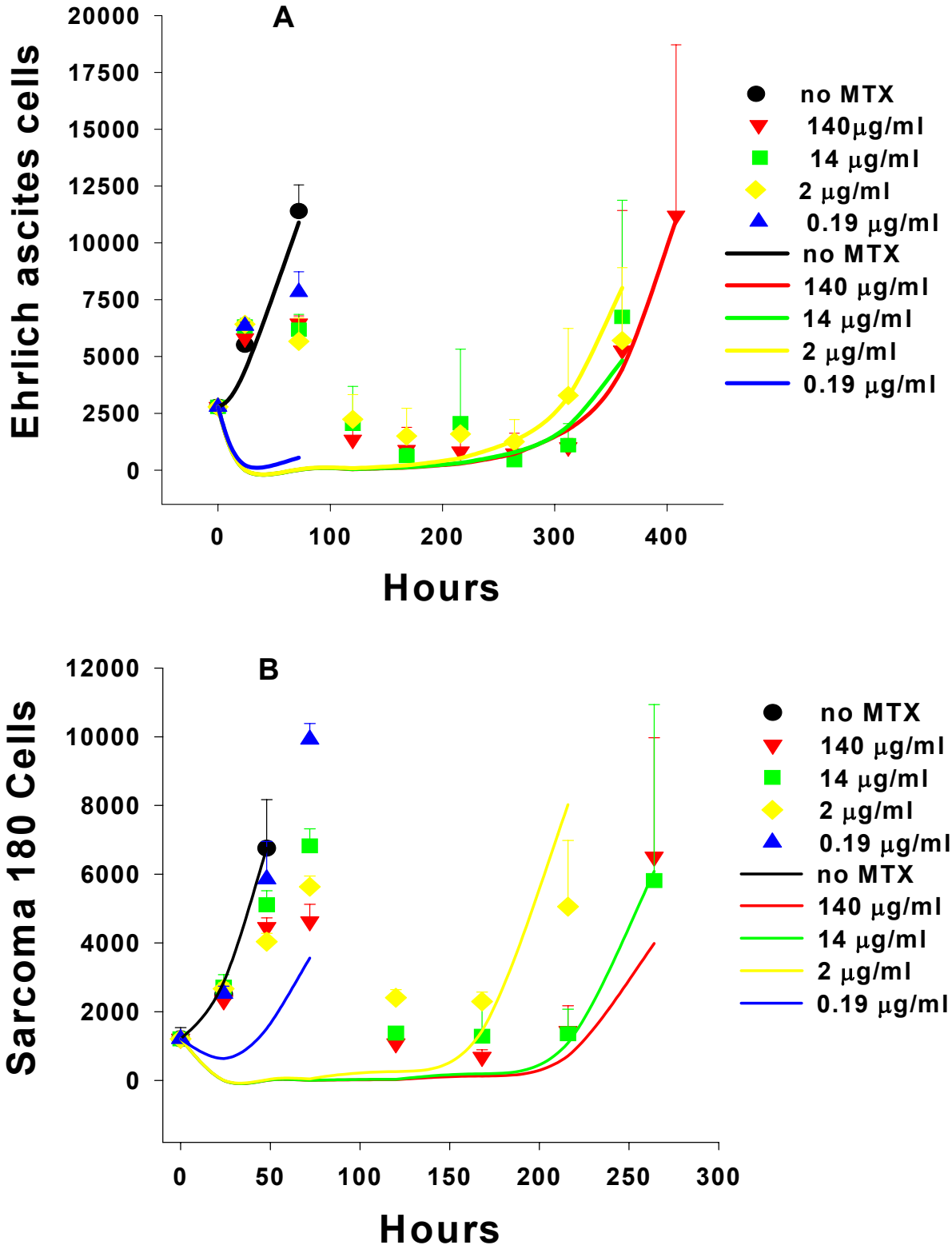
A
Ehrlich ascites cells
20000
17500
15000
12500
10000
7500
5000
2500
0
0
100
200
300
400
Hours
no MTX
140µg/ml
14 µg/ml
2 µg/ml
0.19 µg/ml
no MTX
140 µg/ml
14 µg/ml
2 µg/ml
0.19 µg/ml
B
Sarcoma 180 Cells
12000
10000
8000
6000
4000
2000
0
0
50
100
150
200
250
300
Hours
no MTX
140 µg/ml
14 µg/ml
2 µg/ml
0.19 µg/ml
no MTX
140 µg/ml
14 µg/ml
2 µg/ml
0.19 µg/ml

Figure 3

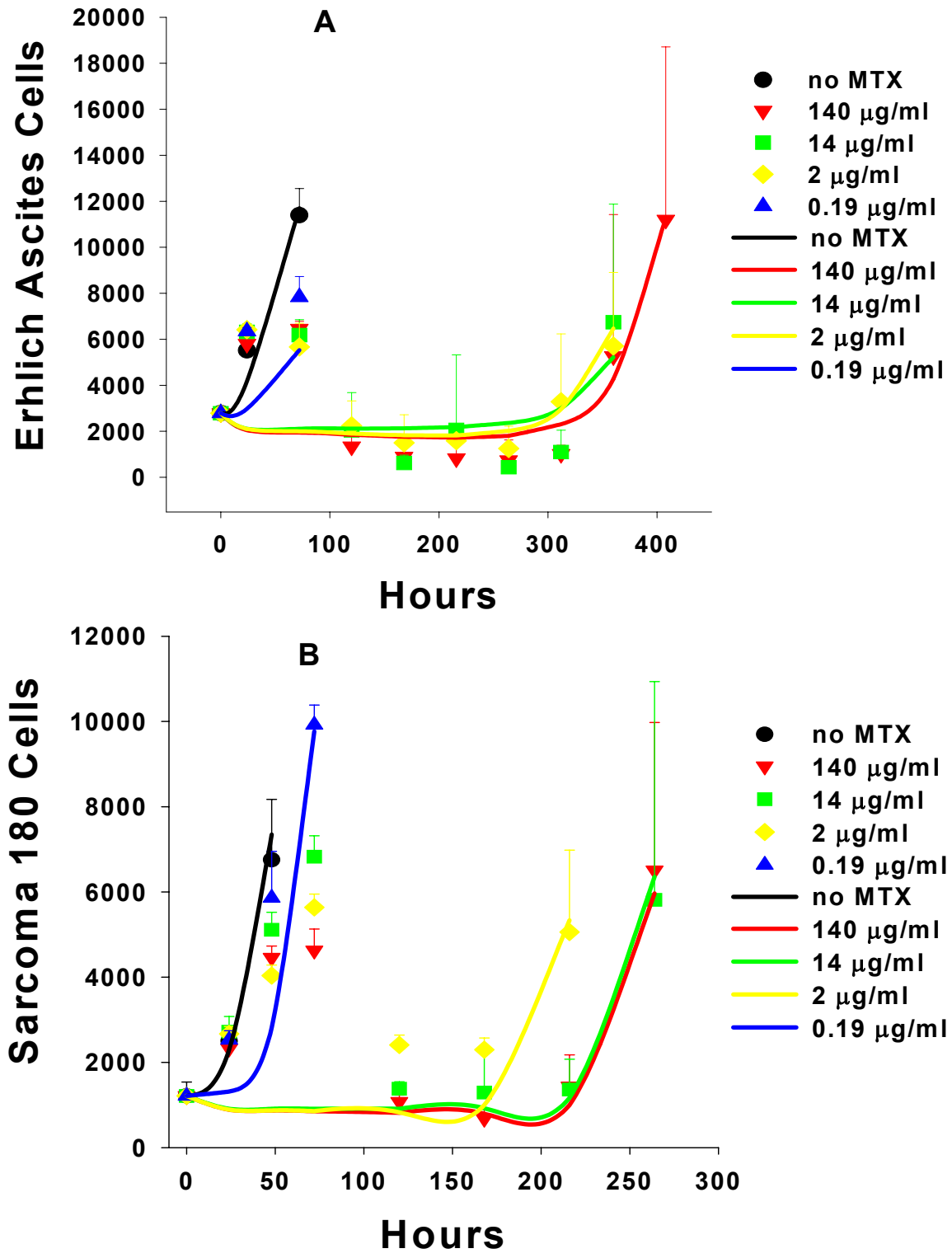
A
Erhlich Ascites Cells
20000
18000
16000
14000
12000
10000
8000
6000
4000
2000
0
0
100
200
300
400
Hours
no MTX
140 µg/ml
14 µg/ml
2 µg/ml
0.19 µg/ml
no MTX
140 µg/ml
14 µg/ml
2 µg/ml
0.19 µg/ml
B
Sarcoma 180 Cells
12000
10000
8000
6000
4000
2000
0
0
50
100
150
200
250
300
Hours
no MTX
140 µg/ml
14 µg/ml
2 µg/ml
0.19 µg/ml
no MTX
140 µg/ml
14 µg/ml
2 µg/ml
0.19 µg/ml

Figure 4

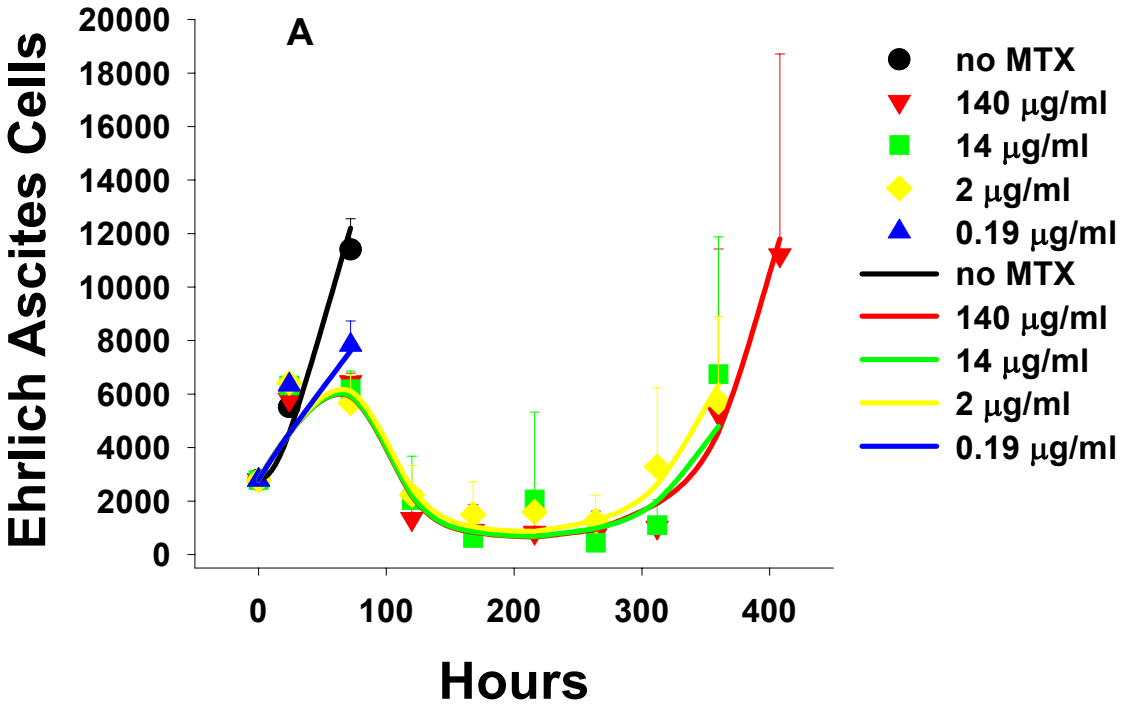
A
Ehrlich Ascites Cells
20000
18000
16000
14000
12000
10000
8000
6000
4000
2000
0
0
100
200
300
400
Hours
no MTX
140 µg/ml
14 µg/ml
2 µg/ml
0.19 µg/ml
no MTX
140 µg/ml
14 µg/ml
2 µg/ml
0.19 µg/ml

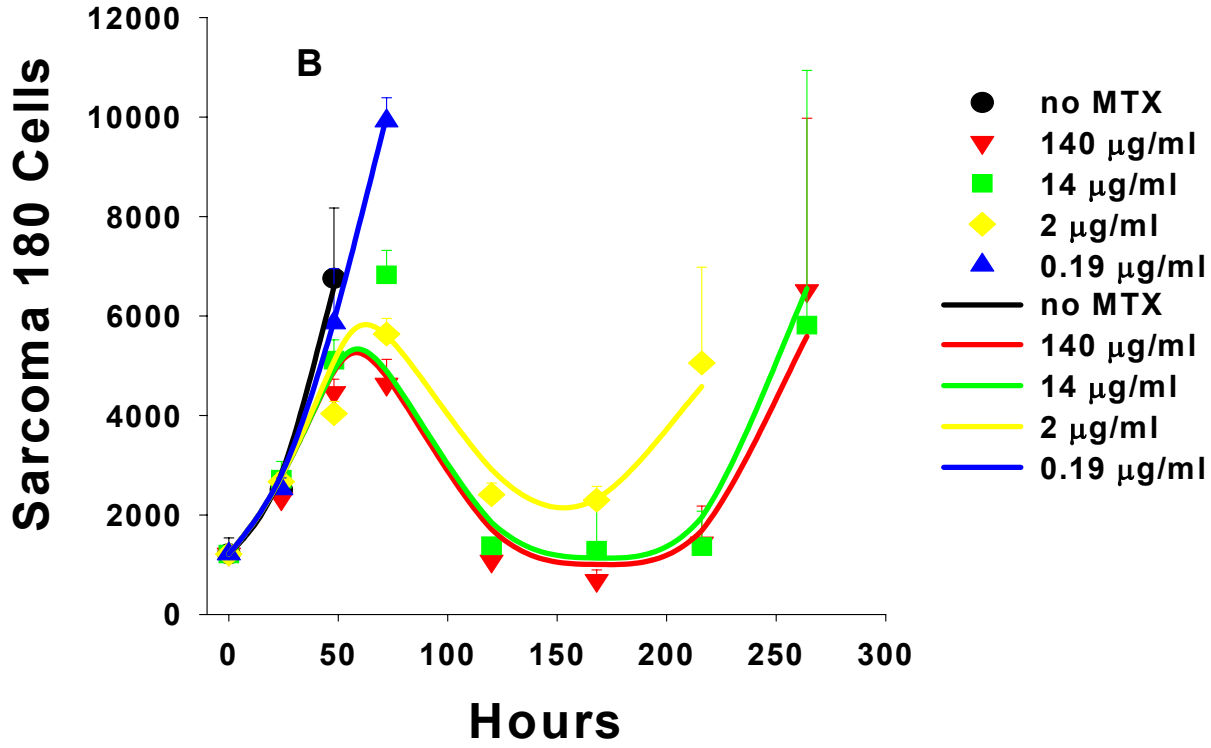
B
Sarcoma 180 Cells
12000
10000
8000
6000
4000
2000
0
0
50
100
150
200
250
300
Hours
no MTX
140 µg/ml
14 µg/ml
2 µg/ml
0.19 µg/ml
no MTX
140 µg/ml
14 µg/ml
2 µg/ml
0.19 µg/ml

CHAPTER SEVEN

Prediction of protocol dependence in chemotherapeutic selectivity with in vivo toxicity data and in vitro cytotoxicity data.

Abstract

Chemotherapeutic selectivity (i.e. the ratio of drug efficacy to drug toxicities) of chemotherapeutic drugs is highly dependent on the dosing protocol. We have proposed that chemotherapeutic selectivity may be predicted from in vivo toxicity studies and in vitro cytotoxicity data. The approach was investigated using methotrexate (MTX) in two cancer cell lines, sarcoma 180 cells (S180) and Ehrlich ascites cells (EAC). In vitro cytotoxicity studies were conducted at MTX concentration and duration of exposure obtained from MTX toxicity and pharmacokinetic studies in mice. Tumor cells were exposed to MTX concentrations for 4 h, 24 h, 72 h and 168 h. MTX efficacy was also investigated in mice bearing peritoneal tumors of S180 or EAC at the maximally tolerated dose of i.p. MTX following bolus and infusions of 24 h, 72 h and 168 h. In vitro MTX cytotoxicity results for S180 indicted that 4 h and 72 h MTX exposure would be equally effective and results for EAC indicated that 4 h, 72 h and 168 h exposures would be equally effective. In tumor bearing mice, the survival time with 24 h exposure was significantly ($p<0.05$) longer in S180 bearing mice whereas 72 h exposure was most effective for EAC bearing mice. In vitro cytotoxicity data and in vivo efficacy results indicated that equally toxic MTX exposures were not equally effective. Unfortunately, the in vitro cytotoxicity data failed to predict chemotherapeutic selectivity in peritoneal tumor bearing mice.

Keywords: chemotherapeutic selectivity, dosing protocol, cell growth inhibition, survival time, correlation.

1. Introduction

The relationships between dose and toxicity, dose and efficacy and dose and selectivity for many cell cycle phase specific chemotherapeutic drugs (such as arabinosyl cytosine， methotrexate, etoposide, paclitaxel, topotecan, etc) are often dependent on the duration of drug exposure [1-5]. The importance of time dependencies in chemotherapeutic toxicity and efficacy has led to the design of numerous clinical trials to assess the effects of drug administration on drug toxicity and efficacy [4, 5]. For example, many different dosing protocols of topotecan have been investigated in the phase I clinical trials such as constant-rate infusions of topotecan varying from 30 min to 21 days [5].

In clinical experimentation, it has been difficult to develop a general understanding of time dependencies of chemotherapeutics from results obtained from the toxicity and efficacy studies due to tremendous differences in patient population. High degree of inter-patient variability in chemotherapeutic pharmacokinetics and pharmacodynamics confounds any meaningful assessment of chemotherapeutic selectivity for a given dosing protocol [6, 7]. Further, high degree of intra-patient variability makes it difficult to assess the effect of different protocols in the same patient [8]. Consequently, optimal dosing protocol in terms of dose and duration remains unknown for many chemotherapeutics.

We feel that animal experimentation would provide the opportunity to probe the time dependencies between dose and toxicity, dose and efficacy and dose and selectivity. Further, understanding the time dependencies between dose and chemotherapeutic effects may allow for prediction of chemotherapeutic selectivity in vivo. An approach was proposed to permit prediction of chemotherapeutic selectivity from in vitro cytotoxicity data. The approach involved investigation of the relationship between dose and drug toxicity following drug administration. In vitro cytotoxicity studies were then conducted at equally toxic drug exposures i.e. drug exposures at the maximally tolerated dose to assess the selectivity of the drug.

We have tested the applicability of the approach with MTX as a model drug in a murine model of peritoneal cancer. Firstly, we investigated the relationship between i.p. MTX administration and MTX-induced toxicity in mice [9]. The maximally tolerated dose of MTX was determined following four i.p. administration protocols, bolus injection and constant-rate infusions of 24 h, 72 h and 168 h.

In this report, we investigated the relationship between MTX exposure and MTX cytotoxicity (in vitro and in vivo). MTX cytotoxicity was tested against two murine cancer cell lines, S180 and EAC. In vitro cell growth inhibition was tested at exposure times and concentrations achieved in vivo at the maximally tolerated dose for each treatment protocol. In vitro MTX cytotoxicity was measured as cell

growth delay (in days) for each cell line in the presence of MTX. The median survival times were determined in mice bearing peritoneal tumors of S180 and EAC following i.p. MTX treatment. The results of the in vitro MTX cytotoxicity were compared with the median survival time observed in MTX treated peritoneal tumor bearing mice.

2. Experimental

2.1 Materials

MTX, 3-[4,5-dimethylthiazol-2-yl]-2,5-diphenyl-tetrazolim bromide (MTT), sodium hydrosulfite and xylazine were purchased from Sigma Chemical (St. Louis, MO). Sodium dodecyl sulfate was obtained from Bio-Rad laboratories (Hercules, CA). Ketamine and sterile 0.9% sodium chloride were obtained from Henry Schein (Melville, NY). ALZET® micro-osmotic pumps 1003D and 2007D were obtained from Alza Corporation (Palo Alto, CA). RPMI 1640 media, certified fetal bovine serum and gentamicin were obtained from Invitrogen Corporation (Grand Island, NY).

2.2 Cell Lines

EAC and S180 cell lines were obtained from American Type Cell Culture (Manassas, VA). RPMI 1640 media was prepared to contain approximately 20 nM folic acid, 10% fetal bovine serum and 100 μg/ml gentamicin. The cancer cell lines were grown in cell culture flask (75 cm^2, 250 ml) and maintained in a humidified, 5% CO_2 incubator at 37°C.

2.3 MTX stability in cell culture media

The stability of MTX in the media at 37°C was determined in the concentration range and exposure times tested in the cell inhibition studies. Media (100 μl) containing MTX was incubated for 4 h (5100 μg/ml and 68 μg/ml), 24 h (14 μg/ml and 0.19 μg/ml) and 72 h (1.74 μg/ml and 0.1 μg/ml) at 37°C in a humidified 5% CO_2 incubator in 96 well plates. Each concentration was tested in three wells. MTX concentration was analyzed before and at the end of the incubation period. Samples were diluted and assayed with a slight modification of previously reported HPLC assay for MTX [10]. Briefly, a solution of 100 μl of media containing MTX, 25 μl folic acid solution (5000 ng/ml, internal standard), 100 μl phosphate saline buffer (pH 7.4), 100 μl sodium acetate/acetic acid (2 M / 5 M) buffer (pH 6.0) and 50 μl freshly prepared sodium hydrosulfite solution (10 mg/ml) was heated to 92 ºC for 30 min. Standard curves were prepared with blank media and phosphate saline buffer containing known concentrations of MTX (50 to 1000 ng/ml). Samples were cooled, centrifuged at 10,000 *g* for 4 min and 200 μl of the supernatant solution was injected on the column.

2.4 In-vitro cell growth inhibition studies

MTX concentrations in the peritoneum and plasma were estimated at the maximally tolerated dose following bolus injection (760 mg/kg) and constant-rate infusions of 24 h (10 mg/kg), 72 h (3.8 mg/kg), and 168 h (6.7 mg/kg) [9]. From pharmacokinetics studies of MTX, the half-life of MTX in mice was found to be approximately 30 min. For bolus injection, an average exposure time of 4 h (>

seven $t_{1/2}$) was tested in vitro. Also, average MTX plasma and peritoneal concentrations were estimated from the area under predicted MTX concentration-time profile at 760 mg/kg of bolus injection. Three MTX concentrations were tested; the steady-state peritoneal concentration, Cp, steady-state systemic concentration, Cs and an intermediate concentration, Cm. The duration of exposures were 4 h, 24 h, 72 h and 168 h. The concentrations of MTX and the duration of exposures are summarized in Table 1. Single cell suspensions containing 10,000 cells/ml and 5,000 cells/ml were prepared for EAC and S180, respectively. Twelve 96 well plates for each cell line were plated with 100 μl of cell suspension. Cells were allowed to attach for 48 h. After 48 h, media was aspirated from the wells with a 25-gauge needle attached to the aspirating pipette. Preliminary studies demonstrated that the method of aspiration did not result in significant cell loss (100.7 ± 6.3% recovery, n=12). Following aspiration, 100 μl of media containing MTX was added to the wells. Each concentration of MTX was tested in 4 wells. Cells were incubated with MTX for the given exposure times, and media was then aspirated. Each well was washed 3 to 4 times with 100 μl MTX-free media. Media in the wells was replaced every 2 days. Cell number was determined on the following day: 1, 3, 5, 7, 9, 11, 13, 15, 17, 20, 22 and 24 for EAC and on day: 1, 2, 3, 5, 7, 9, 11, 13, 14, 15, 17, 19, 21 for S180, using one plate per assay with the tetrazolium assay [11]. Briefly, media was removed from all the wells and 100 μl of fresh media, 25 μl of MTT solution (5 mg/ml in phosphate saline buffer, pH 7.4) was added to each well and the plate was then incubated for 4.5 h at 37°C. After incubation, 100 μl of 10%

SDS-HCL (0.01 M HCL) was added to each well and incubated overnight at 37°C. Absorbance in each well was determined at 590 nm using a plate reader (Spectromax, Molecular Devices). Standard cell solutions were run on each plate in the range of 156 to 10,000 cells. The time to reach 10,000 or greater cell number was monitored to assess MTX inhibition. The time to reach a mean cell number of 10,000 or greater on the day of analysis was determined in control and treated wells. Cell growth delay was defined as the time required by the cells to recover from MTX inhibition. Growth delay in days was calculated as the difference in the time for the treated cells and control cells to reach 10,000 or greater cell number.

2.4 In vivo survival studies in mice bearing peritoneal tumors

In vivo efficacy studies were conducted using 5-6 week-old (20-25 g) Swiss Webster male mice (Harlan Sprague-Dawley Inc., Indianapolis, IN). Animals were provided with food and water ad libitum and housed on a standard light-dark cycle. Cells growing exponentially in media were washed and suspended in sterile 0.9% sodium chloride. Animals received an i.p. bolus injection of either 10^6 cells of S180 (0.5 ml) or 5 x 10^6 cells of EAC (1ml). MTX treatment was initiated the following day after tumor inoculation. Animals were separated in groups of 10 each and were treated with the following i.p MTX administration protocol, a) bolus injection, 760 mg/kg; b) 24 h constant-rate infusion, 10 mg/kg; c) 72 h constant-rate infusion, 3.8 mg/kg; d) 168 h constant-rate infusion, 6.7 mg/kg. Control animals were treated with bolus injection of sterile 0.9% sodium chloride.

Constant-rate infusions were administered with pre-equilibrated osmotic pumps (37°C, sterile 0.9% sodium chloride, overnight) attached with peritoneal catheter and implanted subcutaneously in mice. Briefly, animals were anesthesized with i.p. ketamine / xylazine (100 / 10 mg/kg). The osmotic pumps were placed subcutaneously near the shoulder blade on the dorsal side. Cannulas were inserted into the peritoneal cavity through a small opening made in the abdominal muscle. The body weight of the animals were monitored daily.

MTX dose that caused more than 50% deaths before any control animals died of tumor growth was reduced by 50% and tested for survival in tumor bearing mice. Tumor bearing animals were sacrificed when their body weight reached 120% of their body weight on day zero (i.e. day of treatment). The peritoneal cavity was opened and confirmed for ascites fluid in the sacrificed animals. Survival time was defined as the time required for the animal to reach 120% body weight or the time to death. Percent increase in life span was calculated as ([median survival time in treated animals/ median survival time in controls]-1) x 100. The survival curves were compared using log rank test and hazard ratio with Prism software (GraphPad software Inc, San Diego, CA).

3. Results

3.1 MTX stability in media

The stability of MTX in the media was assessed at concentrations and exposure times tested for cell growth inhibition studies. At the end of the incubation period

at 37ºC, the percent of unchanged MTX recovered was 95 to 107% of the initial MTX concentrations as shown in Table II.

3.2 In vitro cell inhibition studies

3.2.1 Sarcoma 180. The time course of cell growth in the presence of MTX concentration at various exposure times is shown in Fig. 1. The doubling time for S180 cells was estimated to be 19 h. The time to reach greater than 10,000 cells for the control cells was 3 days. The peak MTX effects i.e. nadir cell count was found to be delayed relative to MTX exposure. The time for nadir cell count was 216 h, 168 h, 312 h and 264 h for 4 h, 24 h, 72 h and 168 h exposure times, respectively. The cell growth inhibition determined as growth delay was found to be both concentration-dependent and time-dependent. The growth delay in days on MTX treatment for S180 is summarized in Table III. For a given exposure time, growth delays increased with increase in MTX concentrations. MTX peritoneal concentrations at 4 h and 72 h provided the highest growth delay (18 days) while 24 h exposure had the lowest growth delay (10 days).

3.2.2 Ehrlich ascites cell. The time course of cell growth for EAC in the presence of MTX at different exposure times is shown in Fig. 2. The doubling time of EAC was estimated to be 37 h. The time to reach greater than 10,000 cells was 3 days for EAC. The peak effect was delayed relative to MTX exposure. The time for nadir cell count was 360 h, 264 h, 360 h and 408 h for 4 h, 24 h, 72 h and 168 h exposure. The growth delays for different exposure time are shown in Table III.

The growth delay was both concentration and time dependent. MTX exposures at 4 h, 72 h, 168 h had similar growth delay (21 days) whereas 24 h exposure had the lowest growth delay (14 days).

3.3 In vivo efficacy studies

3.3.1 Sarcoma 180 tumor bearing mice. The survival curves for control animals and MTX treated animals are shown in Fig. 3. The survival curves for MTX treated animals were significantly different than the control group ($p < 0.01$). The median survival time for control animals was 9 days. Eighty percent of the animals treated with 72 h constant-rate infusion at 3.8 mg/kg died of MTX toxicity with a median survival time of 6 days. The median survival time (MST) for bolus (760 mg/kg), 24 h infusion (10 mg/kg), 72 h infusion (1.9 mg/kg) and 168 h infusion (6.7 mg/kg) was 11, 22, 11, and 18 days, respectively. The increase in life span for animals treated with bolus, 24 h infusion, 72 h infusion and 168 h infusion were 22%, 144%, 22% and 100%, respectively. The survival curve for 24 h dosing protocol was significantly different from bolus ($p<0.05$), 72 h infusion ($p<0.01$) and 168 h infusion ($p<0.0001$).

3.3.2 EAC tumor bearing mice. The survival curves for control and MTX treated animals are shown in Fig. 4. MST for the control animals was 8 days. Administration of MTX as 72 h infusion at the 3.8 mg/kg had a median survival time of 6.5 days. The survival in animals treated with 24 h and 168 h dosing protocol was not significantly different from the control animals ($p>0.05$). The

survival curves for bolus ($p<0.01$) and 72 h infusion (1.9 mg/kg) ($p<0.0001$) dosing protocols were significantly different from the control animals. The survival in animals treated with bolus and 72 h infusion were not significantly different ($p>0.05$). The median survival times for bolus, 24 h infusion, 72 h infusion and 168 h infusion were 21, 14.5, 27 and 9.5 days, respectively and the percent increase in life span was 162%, 81%, 237% and 19%.

4. Discussion

Administration of chemotherapeutic drug to a population of cancer patients is associated with high degree of pharmacokinetic and pharmacodynamic variability. High variability in drug exposure may have serious pharmacodynamic implications. High drug concentration may result in severe drug toxicity whereas low drug concentrations may lead to ineffective cancer treatment. Drugs that are cleared primarily through renal filtration, variability in systemic clearance has shown to correlate with clinical relapse [12]. Acute lymphocytic leukaemia patients with rapid clearance for MTX were observed to have significantly higher probability of relapse. Similarly, cancer cell killing effect may differ substantially from patient to patient probably due to differences in tumor sensitivity, disease progression, drug resistance and prior treatments.

In an attempt to improve clinical response in individual patients, Galpin at al. proposed therapeutic drug monitoring for cancer patients with the goal of achieving targeted systemic exposure through dosage adjustments [12]. The

approach involved characterization of the relationship between drug exposures (eg. Cmax or Css or AUC) and drug effects [13, 14]. The drug exposure associated with desirable chemotherapeutic selectivity was targeted in individual patients by monitoring plasma drug concentrations. The approach was successfully applied and tested in patients for some chemotherapeutics (eg. methotrexate, teniposide, carboplatin) [7, 15-18].

Gazdar et al. investigated a pharmacodynamic approach using in vitro cytotoxicity drug sensitivity testing to individualize chemotherapy for patients [19]. In this approach, patient's tumor was obtained through a biopsy sample and tested against a panel of available chemotherapeutics. Tumor cell suspensions were prepared and incubated for 1 h with drug concentration or combination of several drugs. Treatment protocol that produced 50% cell growth inhibition or had the highest cell inhibition was selected for treating the patient [20, 21]. The focus of the approach was to identify drug or drugs most likely to be effective against the patient's tumor.

The individualization approaches discussed above may not be applicable to administration protocol dependent chemotherapeutics where effects are dependent on both dose and duration of exposure. In both the approaches, chemotherapeutic effects were investigated following a particular administration protocol. We have proposed an approach to predict chemotherapeutic selectivity

for administration protocol dependent chemotherapeutics using toxicity data and in vitro chemosensitivity testing.

We have investigated the approach using MTX as a model drug. MTX cytotoxic effects have shown to be dependent on both dose and duration of exposure [2, 22, 23]. Toxicity studies were conducted to identify the maximally tolerated dose for MTX following different administration protocols [9]. Four i.p. administration protocols were investigated: bolus, 24 h infusion, 72 h infusion and 168 h infusion. The maximally tolerated dose was found to be dependent on the dosing protocol and varied from 3.8 (72 h infusion) to 760 mg/kg (bolus) in mice. Pharmacokinetics of MTX was investigated in the dose range of 3 to 600 mg/kg. A pharmacokinetic model was developed to predict MTX concentration-time profile at the maximally tolerated doses.

MTX concentrations and duration of exposures tested in vitro were similar to MTX concentrations and exposure times predicted at the maximally tolerated dose of MTX. The concentration producing 50% reduction in cell number i.e. IC_{50} is commonly determined to compare the sensitivities of different chemotherapeutics. However, IC_{50} is also dependent on the duration of exposure and as such could not be applied to the in vitro investigations. Instead, we examined the time course of cell growth to assess MTX cell growth inhibition following the different exposure times.

The time courses of cell growth inhibition for EAC and S180 in the presence of MTX are shown in Fig. 1 and Fig. 2. The time to peak effect i.e. the lowest cell count was significantly delayed relative to MTX exposure. For example, cells on exposure to 4 h of MTX produced peak effects at 216 h (Fig. 1A and Fig. 2A). Interestingly, the cell number was observed to increase even in the presence of MTX and after MTX removal (for example, 4 h and 24 h exposures). The apparent time dissociation between MTX exposure and the time to peak effect may be due to the indirect nature of MTX cytotoxic effect on the cells [24].

The growth delay was defined as the delay in cell growth in the presence of MTX. Table II summarizes the results for S180 and EAC. The growth delay was found to be dependent on MTX concentration and on the duration of MTX exposure. For example, the growth delay for 24 h treatment protocol in S180 increased with increasing MTX concentration. The growth delays were 2 days, 7 days and 10 days at 0.2 μg/ml, 2 μg/ml and 14 μg/ml, respectively. Nearly 160-fold difference in total MTX exposure (concentration x time) showed equivalent growth delay. For example, 5100 μg/ml x 4 h and 1.74 μg/ml x 72 h treatment protocols had equivalent growth delay in the two tumor cell lines (Table III). This may be due to the phase specific cell killing effect of MTX.

The growth delay results at the peritoneal concentration for the different exposure treatments were compared to make prediction regarding chemotherapeutic selectivity. The data suggested that 4 h, 72 h and 168 h

treatment protocols at peritoneal concentration were equally effective for EAC. For S180, the in vitro cytotoxicity results indicated that 4 h and 72 h exposures may provide the maximum MTX efficacy. The data also indicated that 24 h exposure treatment for both EAC and S180 would be the worse protocol. We tested the predictions of the in vitro cytotoxicity data in peritoneal tumor bearing mice.

In vivo survival studies were investigated in mice bearing S180 or EAC in the peritoneum. Four i.p. MTX administration protocols, bolus injection and constant-rate infusions of 24 h, 72 h and 168 h were evaluated at the maximally tolerated dose. The median survival time for the four equally toxic dosing protocols were different suggesting that equally toxic dosing protocols were not equally effective in mice (Fig. 3). In S180 tumor bearing mice, the 24 h treatment protocol had the longest median survival time of 22 days. The survival of animals treated with 24 h protocol was also significantly different ($p<0.05$) from the bolus (MST=12 days), 72 h infusion (MST=12 days), and 168 h infusion (MST=18 days) treatments. The in vitro cytotoxicity data had predicted that 24 h treatment protocol would be least effective relative to the other treatment exposures. Thus, comparison of the in vivo efficacy results and the in vitro cytotoxicity results indicated a negative correlation for S180 tumor cell line.

Similarly, MTX efficacy in peritoneal EAC tumor bearing mice was highly dependent on the administration protocol (Fig. 4). Equally toxic dosing protocols

were not equally effective. The most effective dosing protocol was 72 h infusion with longest median survival time of 27 days. The survival of animals treated with 72 h infusion was significantly different from animals treated with 168 h infusion ($p<0.05$). The survival of animals treated with bolus and 72 h infusion were not different. The in vitro cytotoxicity data had indicated that bolus, 72 h infusion and 168 h infusion exposures would be equally effective. However, in vivo the median survival times for bolus (MST=21 days), 72 h infusion (MST=27 days) and 168 h infusion (9.5 days) protocols were different. Further, we did not find any positive correlation between in vitro growth delay results and in vivo median survival time for EAC.

We had proposed that chemotherapeutic selectivity in vivo could be predicted from in vitro cell inhibition results. Unfortunately, our results did not find any positive correlation between the in vitro and in vivo cytotoxicity results for the two tumor cell lines. The lack of correlation may possibly be due to a number of factors such as differences in cell growth rates in vitro as compared to in vivo, differences in tumor growth environment, formation of multicellular tumors in vivo, differences in tumor sensitivities in vitro and in vivo and the effect of the immune system in vivo. The in vitro and in vivo cytotoxicity results for MTX suggested that the monolayer cell culture model may not be a suitable model to predict in vivo selectivity. Drug cytotoxicity in monolayer and multicellular spheroid cell culture models have shown different sensitivities (IC_{50}) for the two tumor models [25-27].

In future, multi-cellular spheroid model would be examined to predict chemotherapeutic selectivity.

To summarize, we found that MTX efficacy was dependent on MTX concentration and duration of MTX exposure in a monolayer tumor model (in vitro) and in peritoneal bearing tumors (in vivo). We observed that in vitro treatment with equally toxic MTX exposures did not result in equivalent tumor cell growth inhibition. Similarly, in vivo survival studies in peritoneal tumor bearing mice demonstrated that chemotherapeutic selectivity was dependent on the administration protocol. Lastly, we did not find any positive correlation between in vitro cytotoxicity results and in vivo survival results in the two murine cancer cell lines.

REFERENCES

1. Frei Ed, Bickers JN, Hewlett JS, Lane M, Leary WV, Talley RW. 1969. Dose schedule and antitumor studies of arabinosyl cytosine (NSC 63878). Cancer Res 29: 1325-32.

2. Goldie JH, Price LA, Harrap KR. 1972. Methotrexate toxicity: correlation with duration of administration, plasma levels, dose and excretion pattern. Eur J Cancer 8: 409-14.

3. Joel SP, Shah R, Slevin ML. 1994. Etoposide dosage and pharmacodynamics. Cancer Chemother Pharmacol 34 Suppl: S69-75.

4. Kohler DR, Goldspiel BR. 1994. Paclitaxel (taxol). Pharmacotherapy 14: 3-34.

5. Rowinsky EK, Verweij J. 1997. Review of phase I clinical studies with topotecan. Semin Oncol 24: S20-3-S20-10.

6. Mick R, Ratain MJ. 1991. Modeling interpatient pharmacodynamic variability of etoposide. J Natl Cancer Inst 83: 1560-4.

7. Evans WE, Crom WR, Stewart CF, Bowman WP, Chen CH, Abromowitch M, Simone JV. 1984. Methotrexate systemic clearance influences

probability of relapse in children with standard-risk acute lymphocytic leukaemia. Lancet 1: 359-62.

8. Egorin MJ. 1993. Cancer pharmacology in the elderly. Semin Oncol 20: 43-9.

9. Lobo ED, Balthasar JP. 2002. Pharmacokinetic-pharmacodynamic modeling of methotrexate toxicity in mice. J Pharm Pharmacol Thesis Chapter 3, pg 58: .

10. Lobo ED, Balthasar JP. 1999. Highly sensitive high-performance liquid chromatographic assay for methotrexate in the presence and absence of anti- methotrexate antibody fragments in rat and mouse plasma. J Chromatogr B Biomed Sci Appl 736: 191-9.

11. Tada H, Shiho O, Kuroshima K, Koyama M, Tsukamoto K. 1986. An improved colorimetric assay for interleukin 2. J Immunol Methods 93: 157-65.

12. Galpin AJ, Evans WE. 1993. Therapeutic drug monitoring in cancer management. Clin Chem 39: 2419-30.

13. Gianni L, Kearns CM, Giani A, Capri G, Vigano L, Lacatelli A, Bonadonna G, Egorin MJ. 1995. Nonlinear pharmacokinetics and metabolism of paclitaxel and its pharmacokinetic/pharmacodynamic relationships in humans. J Clin Oncol 13: 180-90.

14. Nagai N, Ogata H. 1997. Quantitative relationship between pharmacokinetics of unchanged cisplatin and nephrotoxicity in rats: importance of area under the concentration-time curve (AUC) as the major toxicodynamic determinant in vivo. Cancer Chemother Pharmacol 40: 11-8.

15. Evans WE, Relling MV, Rodman JH, Crom WR, Boyett JM, Pui CH. 1998. Conventional compared with individualized chemotherapy for childhood acute lymphoblastic leukemia. N Engl J Med 338: 499-505.

16. Rodman JH, Relling MV, Stewart CF, Synold TW, McLeod H, Kearns C, Stute N, Crom WR, Evans WE. 1993. Clinical pharmacokinetics and pharmacodynamics of anticancer drugs in children. Semin Oncol 20: 18-29.

17. Jodrell DI, Egorin MJ, Canetta RM, Langenberg P, Goldbloom EP, Burroughs JN, Goodlow JL, Tan S, Wiltshaw E. 1992. Relationships

between carboplatin exposure and tumor response and toxicity in patients with ovarian cancer. J Clin Oncol 10: 520-8.

18. Egorin MJ, Reyno LM, Canetta RM, Jodrell DI, Swenerton KD, Pater JL, Burroughs JN, Novak MJ, Sridhara R. 1994. Modeling toxicity and response in carboplatin-based combination chemotherapy. Semin Oncol 21: 7-19.

19. Gazdar AF, Steinberg SM, Russell EK, Linnoila RI, Oie HK, Ghosh BC, Cotelingam JD, Johnson BE, Minna JD, Ihde DC. 1990. Correlation of in vitro drug-sensitivity testing results with response to chemotherapy and survival in extensive- stage small cell lung cancer: a prospective clinical trial [see comments]. J Natl Cancer Inst 82: 117-24.

20. Cortazar P, Gazdar AF, Woods E, Russell E, Steinberg SM, Williams J, Ihde DC, Johnson BE. 1997. Survival of patients with limited-stage small cell lung cancer treated with individualized chemotherapy selected by in vitro drug sensitivity testing. Clin Cancer Res 3: 741-7.

21. Cortazar P, Johnson BE. 1999. Review of the efficacy of individualized chemotherapy selected by in vitro drug sensitivity testing for patients with cancer. J Clin Oncol 17: 1625-31.

22. Gimmel S, Maurer HR. 1994. Growth kinetics of L1210 leukemic cells exposed to different concentration courses of methotrexate in vitro. Cancer Chemother Pharmacol 34: 351-5.

23. Pinedo HM, Chabner BA. 1977. Role of drug concentration, duration of exposure, and endogenous metabolites in determining methotrexate cytotoxicity. Cancer Treat Rep 61: 709-15.

24. White JC, Loftfield S, Goldman ID. 1975. The mechanism of action of methotrexate. III. Requirement of free intracellular methotrexate for maximal suppression of (14C)formate incorporation into nucleic acids and protein. Mol Pharmacol 11: 287-97.

25. Bhuyan BK, Folz SJ, DeZwaan J, Northcott SE, Alberts DS, Garcia D, Wallace TL, Li LH. 1991. Cytotoxicity of tetraplatin and cisplatin for human and rodent cell lines cultured as monolayers and multicellular spheroids. Cancer Commun 3: 53-9.

26. Erlichman C, Wu A. 1991. Effects of 5-fluorouracil and leucovorin in spheroids: a model for solid tumours. Anticancer Res 11: 671-5.

27. Erlichman C, Vidgen D. 1984. Cytotoxicity of adriamycin in MGH-U1 cells grown as monolayer cultures, spheroids, and xenografts in immune-deprived mice. Cancer Res 44: 5369-75.

CAPTION FOR FIGURES

Fig. 1. In vitro inhibition of cell growth in Ehrlich ascites cell following MTX exposure. Mean cell count and standard deviation are represented as symbols and error bars, respectively. A. Cell growth following 4 h exposure of MTX at 0 μg/ml (●), 68 μg/ml (▽), 680 μg/ml (▼) and 5100 μg/ml (○). B. Cell growth following 24 h exposure of MTX at 0 μg/ml (●), 0.19 μg/ml (▽), 2 μg/ml (▼) and 14 μg/ml (○). C. Cell growth following 72 h exposure of MTX at 0 μg/ml (●), 0.23 μg/ml (▽), 0.2 μg/ml (▼) and 1.74 μg/ml (○). D. Cell growth following 168 h exposure of MTX at 0 μg/ml (●), 0.018 μg/ml (▽), 0.2 μg/ml (▼) and 1.34 μg/ml (○).

Fig. 2. In vitro inhibition of cell growth in sarcoma 180 following MTX exposure. Mean cell count and standard deviation are represented as symbols and error bars, respectively. A. Cell growth following 4 h exposure of MTX at 0 μg/ml (●), 68 μg/ml (▽), 680 μg/ml (▼) and 5100 μg/ml (○). B. Cell growth following 24 h exposure of MTX at 0 μg/ml (●), 0.19 μg/ml (▽), 2 μg/ml (▼) and 14 μg/ml (○). C. Cell growth following 72 h exposure of MTX at 0 μg/ml (●), 0.23 μg/ml (▽), 0.2 μg/ml (▼) and 1.74 μg/ml (○). D. Cell growth following 168 h exposure of MTX at 0 μg/ml (●), 0.018 μg/ml (▽), 0.2 μg/ml (▼) and 1.34 μg/ml (○).

Fig. 3. Survival curves for mice bearing sarcoma 180 cells. Each mouse was injected with 10^6 sarcoma cells in the peritoneum. Treatment was initiated 24 h after tumor inoculation. Percent of animals surviving after treatment with bolus injection of saline (●), 760 mg/kg MTX as bolus injection (○), 10 mg/kg MTX as 24 h infusion (▼), 1.9 mg/kg MTX as 72 h infusion (▽) and 6.8 mg/kg MTX as 168 h infusion (■). The survival curves for MTX treated animals were significantly different from saline treated animals.

Fig. 4. Survival curves for mice bearing Ehrlich ascites cells. Mice were injected with $5x10^6$ cells in the peritoneum. Treatment was initiated 24 h after tumor inoculation. Percent of animals surviving after treatment with bolus injection of saline (●), 760 mg/kg MTX as bolus injection (○), 10 mg/kg MTX as 24 h infusion (▼), 1.9 mg/kg MTX as 72 h infusion (▽) and 6.8 mg/kg MTX as 168 h infusion (■). The survival curves for MTX treated animals were significantly different from saline treated animals.

Fig. 1

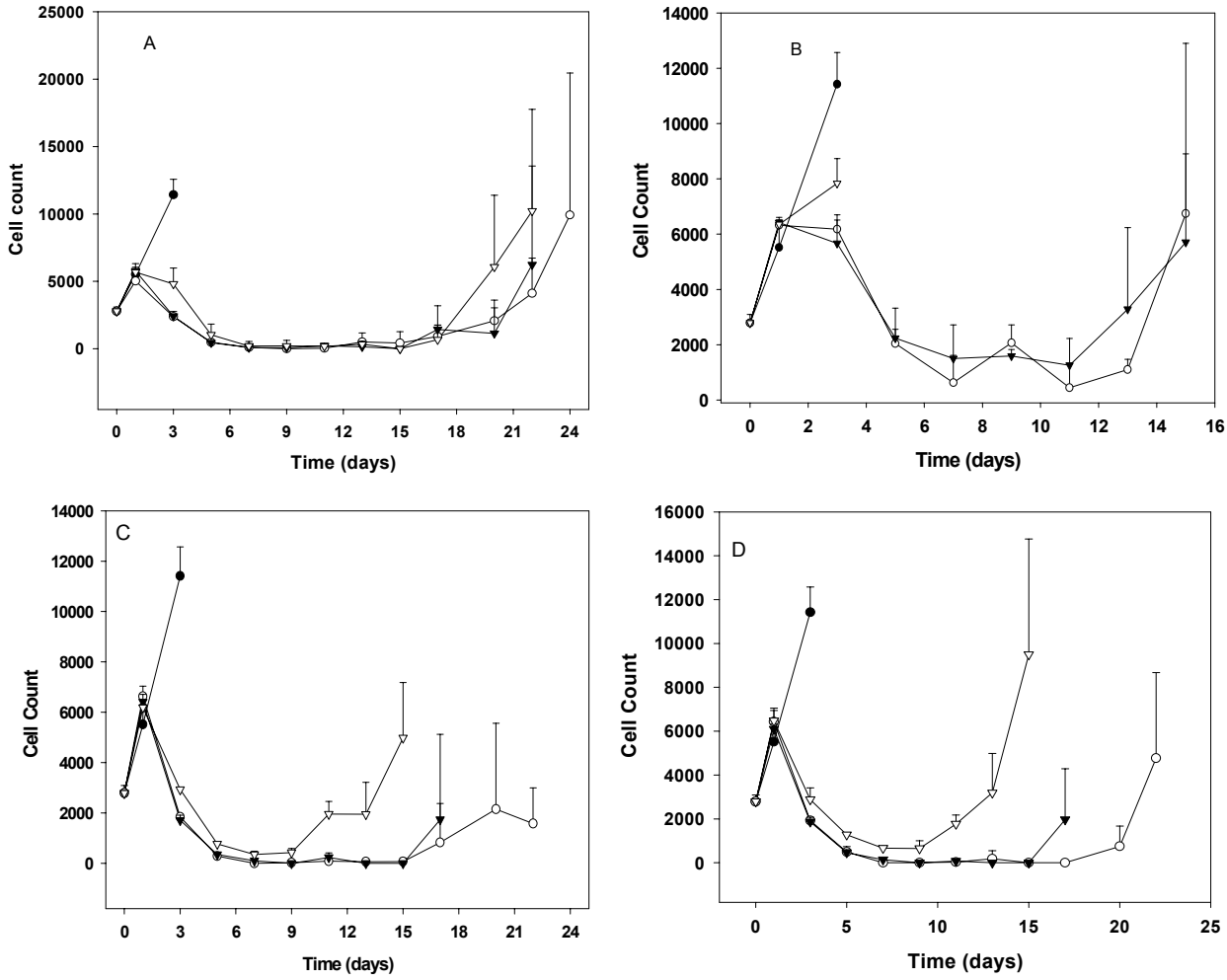
A
Cell count
Time (days)
B
Cell Count
Time (days)
C
Cell Count
Time (days)
D
Cell Count
Time (days)

Fig. 2.

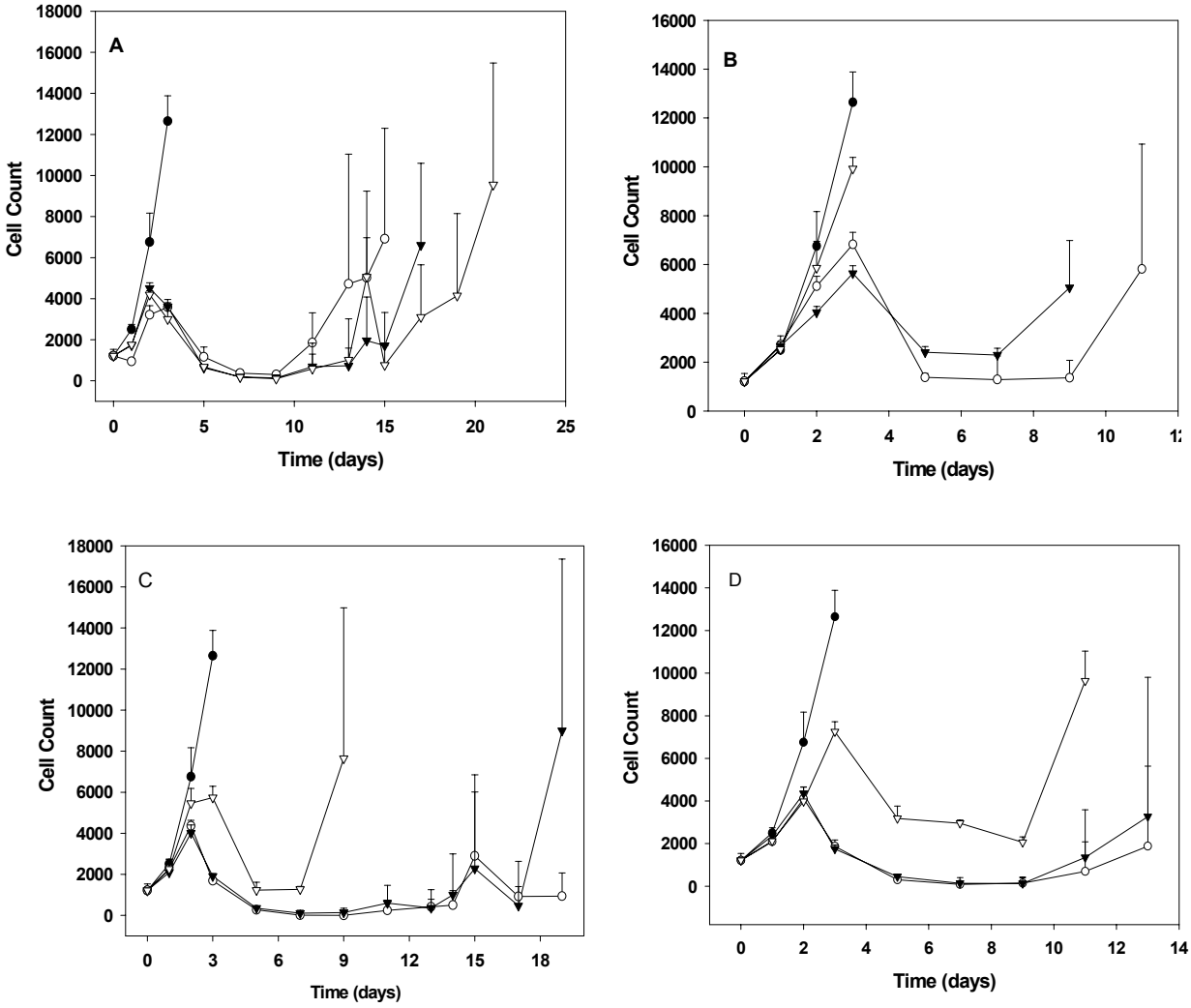

Fig. 3.

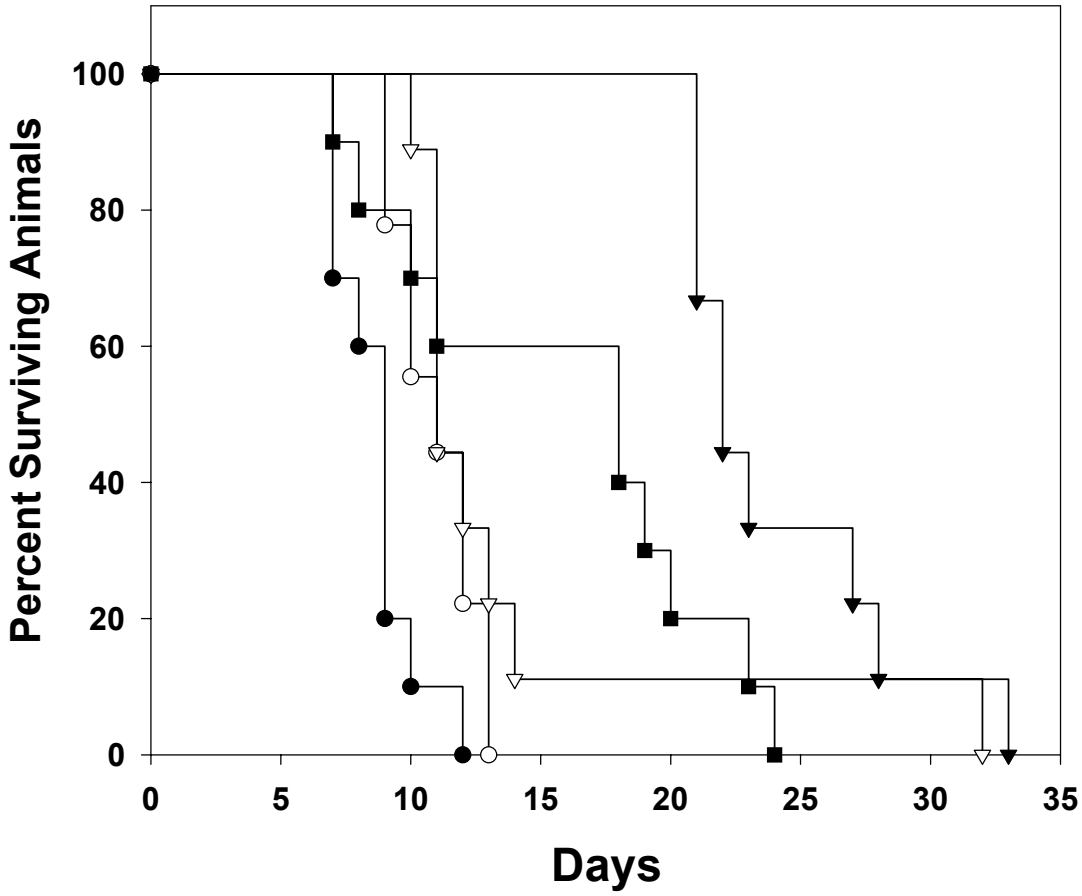
Percent Surviving Animals
100
80
60
40
20
0
0
5
10
15
20
25
30
35
Days

Fig. 4

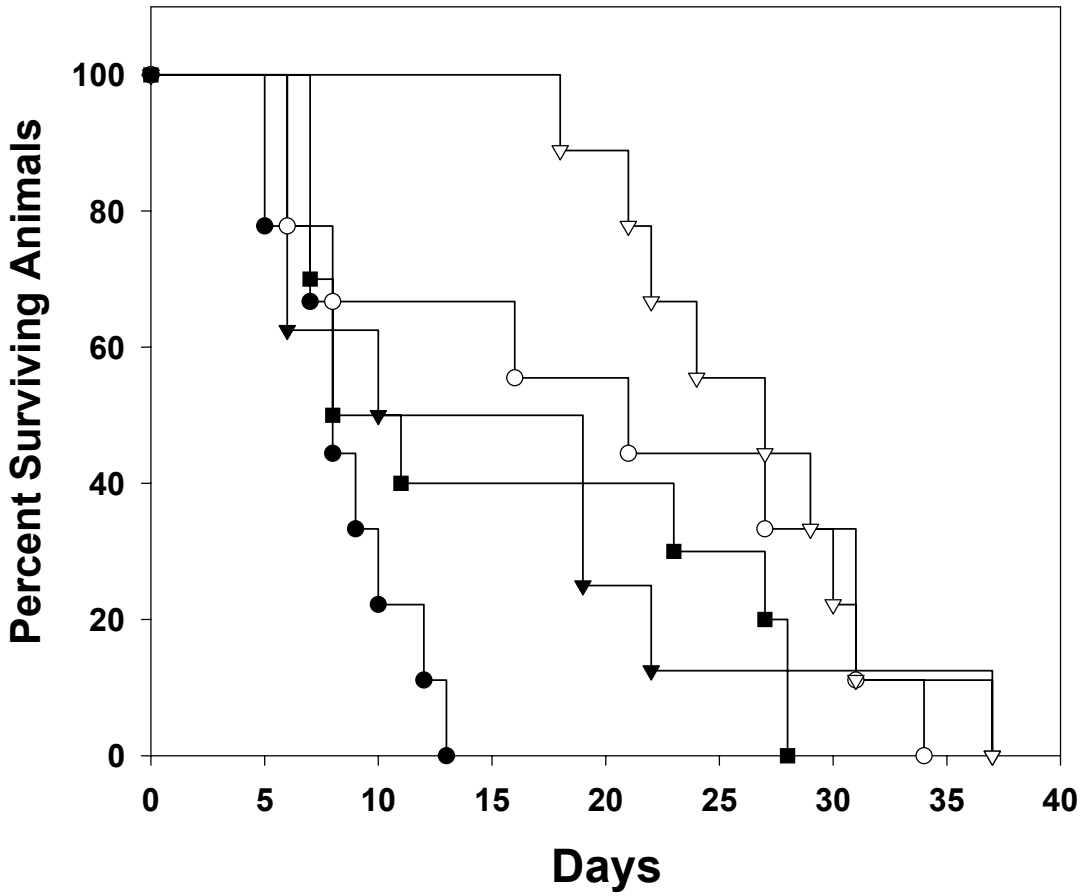
Percent Surviving Animals
100
80
60
40
20
0
0
5
10
15
20
25
30
35
40
Days

Table I. MTX concentrations and duration of exposures tested for in vitro MTX cytotoxicity studies[a].

Exposure time (h)	Maximally tolerated dose (mg/kg)	Cp (μg/ml)	Ci (μg/ml)	Cs (μg/ml)
4 h	760	5100	680	68
24 h	10	14	2	0.19
72 h	3.8	1.74	0.23	0.023
168 h	6.7	1.34	0.2	0.018

a: Maximally tolerated dose was determined from the toxicity studies conducted in mice and was defined as the dose causing 10% nadir body weight loss in mice. Cp and Cs are the predicted MTX concentration in the peritoneum and in the plasma at the given dose, respectively. Ci is an intermediate concentration between Cp and Cs.

Table II: Stability of methotrexate in cell culture media at 37 ºC

[a] MTX Concentration (μg/ml)	Exposure Time (h)	% Recovery
5100	4	97.1
68	4	105.5
14	24	95.0
0.19	24	97.6
1.74	72	101.0
1.34	72	103.8
0.1	72	107.4

a: Methotrexate in media was incubated at the exposure time examined in cell growth inhibition studies. Each concentration was tested in triplicate. Methotrexate was analyzed with an HPLC assay with limited of quantitation of 25 ng/ml.

Table III. Growth delay for cancer cell lines exposed to methotrexate in cell culture[a]

Sarcoma 180

Exposure time	Growth delay (days)		
	Cs	Ci	Cp
4 h	18	18	18
24 h	2	7	10
72 h	8	16	18
168 h	8	11	11

Ehrlich ascites cell

Exposure time	Growth delay (days)		
	Cs	Ci	Cp
4 h	19	21	21
24 h	2	14	14
72 h	14	19	21
168 h	14	19	21

a: Growth delay was defined as the difference in the time for MTX treated cells to reach 10,000 cell number and the time for untreated cells to reach 10,000 cell number. Cs, Ci and Cp refer to systemic methotrexate concentration, intermediate methotrexate concentration and peritoneal methotrexate concentration.

CHAPTER EIGHT

Conclusion

This dissertation investigated the utility of anti-methotrexate Fab fragments to improve the safety and therapeutic efficacy of intraperitoneal methotrexate (MTX) chemotherapy. Previous work in this group has shown that systemic anti-MTX Fab reduced systemic MTX exposure of i.p. MTX therapy. In this dissertation work, the utility of anti-MTX Fab to reduce MTX-induced toxicity, increase the maximum tolerated dose of MTX, and improve MTX efficacy was examined in an animal model of peritoneal tumor. A primary focus of this dissertation was to apply pharmacokinetic-pharmacodynamic (PKPD) modeling to facilitate optimization of intraperitoneal chemotherapy.

In chapter 1, we reviewed the utility of anti-drug antibodies to reduce systemic drug toxicities. Anti-drug antibodies and antibody fragments produce favorable reductions in peak plasma free drug concentrations and cumulative systemic exposure to free drug. However, anti-drug antibodies have been shown to increase the half-life of the drug and increase the duration of free drug exposure. The alteration in free drug exposure may be very significant for chemotherapeutic drugs where effects are dependent on both the dose and the duration of exposure, potentially leading to increases in drug toxicities.

Given that anti-drug antibodies altered the duration of free drug exposure, we proposed to develop a PKPD model that would relate the time course of MTX exposure to MTX-induced toxicities and allow for prediction of MTX-induced toxicities in the presence of anti-MTX antibodies. The pharmacokinetics of MTX

was investigated with an HPLC assay capable of measuring total and free MTX concentration in mouse plasma (chapter 2). The method was shown to be accurate as the recoveries were within 6% of the theoretical values and the coefficient of variation was less than 8%. Toxicity studies presented in chapter 3 indicated that MTX-induced body weight loss was highly dependent on the administration protocol. The maximally tolerated dose for MTX varied from 3.8 mg/kg (following 72 h infusion) to 760 mg/kg (bolus injection). MTX pharmacokinetics were linear in the dose range of 3 - 600 mg/kg. The data was characterized with a time-dissociated PKPD model that related the time course of MTX exposure to the magnitude of MTX-induced nadir body weight loss. The model characterized the protocol dependence of MTX toxicity satisfactorily with a median prediction error of 3.9%.

The PKPD model for MTX toxicity was integrated with a pharmacokinetic model to predict the effect of anti-MTX antibodies on the time course of MTX exposure and MTX-induced toxicity (chapter 4). Computer simulations conducted with the model predicted that i.v. anti-MTX antibodies could either increase or decrease MTX-induced body weight loss following i.p. MTX therapy. Simulation studies also indicated that the effects of anti-MTX antibodies would be dependent on the dosing protocol, molar dose ratio of antibody to MTX, antibody affinity and on the antibody (IgG or Fab). The dosing protocols of i.v. anti-MTX antibodies and i.p. MTX predicted to produce either an increase or a decrease in MTX-induced body weight loss were tested in mice. A new hybridoma secreting monoclonal anti-

MTX IgG1 was developed. Anti-MTX IgG and anti-MTX Fab were produced, purified and characterized. Consistent with the model predictions, 24 h constant-rate infusions of i.p. MTX and i.v. anti-MTX IgG significantly increased MTX-induced body weight loss and MTX-related mortality compared to 24 h constant-rate infusion of i.p. MTX + i.v. saline (or i.v. mouse IgG). Similarly, 72 h constant-rate infusions of i.p. MTX and i.v anti-MTX Fab significantly reduced MTX-induced nadir body weight loss and MTX-related mortality compared to 72 h constant-rate infusions of i.p. MTX + i.v. saline. Thus, these data demonstrated that a PKPD model may be useful for predicting in vivo effects of anti-drug antibodies.

In chapter 5, we tested the hypotheses that anti-MTX Fab would allow for increases in the maximally tolerated dose of MTX and increase the efficacy of i.p. MTX therapy. Pharmacokinetics of anti-MTX Fab was investigated following i.v. and s.c. administration. Subcutaneous administration of anti-MTX Fab allowed for more than 5-fold increase in the maximally tolerated dose of i.p. MTX. Anti-MTX Fab increased the median survival time in mice bearing peritoneal tumor following i.p. MTX therapy. Thus, results with MTX and anti-MTX Fab indicated that anti-drug antibodies may have utility in improving the ratio of drug efficacy : drug toxicities of intraperitoneal drug administration.

In an attempt to predict chemotherapeutic selectivity in vivo (ratio of drug efficacy: drug toxicities), an approach was examined that utilized MTX toxicity

data and in vitro MTX cytotoxicity results (chapter 7). MTX efficacy was determined with four equally toxic MTX exposures (determined from in vivo toxicity studies) against two cancer cell lines grown in cell culture and in mice bearing peritoneal tumors. MTX-induced cell growth inhibition was found to be dependent on MTX concentration and the duration of MTX exposure. Equally toxic MTX exposures were not equally effective both in vitro and in vivo. Thus, chemotherapeutic selectivity like chemotherapeutic toxicity was also dependent on the administration protocol. Unfortunately, the in vitro cytotoxicity results failed to predict in vivo chemotherapeutic selectivity for either cell line.

In chapter 6, we have applied a transit compartment model to characterize the time delays associated with the development of chemotherapeutic effects. In vitro data showed that the peak MTX effect (i.e. the time to reach the lowest cell number on MTX treatment, 168-264 h) was delayed tremendously relative to the time course of MTX exposure (24 h). In comparison to the established PKPD models for chemotherapeutic effects, the transit compartment model provided superior fitting of the data. Thus, the transit compartment models may find broad use in the characterization of chemotherapeutic effects.